ABSTRACT

Title of Thesis:	ALGAE-BASED PURIFICATION OF LANDFILL BIOGAS USING A CO2 REMOVAL SYSTEM AND HELICAL PHOTOBIOREACTOR IN SERIES
Authors:	Jason Albanese, Mindy Chen, Jay Chiao, Lawrence Cho, Hubert Huang, Brif an Lin, Melissa Meyerson, Praveen Puppala, Anjana Sekaran, Yoon Shin, David Wang, Melissa Yu, and Cary Zhou
Directed By:	Dr. Steven Hutcheson

Biogas is a mixture of methane and other gases. In its crude state, it contains carbon dioxide (CO_2) which reduces its energy efficiency and hydrogen sulfide (H_2S) which is toxic and highly corrosive. Because chemical methods of removal are expensive and environmentally hazardous, this project investigated an algal-based system to remove CO_2 from biogas. An anaerobic digester was used to mimic landfill biogas. Iron oxide and an alkaline spray were used to remove H_2S and CO_2 respectively. The CO_2 laden alkali solution was added to a helical photobioreactor where the algae metabolized the dissolved CO_2 to generate algal biomass. Although technical issues prevented testing of the complete system for functionality, cost analysis was completed and showed that the system, in its current state, is not economically feasible. However, modifications may reduce operation costs.

ALGAE-BASED PURIFICATION OF LANDFILL BIOGAS USING A CO_2 REMOVAL SYSTEM AND HELICAL PHOTOBIOREACTOR IN SERIES

By

Team BE PURE (Biogas Efficiency Producing and Utilizing Renewable Energy)

Jason Albanese, Mindy Chen, Jay Chiao, Lawrence Cho, Hubert Huang, Brian Lin, Melissa Meyerson, Praveen Puppala, Anjana Sekaran, Yoon Shin, David Wang, Melissa Yu, and Cary Zhou

Mentor: Dr. Steven Hutcheson

Thesis submitted in partial fulfillment of the requirements of the Gemstone Program
University of Maryland, College Park
2014

Acknowledgements

We would like to thank Dr. Stephanie Lansing and her graduate students for their immense knowledge, advice on anaerobic digesters and the inocula used for starting our biodigester; Dr. Ganesh Sriram and Andrew Quinn for supplying us with and helping us grow the algae; the ACCIAC Fellows Program, University Sustainability Fund, and the Gemstone Program for funding our project; our librarian, Nedelina Tchangalova, for her help with our literature review; Dr. Gantt and Dr. Cunningham for allowing us to use their photometer and regulator; the Gemstone staff for their guidance and support through the peaks and the valleys; Alma Polo-Barrios and Jay Corckran for their help; and finally our mentor, Dr. Steven Hutcheson, for his patience, encouragement, expertise, editorial services and lab space, without which we would never have accomplished as much as we did.

A special acknowledgement to our former teammate, Alex Song, for his leadership and initiative during the early stages of our project. We wish him all the best.

Table of Contents

List of Abbreviations

C&D- construction and demolition
HRT- hydraulic retention times
LED- light-emitting diode
MEA- monoethanolamine
OLR- organic loading rate
PVC- polyvinyl chloride
RSF- rapid sand filtration
S/I- substrate-to-inoculum
SSF- slow sand filtration
TS- total solids
UV- ultra-violet
VFA- volatile fatty acids
VS- volatile solids

List of Figures

List of Tables

Chapter 1: Introduction

Industrial energy demands are rapidly outpacing the supply of carbon-based fossil fuel sources (Demirbas, 2010). Several studies have indicated that fossil fuel reserves may be depleted by the year 2112 (Shafiee & Tofal, 2009). Consumption of fossil fuels leads to rising levels of greenhouse gases, which in turn have been directly attributed to global warming. The most abundant greenhouse gases are carbon dioxide (CO_2) and methane (CH_4), which comprise 0.039445% and 0.000179% of all atmospheric greenhouse gases, respectively (International Panel on Climate Change, 2001). CO_2 has the most significant contribution to greenhouse gases due to the vast quantities present in the atmosphere. However, when compared to CO_2 on a molar basis, CH_4 has a global warming potential that is 3.7 times higher (Lashof & Ahuja, 1990). The increased temperatures caused by global warming could have a wide range of effects on the environment, including rising sea levels, drastic climate changes, and mass extinctions (Hoegh-Guldberg & Bruno, 2010).

In light of the limitations of fossil fuels and their environmental destructiveness, the need for alternative energy sources is widely recognized. Biogas has been proposed as one of these new sources of energy. Biogas is a combustible mixture of gases produced via anaerobic digestion, where bacteria metabolize organic material in an oxygen-free environment (Lastella, 2002). Sites that collect organic waste, such as landfills and wastewater treatment plants, naturally produce large quantities of biogas. Thus, biogas has a wide availability and renewable nature due to the organic materials and microorganisms required for biogas synthesis.

Biogas consists primarily of CH_4 (45% to 75%), CO_2 (25% to 55%), and traces of other compounds such as hydrogen sulfide (H_2S), the concentration of which can range from a hundred to a thousand ppm (Mann et al., 2009). The CH_4 in biogas provides a valuable source of energy while the other components, including CO_2 and H_2S, impede the energy efficiency of biogas (Abatzoglou & Boivin, 2008). CO_2 produces no energy through combustion and thus dilutes the biogas, while H_2S is toxic, odorous, and highly corrosive, often damaging machinery for producing and transporting biogas. H_2S, when combusted, also forms sulfur dioxide, a harmful pollutant and major component of acid rain (Kapdi et al., 2005). These impurities must be removed to make biogas an efficient, odorless energy source.

Natural gas is a non-replenishable fossil fuel found in deposits underneath the earth's surface that currently accounts for 24% of the United States' energy use. Similarly to biogas, natural gas must be treated to remove impurities such as H_2S and CO_2 after extraction. However, its composition consists predominantly of CH_4 (70% to 90%) and little CO_2 (0% to 8%), producing a higher energy yield than that of raw biogas (Environmental Protection Agency, 2013c; Speight, 2007). In order for biogas to serve as a competitive source in the energy market, CH_4 content must be enriched by removing CO_2, a major impurity.

Current methods of biogas purification involve chemical or mechanical processes, including chemical scrubbing, chemical adsorption, filters, and membranes. Such methods are often expensive and environmentally hazardous due to the nature of the chemicals used, preventing biogas from becoming a competitive alternative energy source (Osorio & Torres, 2009).

Biological methods of purifying biogas exist, but are not utilized on an industrial scale. Photosynthetic algae and other autotrophic microorganisms can metabolize CO_2 to produce sugars through photosynthesis, which can also be used as biofuels (Weyer et al., 2010). Other microorganisms (i.e. purple and green sulfur bacteria) consume H_2S during metabolism and produce solid elemental sulfur (Biebl & Pfennig, 1977). These microorganisms form the foundation for biological methods of CO_2 and H_2S removal from biogas. Because these microorganisms are renewable and self-sustaining (i.e. requiring minimal nutrients), a biological system could be more cost-efficient and environmentally sustainable than conventional chemical methods.

This study analyzed the use of biological methods for biogas purification on a laboratory scale, focusing on scalability. Landfills account for about 16% of the CH_4 produced annually in the United States, with the potential to produce 215 billion cubic feet of biogas per year (Environmental Protection Agency, 2013a). However, landfills remain a largely untapped resource in the United States. Rather than collecting and utilizing the biogas, landfills burn or freely vent the methane into the atmosphere, wasting a potent energy source as well as contributing to global warming. This is especially problematic due to the potency of CH_4 as a greenhouse gas (Lashof & Ahuja, 1990). Burning the biogas converts the CH_4 to CO_2, lowering the potency of the greenhouse gases emitted (Environmental Protection Agency, 2013a; Jaffrin et al., 2003). As of July 2013, the Environmental Protection Agency has incorporated 621 landfills into their Landfill Methane Outreach Program that encourages the collection and utilization of landfill gas (Environmental Protection

Agency, 2013b). They have also identified about 450 potential landfills to add to the program. Because of the wide availability of landfill biogas, we chose to incorporate it into our study. Our purification system aimed to effectively convert this waste product into a powerful energy source, while reducing the potency of the greenhouse gas emissions.

This study aimed to develop a biogas purification system using microorganisms to effectively remove CO_2, and then compare the cost-effectiveness of this system to currently established chemical methods. The system as a whole is a connection of five individual components in series: anaerobic digester, H_2S scrubber, CO_2 column, algal system, and water recycling column. The anaerobic digester serves to produce biogas for testing that has a composition proportional to that of landfill biogas. The study focused on landfill biogas because it is readily available and a largely untapped resource. H_2S must be removed because it is toxic and will corrode the system. This is accomplished in the H_2S scrubber. CO_2 must also be removed in order to increase the energy potential of the biogas so that it can compete with natural gas standards. Although biological methods exist for both H_2S and CO_2 removal, CO_2 was removed with a biological method while an established chemical method was used for H_2S removal because time limitations prevented testing and development of biological methods for both removal systems. It was also important to ensure that all H_2S was removed in order to prevent damage to the rest of the system. The biological method of CO_2 removal was chosen because of its renewable and self-sustaining characteristics. CO_2 removal was divided into the CO_2 column and algal system to prevent a combustible mixture of CH_4 and O_2. In photosynthesis, O_2 is produced as a

byproduct, which can be problematic due to the combustible nature of O_2 when reacting with hydrocarbon mixtures, such as CH_4. With the use of an aqueous solution, the CO_2 scrubbing column removes CO_2 from the biogas, resulting in a CH_4 enriched biogas, which exits at this stage for collection. The CO_2-laden aqueous solution from the CO_2 column then enters the algal system for use by the algal culture, thereby preventing CO_2 release into the atmosphere. Aqueous solution from the algal system is filtered by the recycling system and returned to the CO_2 column for reuse.

We hypothesized that this purification system using microorganisms would be cost-efficient and sustainable. To test our hypothesis, we collected and compared data on the composition of the biogas before and after it had been cycled through our system. Using results gathered from our laboratory scale studies, we predicted utility costs and revenue that would be generated from an industrial sized model.

Chapter 2: Anaerobic Digester

Introduction

Biogas is a gaseous mixture of CH_4, CO_2, and other trace gases such as nitrogen (N_2) and H_2S. These gases are the combined metabolic products of an assortment of microorganisms. The metabolic processes which convert organic matter into biogas are collectively called anaerobic digestion. Anaerobic digestion occurs in the absence of oxygen (O_2) since O_2 is toxic to the microorganisms involved.

Almost all organic materials can be digested except stable woody materials because few microorganisms can degrade lignin, an integral part of the cell walls of plants and some algae (Appels, Baeyens, Degreve, & Dewil, 2008). Anaerobic digestion is widely prevalent where digestible waste is collected, such as landfills and wastewater treatment plants, making these natural sources of biogas. The exact composition of biogas depends on the source material and varies widely between landfill waste, wastewater, and farm waste. Carbohydrates are composed of carbon, hydrogen, and oxygen. Proteins and nucleic acids are both sources of nitrogen, but proteins are also the primary source of sulfur, whereas nucleic acids are the dominant sources of phosphorous. Biogas is the gaseous byproduct of the metabolism of these carbohydrates, proteins and other cell constituents, converting them into energy, CH_4, CO_2, H_2S, and amines.

This study focused on converting biogas into a natural gas energy substitute. In order to burn biogas for its energy, CH_4 is required in a high concentration. Natural gas is composed of roughly 70-90% CH_4 and 0-20% other burnable hydrocarbons (Speight, 2007). However biogas contains only 50% CH_4 while the other half is

composed of CO_2. Thus, in order to convert biogas into a natural gas substitute, the CH_4 content must be enriched in biogas to similar levels (at least 95%). In particular, landfill biogas was the focus because of it was readily available and was a large source of untapped energy. However, no nearby landfills collected biogas and long-distance transportation of the biogas was not feasible at the time of the study. Therefore, an anaerobic digester was constructed to process a controlled feed of organic material and produce biogas similar to that of a landfill to test the purification system. Because this was a microbial process, manure, a natural source of these microorganisms, was used to provide a starting culture of methanogens. Manure alone, however, results in poor biogas production with a composition dissimilar to landfill biogas. Therefore, a custom anaerobic digester was built to produce a steady supply of biogas that is similar in composition to that produced from landfills.

Literary Review

Biogas Composition

Biogas is ultimately a mixture of CH_4, CO_2, and several trace compounds, including H_2S, N_2, O_2, and volatile organic compounds. The exact composition varies depending on the source of biogas. A study in Finland (Rasi, 2007) compared the biogas produced by digesting waste from a landfill, municipal sewage, and a farm. The study reported the highest CH_4 level from sewage (61% to 65%) and the lowest level from landfills (47% to 57%). The CO_2 levels were 36% to 38% for the sewage biogas and 37% to 41% for landfill biogas. The H_2S level was negligible for the sewage biogas whereas the landfill biogas had an average of 62.5 ppm but other studies have found levels as high as 5400 ppm (Papadias *et al.*, 2012).

Chemistry

Anaerobic digestion consists of four major steps: hydrolysis, acidogenesis, acetogenesis, and methanogenesis. Hydrolysis is considered the rate-limiting step, where insoluble and high-molecular weight organic compounds are broken down into soluble intermediates (i.e. amino acids, fatty acids, and sugars). During acidogenesis, the soluble intermediates are further degraded into volatile fatty acids (VFAs), ammonia (NH_3), CO_2, H_2S, and other by-products (Appels et al., 2008). Acetogenesis converts the acids and alcohols into CO_2, hydrogen, and acetate. Lastly, in methanogenesis, methanogens produce CH_4 and CO_2 from acetate and further reduce the CO_2 to more CH_4 with hydrogen. (Appels et al., 2008; Themelis & Ulloa, 2007).

Variables affecting biogas production

Several factors affect biogas production, including organic loading rate, substrate-to-inoculum ratio, and temperature.

Organic loading rate

Organic loading rate (OLR) is defined as the amount of organic material that is fed into the digester over time. The effect of the OLR on biogas production has been studied by Nagao et al. (2012). Two 3-L anaerobic digesters were used to control for different hydraulic retention times (HRT), defined as the average length of time that the organic feed remains in the digester. The two digesters (Digester 1 and 2) were maintained at an HRT of 8 and 16 days, respectively, by discharging supernatant daily. Volumetric biogas production rate was measured against various OLRs (3.7, 5.5, 7.4, 9.2, 12.9 $kg_{Volatile\ Solid}/(m^3*day)$). The biogas production rate of Digester 1 stabilized at 2.7 $L_{biogas}/(L_{digester}*day)$ at an OLR of 3.7 $kg_{VS}/(m^3*day)$. When the OLR was increased to 5.5 $kg_{VS}/(m^3*day)$, a rapid decrease in biogas

production in Digester 1 was observed by day 5 after the change in OLR. Higher OLRs resulted in a severely reduced biogas production rate in Digester 1.

The biogas production rate of Digester 2 also stabilized at 2.7 $L_{biogas}/(L_{digester}*day)$ at an OLR of 3.7 $kg_{VS}/(m^3*day)$. Unlike Digester 1, however, the biogas production increased to 6.6 $L_{biogas}/(L_{digester}*day)$ as the OLR increased to 9.2 $kg_{VS}/(m^3*day)$. When the OLR increased to 12.9 $kg_{VS}/(m^3*day)$, the biogas production rate decreased to roughly 4 $L_{biogas}/(L_{digester}*day)$.

The study suggested that the changes in the biogas production rate were directly related to the changes in pH and inversely related to VFA levels. The pH level in Digester 1 dropped simultaneously with the decreasing biogas production rate. Digester 2 exhibited a stable pH level until an OLR of 12.9 $kg_{VS}/(m^3*day)$, where the biogas production dropped. The VFA content was low (< 1000 mg/L) in Digester 1 at an OLR of 3.7 $kg_{VS}/(m^3*day)$ and increased to 8149 mg/L at an OLR of 5.5 $kg_{VS}/(m^3*day)$. The VFA concentration increased significantly in Digester 2 to 19210 mg/L at an OLR of 12.9 $kg_{VS}/(m^3*day)$.

In a similar study done by Liu et al. (2012), OLRs of 1.2 – 8.0 $kg_{VS}/(m^3*day)$ were tested for the biogas production rate. The highest OLR of 8.0 $kg_{VS}/(m^3*day)$ led to the highest biogas production rate of 2.94 $L_{biogas}/(L_{digester}*day)$. The pH decreased slowly as OLR increased from 1.2 to 8.0 $kg_{VS}/(m^3*day)$; the VFA concentration increased from 203 to 570 mg/L as OLR increased from 1.2 to 8.0 $kg_{VS}/(m^3*day)$. These studies showed how OLR affects the pH and VFA, which led to changes in the biogas production rate. The trends of pH and VFA vs. OLR were contradictory between the two studies, suggesting that they were feed- and inoculum-dependent and

should be tested in a specific system. However, both studies agree that the ideal OLR for a digester varies between 3.7 - 9.2 $kg_{VS}/(m^3*day)$.

Substrate-to-inoculum ratio

Zhou et al. (2011) researched the effect of varying substrate-to-inoculum (S/I) ratio on the biogas yield. A batch reactor at mesophilic temperature conditions was used to digest fresh okara, or soy flour. The inoculum was obtained from a municipal wastewater treatment plant in Japan. S/I ratios ranging from 0.1 to 3.0 were tested against volumetric biogas yield. The study found that S/I ratios of 0.6 to 0.9 generate the highest biogas yield (762 mL to 775 mL/g_{VS}). The methane-based degradability, which is the ratio of theoretical and experimental methane production, was also highest (90% to 93%) for S/I ratios of 0.6 to 0.9. The study attributed the low biogas yield at a high S/I ratio (2.0) to accumulation of VFAs; high levels of VFA induced inhibitory responses from the microorganisms.

Temperature

Bolzonella et al. (2012) compared the performances of mesophilic (35°C) and thermophilic (55°C) reactors. Both digesters had the same HRT of 20 days and OLR of 2.2 $kg_{VS}/(m^{3*}day)$. The biogas production rate increased from 0.7 to 1.0 $m^3/(m^3*day)$ with temperature. This rise was attributed to the increased hydrolysis activity at higher temperatures. However, extreme temperatures had to be avoided because increased NH_3 levels can inhibit microbial metabolism; sudden changes in temperature were also detrimental to the microorganisms (Appels et al., 2008).

Methodology

Apparatus

Several biogas generators were built and modified as necessary. Although the overall structures and functions of these prototypes remained constant, each model served to improve upon the previous one. The basic anaerobic digester consisted of a heavy-duty, 5-gallon polyvinyl chloride (PVC) bucket, which contained the inoculum. O_2 is toxic to the anaerobic bacteria, so feed and waste valves were installed to limit the introduction of air into the digester. A stir bar was used in the earlier models to provide intermittent mixing, but was removed in the final model because it did not appear to be required. Instead, external mixing through manual rocking of the digester was applied after each feeding to provide more gentle, but necessary mixing in the digester.

All components of the digester were composed of plastic, PVC, and stainless steel to prevent H_2S corrosion. The waste valve featured a faucet that was positioned roughly 10 cm above the bottom of the bucket. A ball valve placed on the lid served as the feed valve. The digester was sealed with silicon sealant and bulkhead fittings at every connection to prevent leaks and the introduction of O_2 (Figure 2.1). Soap-bubble leak tests and pressure leak tests were conducted periodically to ensure that the digester was leak-proof.

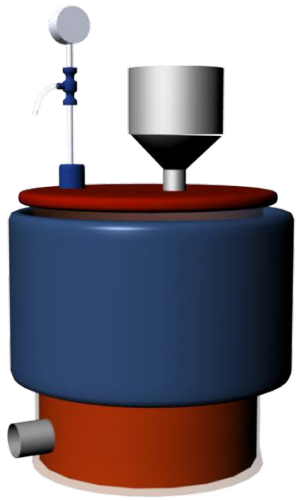

Figure 2.1. Model of the anaerobic digester. The container and parts were PVC, while the fittings were stainless steel. The volume of the container was 18.9 L, filled with 14 L of inoculum and substrate; the remaining space was filled with the produced biogas. Feed was was introduced into the digester through the ball valve shown near the center of the lid. The waste valve is located near the bottom of the digester, and produced biogas exited the digester through the outlet on the lid.

Testing and Production

The digester was fed with organic soy flour at a concentration of 10% (by weight) total solid in deoxygenated water. Soy flour was chosen for its high protein content, providing a sulfur source for H_2S production and more closely mimicking landfill biogas.

After the digester was fully constructed and leak-tested, 14 L of inoculum was added through the feed valve. After roughly 24 hours, the first 100 mL batch of feed was added and then every 2 days. The feeding frequency was increased to every day when biogas production stopped in the initial model. Volume inside the digester was kept constant by removing an equivalent volume of digested material from the waste valve. The pH of the “waste” material was recorded periodically using a pH meter (HM Digital PH-200).

The OLR was 0.714 $kg_{TS}/(m^3*day)$. Note that the OLR was recorded based on total solids (TS) rather than volatile solids (VS), which are the portion of TS that can be converted into biogas. The OLR was considerably lower than that applied by Nagao et al. (2012) to prevent overloading the digester; the optimal OLR for organic soy flour was unknown, so a more conservative OLR was chosen for this study.

Two system temperatures, room temperature (22°C) and 32°C, were tested. The digester was wrapped with two electric heat blankets (Sunbeam 732-500) to increase the temperature above room temperature. The inside temperature was measured using the thermometer built into the pH meter. The digester wall temperature was also approximated using an aquarium thermometer. Biogas production was measured by the pressure increase in the digester according to the pressure gauge installed in the biogas collection outlet. As biogas was produced in the digester, the pressure increased when all ports and valves were closed. Assuming that there were no leaks in the system, the differential ideal gas law was applied to measure the change in the number of moles of biogas. This was then converted into volume of gas that would be evolved over time. CO_2 and H_2S concentrations were measured using a 0-60% CO_2 meter with Datalogger (CM-0050) and a GasAlert Extreme H_2S meter (BW Technologies), respectively. For the final model, gas samples were collected and analyzed using a gas chromatography-mass spectrometry (GC/MS).

Results

Rate of Biogas Production

Biogas production was calculated by measuring the change in pressure of the digester over time and converting it to a volumetric flow using the ideal gas law. An example calculation is enumerated in Appendix C. Volumetric flow was not directly

measured because the flows from the digester were too low for any flow meters within our budget. Three trials were conducted at each temperature and the data fit with a linear regression passing through the origin. R^2 values of each trial were consistently near 1.00 (between 0.964 and 0.995) and the overall R^2 value was 0.991 for 22°C and 0.992 for 32°C. The high R^2 values indicate a steady biogas production rate over the short-term. The slopes of the regression lines were used to convert to volumetric biogas production rate. The production rates for each temperature both had a percent error of less than 6% (5.6% for 22°C and 4.1% for 32°C), which suggests the biogas production rate was also consistent in the long-term. The absolute maximum pressure reached over all trials was 1.2 psi.

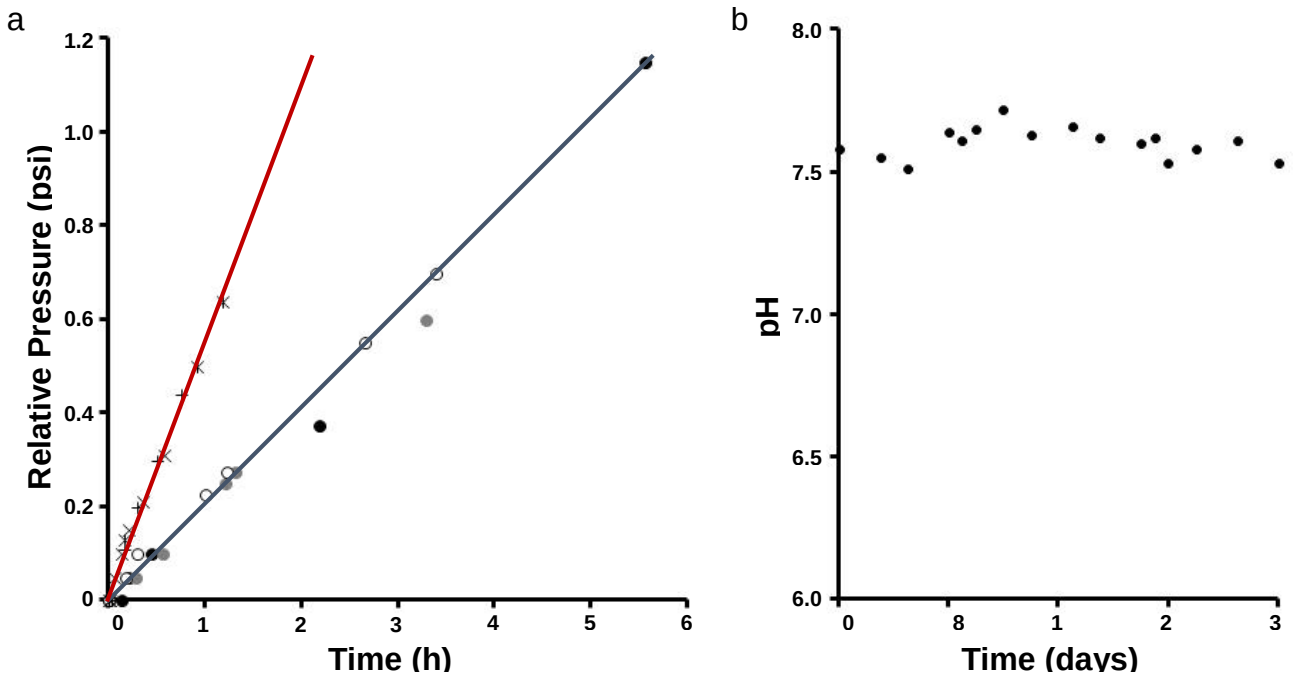

Figure 2.2. Biogas production over time. **(a)** The change in internal pressure in the digester at 22°C and 32°C recorded over time for three trials each. The pressure was normalized to 0 psi at time 0 hr. The circles represent the three 22°C trials while the hatch marks represent the three 32°C trials. The R^2 values are consistently above 0.96, indicating a steady biogas production rate over a short period of time, while the slopes of the three trials are within 6% of each other for each temperature, indicating a consistent biogas production rate over a long period of time. The biogas production rate at 32°C was roughly 2.5 times higher than that at 22°C. **(b)** The pH of the waste collected from the final digester model was measured over the course of the experiment (32 days). The pH was consistently near 7.6, indicating a stable culture.

Temperature

Two different digester temperatures, 22°C and 32°C, were tested to determine which resulted in a more biogas production. The slopes seen in Figure 2.2(a), noted as pressure change over time (psig/h), and corresponding biogas production (L/day) are tabulated in Table 2.1

Table 2.1. Effect of temperature on biogas production.

Temperature	22°C	32°C
Pressure Change (psig/h)	0.202	0.572
	0.188	0.593
	0.210	0.546
Average	*0.200 ± 0.011*	*0.5700 ± 0.024*
Volumetric Biogas Production (L/day)	1.51	4.13
	1.40	4.29
	1.57	3.95
Average	*1.49 ± 0.083*	*4.12 ± 0.170*

Three trials were conducted for each temperature, and each trial was taken on a different day, to take into account the variability that may occur due to the feed cycle (once every two days). As shown in Table 2.1, biogas production was almost 2.5 times greater at 32°C (average of 4.12 L/day ± 4.1%) compared to 22°C (average of 1.49 L/day ± 5.6%). A two-sample t-test comparing the slopes of the pooled data sets (Howell, 2010) found that the biogas production rates were significantly different with a p-value of 0.039.

pH

The pH of the final digester was recorded and graphed in Figure 2.2(b). The digester was freshly inoculated on January 5th (time = 0 days). As shown, the pH remained between 7.51 and 7.61 over the course of 32 days, a 0.055 tolerance (calculated as standard deviation). The consistent pH indicated a stable culture within the digester.

Biogas Composition

The CH_4 concentrations of the produced biogas were recorded periodically by GC/MS analysis. Samples from three different days were run three times each on the GC/MS. The average CH_4 concentration across all three days was 69.9 ± 5.29%; the

average H_2S concentration was 3520 ± 624 ppm. The CH_4 concentration decreased from 75.2% to 63.5% over the course of the 13 days. Remaining composition of biogas was assumed to be CO_2, which had an average composition of 30.1%.

Table 2.2. Composition of biogas using Gas Chromatography.

Date	CH_4 Concentration (%)				H_2S Concentration (ppm)				CO_2 Concentration (%) (100% - %CH_4)
	Trial 1	Trial 2	Trial 3	Avg	Trial 1	Trial 2	Trial 3	Avg	
Jan 16	72.5	78.7	74.3	75.2	3860	4040	3840	3910	24.8
Jan 22	66.6	74.9	71.5	71.0	2180	3280	3190	2880	29.0
Jan 29	64.1	62.8	63.5	63.5	3790	3690	3800	3760	36.5
Average				*69.9*				*3520*	*30.1*

Discussion

The final working model of the anaerobic digester used in the testing of the completed system operated at a temperature of 32°C and was mixed manually each time feed was added. Inoculum in the digester, provided by manure, was fed daily with a soy flour feedstock that provided the sulfur components necessary for production of the H_2S gas component.

Testing of the final digester model showed that biogas was produced at a steady rate of 4.12 ± 0.170 L/day at 32°C. However, the GC/MS data suggested the biogas composition was inconsistent, with methane content decreasing as days passed. A control must therefore be used in any system testing to adjust for the variable initial biogas composition. In later studies, a gas sample obtained directly from the digester was analyzed for every gas sample collected after passing through

the purification system to provide this control. Maximum pressure produced by the anaerobic digester was approximately 1.2 psig.

The average biogas composition produced by the digester was 69.9 ± 5.29% CH_4, 30.1 ± 5.29% CO_2, and 3520 ± 624 ppm H_2S as measured by GC/MS. Landfill biogas, however, averages 47-57% CH_4, 37-41% CO_2, and 62.7-5400 ppm H_2S. The H_2S levels were within observed levels from landfills. The significant difference in CO_2 concentration may make application of our data to purifying landfill biogas difficult. However, the CO_2 composition was substantial and could still demonstrate the removal power of our system. The composition of biogas in general is also highly variable. While not the average landfill composition, the biogas produced was still within the compositions of biogas that has been observed from some landfills. Any purification system must also be able to handle a wide range of biogas compositions. Therefore, the biogas produced by the anaerobic digester was acceptable for testing our purification system for purification of landfill biogas. Note however, that the CO_2 composition of the produced biogas may be less than 30% since the value reported is that of all gases that are not CH_4 or H_2S, which may include small amounts of N_2 and NH_3. Measurements using the H_2S and CO_2 meters were unreliable due to water vapor and inconsistent flow issues. The readings never stabilized and so are superseded by the GC/MS data. The reported volumetric biogas production rate is dependent on the assumption that biogas is an ideal gas. Error in this value may therefore be higher than the reported experimental error.

Several design issues were prominent during testing of the digester, which led to the major design changes specified above. Constructing a gas-tight digester proved

to be difficult, leading to unreliable performance in early models. The gas leaks were attended to in the final model by applying a silicone sealant to the ports. The digester was also tested repeatedly for gas leaks by applying soap to the gaps and carefully monitoring the internal pressure. The stir bar resulted in another issue: excessive stirring resulted in poor biogas production. Too much turbulence inside the digester likely interfered with contact between bacteria and the feed. The stir bar was removed in the final model, and contents inside the digester were mixed after each feeding using a manual rocker, which provided a gentler mixing method.

Two internal temperatures for the digester were tested. Elevating the temperature of the digester to 32°C resulted in a significantly increased biogas production rate over room temperature (22°C). An increase in the OLR also led to a greater gas production because at lower OLRs, the amount of nutrients was insufficient to sustain the bacteria, leading to a cessation of biogas production after certain points. Therefore, the final model added heating blankets to maintain an elevated temperature and the feeding frequency was increased two-fold.

Various feed stocks could not be thoroughly tested due to restrictions in time and the available space. Therefore, soy flour was chosen for its protein content in order to most closely mimic the composition of landfill biogas. The protein to sugar ratio in the feed corresponds to the sulfur to carbon content which defines the proportion of H_2S in the resulting biogas. Soy flour is approximately 34% protein by weight and proteins on average contains 1.26% sulfur by weight. Therefore, soy flour should provide approximately 4300 ppm of H_2S versus 62-5400 ppm in landfill biogas. A manure inoculum was chosen over a defined microorganism culture

because manure is cheaper, more readily available, and contains a complete microbiome known to produce biogas.

Chapter 3: H_2S Scrubbing

Introduction

Biogas contains trace amounts of H_2S in widely varying concentrations, depending on the source material. Landfills that process construction and demolition waste produce biogas that typically contains 50 – 15,000 ppm of H_2S, while landfills that do not process such waste generally produce biogas with less than 100 ppm. Even in such small amounts, H_2S poses serious logistical and environmental concerns. H_2S is extremely corrosive to metals within a system, resulting in high maintenance costs and potential engineering problems (Ma et al, 2000). In addition, H_2S is an environmental concern as it forms a pollutant, sulfur dioxide (SO_2), upon combustion (Kapdi et al., 2005). H_2S is also highly toxic and odorous even in trace quantities. The IDLH (level at which a substance is immediately dangerous to life and health) is 100 ppm, but H_2S is known to be irritating in levels as low as 0.1 ppm (Centers for Disease Control and Prevention, 1994). H_2S must therefore be removed completely from biogas before the biogas can be used as a natural gas substitute.

Since H_2S is such a major problem, many industrial methods are available to remove H_2S from a gas. Certain microorganisms also use H_2S as an energy source, ultimately oxidizing it into non-gaseous sulfates (Kabil and Banerjee, 2010). A biological H_2S removal system may prove to be cost effective and sustainable; however, testing such a system is beyond the scope of this study. Therefore, in our biogas purification system, we include a chemical H_2S scrubber to remove H_2S to prevent corrosion of the later components of our system and avoid health risks. Two

scrubbers were tested: an iron oxide adsorption column and a copper sulfate ($CuSO_4$) absorption column, due to their simplicity, relatively inexpensiveness, and widely demonstrated ability to be effective at removing H_2S. We hypothesized that both scrubbers would remove H_2S from biogas below detectable levels; however, the $CuSO_4$ scrubber would prove to be more practical for testing our system because the gas is more easily observable in a liquid phase.

Literature Review

H_2S removal through oxidation

One method of removing H_2S involves oxidation with air. In the Claus process, H_2S is oxidized by air to produce SO_2, which then reacts with H_2S to produce elemental sulfur. Performing the Claus process using two reactors can achieve an efficiency of 95%; four reactors can increase this efficiency to 98% (Nagl, 1997). This process is advantageous because it removes high amounts of H_2S and is cost-effective due to its utilization of air as the oxidant. The disadvantage stems from the oxygen to H_2S ratio negatively affecting the efficiency of the process. This ratio must therefore be closely monitored and controlled. As such, the process should only be considered when the stream has a relatively fixed and large amount of H_2S (Nagl, 1997). Another study by El-Bishtawi and Haimour (2004) improved the Claus process by enriching the oxygen in the air and recycling it back into the feed. The modified process reduced the equipment size and cost while increasing the adiabatic flame temperature. This allowed for higher concentrations of H_2S to be in the feed.

Another type of oxidation used for removing H_2S is the liquid phase process. Metallic compounds (i.e. iron sulfate ($FeSO_4$), zinc sulfate ($ZnSO_4$), and $CuSO_4$)

dissolved in solution can be used as oxidants to remove the H_2S from biogas. The H_2S is dissolved in an aqueous solution and the sulfide ions are allowed to react with the metal ions to form metal sulfides as precipitate. A study by Maat et al. (2005) found that both $FeSO_4$ and $ZnSO_4$ solutions can yield results but are hindered by pH sensitivity and selectivity of H_2S removal. The $CuSO_4$ solution showed the greatest potential, as it selectively removed large amounts of H_2S in the widest range of pH levels. The efficiency of the $CuSO_4$ solution in removing H_2S was around 99.5% to 99.9%. The process is advantageous due to its high efficiency of H_2S removal, its high adaptability to different pH levels, and its ability to regenerate $CuSO_4$. The disadvantage to this process is the foaming that may cause reductions in efficiency (Maat et al., 2005). Also, $CuSO_4$ is relatively costly when large amounts are desired and produce large amounts of Cu waste. The process can be improved upon by increasing the surface area and residence time (Abatzoglou & Boivin, 2009; Maat et al., 2005).

H_2S removal through adsorption

Another method of removing H_2S is through adsorption with metal oxides, such as iron (III) oxide (Fe_2O_3). In the iron sponge process, Fe_2O_3 is impregnated into wood chips used to pack the reactor. The Fe_2O_3 reacts with H_2S to form iron (III) sulfide (Fe_2S_3) and then reacts with O_2 to produce elemental sulfur. The theoretical efficiency of the iron sponge process in a batch reactor, calculated by Zicari (2003), was about 85%. The advantage of using the iron sponge process is its ability to be regenerated with a reduction in efficiency of only one-third of the previous cycle. However, it has relatively high operating costs and produces hazardous waste

(Abatzoglou & Boivin, 2009). Unlike other methods of removing H_2S, the iron sponge process, due to its popularity, already has design parameter guidelines that are widely accepted. For optimal conditions, these guidelines recommend that the vessel be non-corrosive and provide enough bed length. In addition, a down-flow of gas should first pass through the bed with a suggested residence time of over 60 sec, keeping superficial gas velocity between 0.6 to 3 m/min and temperatures between 18°C and 46°C. Other guidelines include suggestions for bed height, mass loading amount, moisture content, pH level, and pressure (Zicari, 2003).

Adsorption can also be used to remove H_2S by utilizing activated carbon. Activated carbon can be impregnated with cations that act as catalysts in the absorption process to improve the efficiency (Bandosz, 2002). The efficiency of the adsorption greatly depends on the type of activated carbons used and other environmental factors (i.e. humidity) (Bouzaza et al., 2004). Non-impregnated activated carbons removed hydrogen sulfide at a much slower rate; even at low H_2S concentrations and sufficient residence time, the removal rate was slow (Bandosz, 2002). Abatzoglou and Boivin (2009) found that the average adsorption capacities of H_2S for impregnated and non-impregnated activated carbons were 150 $mg_{H2S}/g_{activated\ carbon}$ and 20 $mg_{H2S}/g_{activated\ carbon}$, respectively. Activated carbon is advantageous for its ability to be regenerated upon washing with water. The disadvantages of using activated carbon are that the addition of caustics in the impregnated activated carbon lowers the ignition temperature of the material, which could lead to self-ignition. Although the mechanisms of how H_2S is removed by activated carbon are not yet

fully understood, Yuan and Bandosz (2007) suggested that the process contains both chemical and physical mechanisms.

H_2S removal through amine absorption

Another method of absorbing H_2S is by using amines. H_2S is absorbed and dissolved in an aqueous amine stream, which is then heated to pull the H_2S back out. Lu, Zheng, and He (2006) examined the effects of temperature and gas flow rate on absorption. Increasing the temperature lowered H_2S removal efficiency and selectivity because of the decreased solubility and increased reversibility at higher temperatures. Increasing the flow rate decreased H_2S removal efficiency due to smaller residence time, but increased the selectivity because the mass-transfer resistance of H_2S decreased while that of CO_2 stayed relatively constant. The advantages of this process are the high selectivity and its ability to regenerate amines. The disadvantages of this process are the lower efficiency due to the oxidation of amines, high operation costs, and possibility of foaming (Zicari, 2003).

H_2S removal through a biological method

A biological method of removing H_2S involves the use of a microorganism. One such microorganism is *Thiobacillus ferroxidans* which can remove H_2S by oxidizing $FeSO_4$. The oxidized form, $Fe_2(SO_4^{2-})_3$, can then oxidize H_2S to produce elemental sulfur (Abatzoglou & Boivin, 2009). The advantage of using the biological method of removing H_2S is its flexibility in choosing various species that meet the criteria. However, using a biological process requires constant care of the microorganism, which increases the operation cost. Also, the microorganism must

meet certain criteria, such as the ability to prevent biomass accumulation and survivability in fluctuating environmental conditions (Siefers, 2000).

H_2S removal through other methods

Other methods of removing H_2S include caustic scrubbing and physical solvents. Caustic scrubbing involves an equilibrium-dependent reaction, where a pH increase removes H_2S while a pH decrease produces it. This process can be quite disadvantageous because a purge stream is required to keep salts from precipitating and must not be allowed back into the process stream to prevent the reverse reaction. This prevents the regeneration of caustics, increasing the operation cost (Nagl, 1997). The use of physical solvents involves a liquid dissolving the H_2S and then removing the H_2S by lowering the pressure. The advantage of this process is its simplicity. The disadvantage is that the H_2S must have a high solubility with the solvent or else the operation cost will be too high.

Methodology

$CuSO_4$ column

Two different methods of scrubbing H_2S from biogas were considered: an absorption column using a $CuSO_4$ solution and an adsorption column using iron oxide generated from steel wool. The absorption column used a 1 M solution of $CuSO_4$ as the scrubbing agent inside a glass column with a diameter of 5.3 cm and height of 10.8 cm. Raw biogas from the anaerobic digester entered the column through an air stone sparger at the bottom of the column and bubbled up through the $CuSO_4$ solution. The biogas was collected at the top of the column (Figure 3.1). Teflon tape and a soap bubble test were used to ensure the system was air-tight and leak proof.

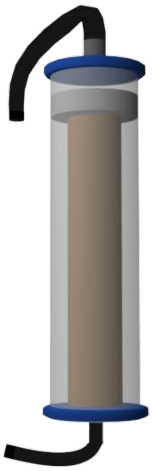

Figure 3.1 H_2S scrubber using the iron oxide method. Biogas from the anaerobic digester enters the column from the bottom. Biogas flows through the steel wool packing removing H2S and exiting through an outlet at the top.

Steel wool scrubber

The iron oxide adsorption column scrubber was constructed from a 67.3 cm long iron pipe with a diameter of 6.2 cm; the ends of the pipe were capped with two screw-on caps, and each cap was fitted with a nipple in the center to attach the tubing. Super fine grade (#0000) steel wool was treated with glacial acetic acid and used to pack the column. The acid generated iron oxide and the steel wool also served as packing to baffle the gas flow and increase the reaction surface area. A stand was employed to hold the pipe up vertically. Raw biogas was introduced into the steel wool through the nipple on the bottom of the pipe. It then flowed upwards and exited out the nipple at the top of the pipe after H_2S was removed. This method required less pressure to flow the biogas through the system than the $CuSO_4$ method. Teflon tape and a soap bubble test were also used to ensure the apparatus was leak-proof.

Scrubber testing

The efficacy of H_2S removal was tested for both methods. A Mylar balloon was filled with biogas from the anaerobic digester and the biogas was driven through the system by placing a brick atop the balloon. The H_2S concentration in the biogas was measured with a GasAlert Extreme H_2S meter (BW Technologies) before and after running the raw biogas through each scrubber. The resolution of the meter was 1 ppm and the maximum accurate reading was 500 ppm. In each trial, the column was flooded with biogas before making any measurements.

A later test was performed by feeding biogas directly into the H_2S column from the anaerobic digester. The initial and effluent biogas compositions were collected in sample bags and analyzed using GC/MS.

Results

For both columns, the initial biogas composition had more than 500 ppm of H_2S while the effluent biogas had less than 1 ppm of H_2S for all trials. This data clearly suggests success in H_2S removal. The H_2S meter, however, was observed to fluctuate wildly, shedding some doubt on the data. A later test using GC/MS showed that the initial H_2S composition was over 3500 ppm, while the effluent was not-observable with GC/MS. This supports the previous data, however, the initial CH_4 composition was 77%, but the effluent gas had non-observable levels of CH_4, suggesting another mechanism for the observed reduction in H_2S.

The $CuSO_4$ scrubber required a minimum pressure of 2 psig to bubble gas through the column, while the iron oxide scrubber did not require any noticeable pressure.

Discussion

Although both the $CuSO_4$ and the iron oxide column seemed able to remove H_2S appropriately, the iron oxide column was ultimately chosen due to pressure requirements and commercial availability factors. For the $CuSO_4$ column, a minimal pressure of 2 psig was required to bubble the biogas through the column. Because the anaerobic digester could only hold a maximum pressure of approximately 1.2 psig, operation of the $CuSO_4$ column under these circumstances required a gas compressor, which was impractical. In contrast, the steel wool column had no required operating pressure due to the solid adsorption process. The pressure of the biogas generated from the anaerobic digester proved more than sufficient to drive the gas flow through the steel wool column. In addition, steel wool is cheaper than pure $CuSO_4$ and produces less waste.

The results of this study should be observed carefully because of oddities in other aspects of the data. The H_2S meter was often observed to fluctuate wildly when measuring a gas of static composition. The meter also responded drastically to minor changes in flow and pressure. The results may therefore not be reliable. The GC/MS data also showed a complete removal of H_2S. However, CH_4 was also removed, indicating an underlying problem. The loss of CH_4 indicates a loss of gas in its entirety, but the positive pressure coming out suggests this is not the case. A mix-up in samples or another anomaly may account for this result. While the efficacy of H_2S removal is in question, the results suggest all the H_2S was removed. Appropriate precautions were taken in case H_2S was not removed completely.

Chapter 4: CO_2 Scrubbing

Introduction

CO_2 is a major component of biogas, accounting for 25-55% of the total volume (Mann et al., 2009). Landfill biogas, specifically, contains 37-41% on average (Rasi, 2007). Natural gas, however typically is less than 5% non-combustible gas, though as much as 10% is acceptable. CO_2 is a non-combustible gas, providing no energy, and therefore must be removed from biogas to reasonable levels before biogas can be used as a natural gas substitute (Abatzoglou & Boivin, 2008).

Currently there are many different chemical and mechanical processes used to remove the CO_2 from biogas, including chemical adsorption, chemical scrubbing, membranes, and filters. The chemicals and materials that are used make these processes expensive and are often hazardous to the environment (Osorio & Torres, 2009). These methods also produce large amounts of waste in the form of reaction byproducts or from the regeneration reactions of the material used in CO_2 removal. Using the photosynthesis of algae to remove the CO_2 from biogas is an alternative method that solves the problems of the common non-biological methods. Algae is self-sustaining with the addition of minimal nutrients and light. While the light is not negligible, the sun can be used as a source of free energy. The products of photosynthesis are sugars, which the algae use to grow and reproduce and oxygen. The algae are a natural waste product and can be harvested as another biofuel source by processing the algal waste into algal oil. The oxygen poses a slight problem, however. If the biogas is directly introduced into the algae-containing media, the produced oxygen will be included in the purified biogas. The oxygen-methane

mixture would be highly flammable and very dangerous. Therefore, we use a two-step process to remove CO_2, first dissolving the CO_2 into an aqueous solution, and then feeding the CO_2-laden media to an open algae system. The open algae system removes CO_2 via photosynthesis while allowing excess oxygen to be vented into the atmosphere.

CO_2 is significantly more soluble in water than CH_4. This is the principle used in our CO_2 absorption column in order to transfer CO_2 to an aqueous media which can be fed to algae. While the solubility differential is higher in some non-aqueous solutions, the algae must be fed with an appropriate media, so an aqueous solution is used to absorb the CO_2 in this study. Increasing the alkalinity of the aqueous solution can enhance the CO_2 solubility in the solution. Such a scrubbing column is common in the chemical and petroleum industries (Chen, Shi, Du, & Chen, 2008). We hypothesized that an alkaline CO_2 absorption column, could successfully reduce CO_2 levels in biogas to less than 10% and ideally less than 5%.

Literature Review

Chemical scrubbing

Several different techniques can be used to absorb CO_2 from biogas, commonly involving scrubbing with water or chemicals. Water columns are effective because CO_2 is several times more soluble than CH_4 in water. However, at room temperature and atmospheric pressure, CO_2 is still relatively insoluble and thus large volumes of water are required to absorb the CO_2 (Andriani, Wresta, Atmaja, & Saepudin, 2013). In order to decrease the volume of water required, many scrubber designs use high pressures or cooled water. The water can then be recycled by running the CO_2-laden water against a countercurrent of air low in CO_2. The

difference in CO_2 concentration causes the CO_2 from the water to be released into the air (Petersson & Wellinger, 2009). One main problem with this method is that the CO_2 is still released into the environment as a greenhouse gas.

Gas solubility in water

Various factors affect the solubility of gases in liquids. These include pressure, temperature, and concentration of the solute. The relationship between pressure and solubility is described by Henry's law, shown below in Equation 1, where P_g is the partial pressure of the solute in the gas phase, C_l is the concentration of the solute in the liquid phase, and K_H is the Henry's law constant.

$$P_g = K_H C_l \qquad \text{Eqn. 1}$$

The Henry's law constant is often used to describe the solubility of the solute in the solvent where a larger value of K_H means a lower solubility. It is also evident from this equation that the higher the partial pressure of the solute the higher the concentration in the liquid (Markham & Kobe, 1941). Temperature and concentration of solute display the opposite effect. As the temperature of the liquid or the concentration of the solute is increased, the solubility of the gas generally decreases (Markham & Kobe, 1941).

Relationship between CO_2 concentration and pH

When CO_2 dissolves in water it reacts with the water producing carbonic acid (H_2CO_3) according to the following reaction, Equation 2.

$$H_2O + CO_2 \leftrightarrow H_2CO_3 \leftrightarrow H^+ + HCO_3^- \quad \text{Eqn. 2}$$

The production of H_2CO_3 lowers the pH of the water, so as more CO_2 dissolves the pH of the water decreases (Wurts & Durborow, 1992). In accordance with Le Chatelier's principle, the higher the alkalinity of the water the more acid can be absorbed and therefore the more CO_2 that can dissolve. This is because additional base neutralizes the acid, allowing more acid to dissociate. In the case of CO_2, the H_2CO_3 on the right side of Equation 2 is neutralized by the base present in solution. This shifts the equilibrium of the reaction to the right causing more of the CO_2 to convert to H_2CO_3 and allowing more CO_2 to dissolve into the water.

CO_2 scrubber design

CO_2 can also be scrubbed using aqueous solutions or organic solvents. Commonly used scrubbing agents include polyethylene glycol, amine solutions, and alkali solutions (Petersson & Wellinger, 2009; Andriani et al., 2013). A study by Tippayawong and Thanompongchart (2010) tested the abilities of NaOH, $Ca(OH)_2$, and monoethanolamine (MEA) to capture CO_2 from biogas. The relevant reactions are shown below.

Chemical scrubbing reactions:

$$CO_2 + 2OH^- \rightarrow CO_3^{2-} + H_2O \qquad \text{Eqn. 3}$$

$$CO_2 + CO_3^{2-} + H_2O \rightarrow 2HCO_3^- \qquad \text{Eqn. 4}$$

$$CO_2 + RNH_2 + H_2O \rightarrow RNH_3^+ + HCO_3^- \qquad \text{Eqn. 5}$$

$$CO_2 + RR'NH \rightarrow RR'NCOO^- + H^+ \qquad \text{Eqn. 6}$$

All three solutions effectively captured the CO_2 from the biogas with more than 90% removal. NaOH was found to have the highest loading capacity and the calcium hydroxide ($Ca(OH)_2$) saturated most quickly. The study concluded that alkali

solutions were not a promising method for CO_2 capture because, unlike amines, they cannot be regenerated (Tippayawong & Thanompongchart, 2010).

Bubble-columns

Continuous bubble-column scrubbers and packed bubble column scrubbers are two of the most common scrubber designs for CO_2 removal systems. Continuous bubble-column scrubbers pipe in the CO_2-laden gas from the bottom of the column and a scrubbing solution from the top of the column. The gas bubbles through the scrubbing solution, transferring the CO_2 to the liquid phase. In the case of alkaline scrubbing solutions, CO_2 is removed through production of carbonate at the interface of gas and solution (Chen et al., 2008). A diagram of a bubble-column scrubber that was used for experimentation can be seen in Figure 4.1 below.

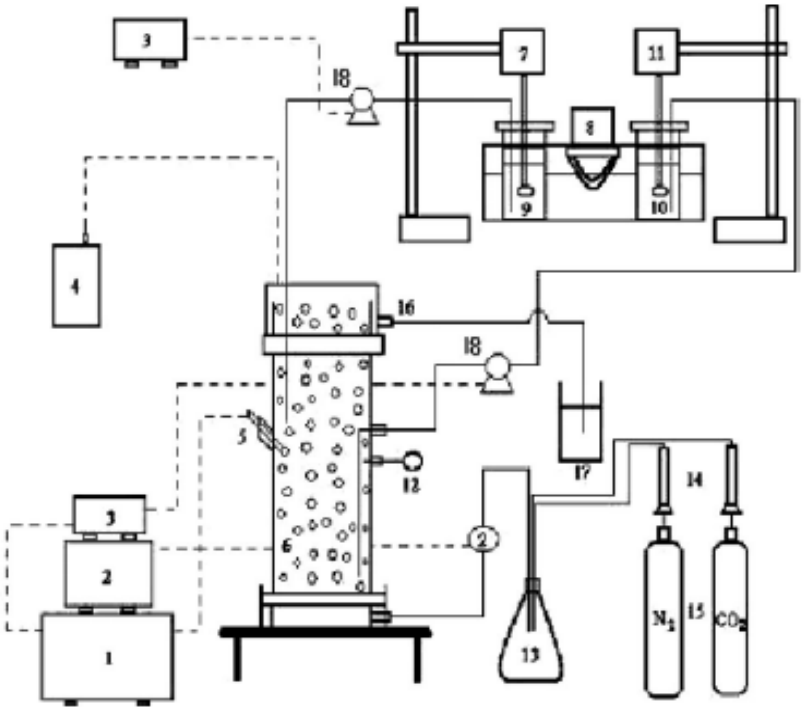

Figure 4.1. CO_2 bubble-column scrubber system schematic (Chen et al., 2008). Legend: 1, pH controller; 2, pressure gauge; 3, speed controller; 4, P_{CO2} meter; 5, pH electrode; 6, bubble column; 7, motor; 8, heater; 9, feed tank for $BaCl_2$ solution; 10, feed tank for NaOH solution; 11, motor; 12, digital temperature meter; 13, mixing bottle; 14, gas flow meters; 15, gas tanks; 16, outlet line; 17, storage tank; and 18, pump.

Packed bubble-columns

Packed bubble column scrubbers are a variation on regular bubble column scrubbers where the column is filled with solid packing material. This filling usually consists of small, specially shaped pieces that reduce the size of the bubbling gas, increasing surface area and thus the CO_2 absorption rate. There are two types of packing material: structured and random. Structured material is arranged to force liquid or gas to pass through the material in a specified manner while random packing is not arranged in any particular manner. Structured packing offers better efficiencies and lower pressure drops than random packing but is usually more expensive.

Spray bubble-columns

Spray column scrubbers are similar in design to bubble column scrubbers. Instead of bubbling gas up through a liquid phase, however, scrubbing solution is sprayed down through a gaseous phase. This design has a similar interface size as bubble column scrubbers. The advantage is that the pressure requirement is shifted from the gas inlet to the liquid inlet and less scrubber solution is required. However, while the transfer rate of CO_2 is similar, the total amount of CO_2 that can be absorbed by a spray system at one time is much smaller than that of bubble column scrubbers. Expensive atomizers are also often required to produce fine droplets to match the CO_2 absorption rate of bubble systems.

Methodology

CO_2 absorption column

The purpose of the CO_2 absorption column was to transfer the CO_2 from the biogas to a soluble form that could be fed to the algae, which would convert the CO_2

into sugars via photosynthesis. The CO_2 absorption column was 10 cm in diameter and 50 cm in height with a volume of 4 L. The column was constructed of PVC pipe, the base was a PVC toilet flange sealed onto one end of the pipe with PVC cement and caulking. The column was capped with a PVC cap, sealed with vacuum grease. The column was packed with 6 mm raschig rings to increase the contact surface area between the gas and the liquid. The column was airtight to prevent any biogas leaks.

The column (Figure 4.2) contained four ports: one near the bottom through which water is pumped out (Port 1), one just above port 1 through which biogas is bubbled into the tank (Port 2), one just below the water line through which water flows in (Port 3), and one at the top through which gas is collected (Port 4). The ports were drilled into the PVC column and tapped, then fitted with brass hose barbs. An airstone sparger was used to decrease the sizes of the biogas bubbles in the column; this improved the surface area to volume ratio of the bubbles, increasing exchange surface area between gas and liquid. The tank was connected to a reservoir of water, and a peristaltic pump (Cole Parmer Masterflex 5749-50) was used to cycle the water between the reservoir and the column. The total volume of water in the column and reservoir was 18 L.

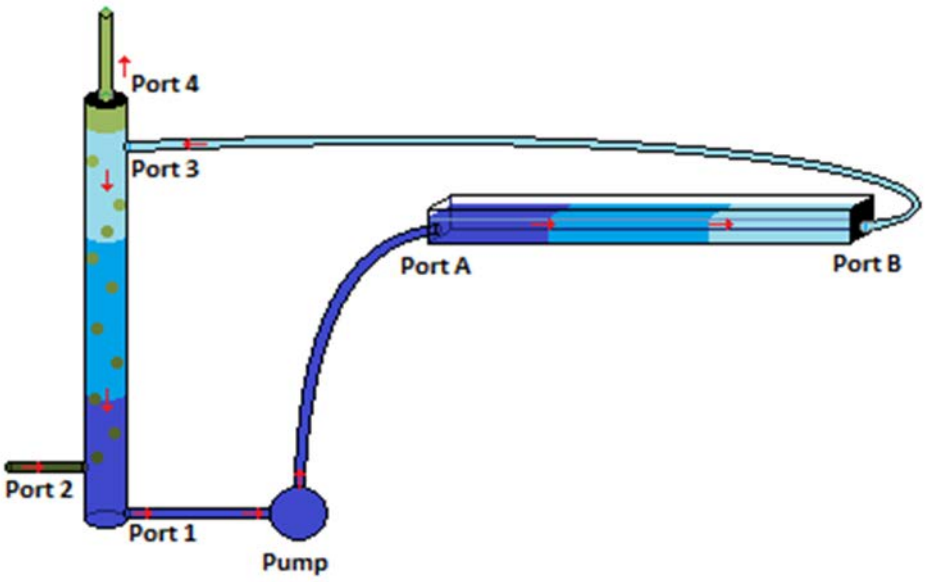

Figure 4.2. Diagram of biological CO_2 purification system. The red arrows indicate the direction of flow. The green bubbles are flowing upwards. The green represents biogas while the blue represents water, and darker colors indicate higher CO_2 concentration.

CO_2 bubble absorption column

The goal for the pilot study was to determine how much CO_2 could be removed by the CO_2 scrubber. Biogas was not yet available for the pilot studies, so a mixture of CO_2 and N_2 was used as synthetic biogas. N_2 is very stable and relatively insoluble in water, so it was used as a cost-effective substitute for the CH_4 in biogas. A mixture of roughly 45% CO_2 and 55% N_2 was used to test the system. This mixture was generated by using rotameters (McMaster-Carr) to regulate the flow rate of CO_2 and N_2 released from respective compressed gas tanks. The synthetic biogas was bubbled through the water from port 2, and the resulting gas was collected from port 4 and measured for its CO_2 concentration using a CO_2 meter (COZIR CM-0050). Water vapor initially caused fluctuations in CO_2 readings, so gas was run through a desiccator before the CO_2 meter.

pH testing

1 M sodium hydroxide (NaOH) solution was used to adjust the pH of the water. After adding the base into the water, the initial pH of the alkaline water was recorded. The alkaline water in the water reservoir was pumped into the absorption column; the alkaline water cycled between the reservoir and the column. The composition of the outlet gas stream was measured with the CO_2 meter every 30 sec, starting from 120 sec, so that the gas had enough time to travel through the column. The initial time, $t_{0,}$ was determined as the point in time when the gas was connected to the column. Trials were run for a total of 10 minutes. Afterwards, the final pH and CO_2 composition were recorded. The final CO_2 composition was determined by disconnecting the gas from the column and reconnecting it directly to the meter. This was done mainly to ensure that the synthetic biogas mixture composition stayed constant throughout the experiment.

CO_2 spray absorption column

The CO_2 bubble column required a large amount of pressure to force the gas to bubble up through the water column. The digester could not produce a sufficient pressure to accomplish this so the absorption column was redesigned. A spray column was used instead with a minimal water column (less than 5 cm). Alkaline aqueous solution was sprayed down from the top of the column onto the ceramic raschig ring packing. The spray nozzle used was FullJet 1/8GG-1.5. Gas was introduced from the bottom of the column through the air stone sparger below the water out port. This was later raised to above the water out port to prevent gas from escaping through the water out port. The water was set to flow through the column at a rate of 566 mL/min.

Testing

Trials were conducted similarly to those done on the bubble absorption column. The adjustments were as follows: 2 L of aqueous NaOH at pH 13 was placed in the reservoir. While the pump was turned off, gas was allowed to flow through the column for 10 min to replace the air in the column with the gas mixture. Rotameters were used to control the gas flow; N_2 output was set to 0.6 standard cubic feet per hour (scfh) and CO_2 output was set to 0.4 scfh. A y-connector was used to connect the N_2 and CO_2 exiting the rotameters. The single tube containing both gases was then connected to the "gas-in" port at the top of the column where it traveled down through the tube and was released into the column through a sparger. The water-out port was clamped to prevent gas from escaping before the water level rose above the out port level. The CO_2 meter and desiccator were attached to the "gas-out" port. The pump was then turned on and CO_2 levels were measured at 10 sec intervals for 5 min. The clamp was removed from the water-out port 30 sec after turning the pump on, allowing water to flow into the empty reservoir.

Results

Effect of pH on CO_2 absorption

When the pH was increased, the amount of CO_2 absorbed by the bubble column increased (Figure 4.3).

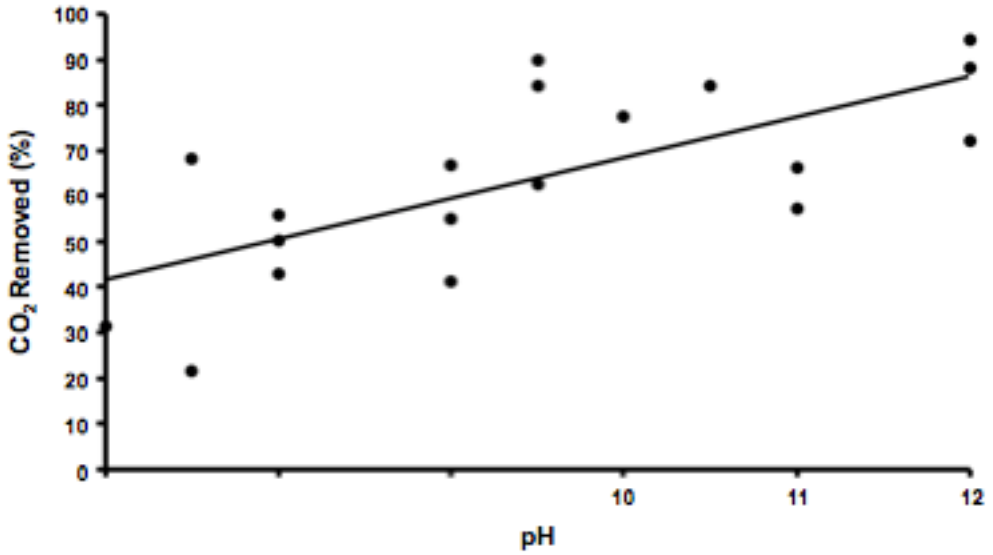

Figure 4.3. Effects of pH on percentage of CO_2 removal. pH was varied by adding various amounts of 1M NaOH. As the amount of NaOH added increased, the percentage of CO_2 removed from the CO_2/N_2 gas mixture also increased. A linear regression line had a $R^2 = 0.494$.

At pH 12, the average amount of CO_2 removed from the synthetic biogas when the water was partially saturated was 73%, corresponding to approximately 10% CO_2 remaining in the synthetic biogas. This corresponds to 3.4 mol of CO_2 removed from the synthetic biogas and a concentration of CO_2 in the water of 0.19 M (Appendix D). Lower pH did not remove as much CO_2, roughly correlating pH and CO_2 removal ($R^2 = 0.494$). A linear regression hypothesis test showed a p-value of $6.09*10^{-7}$ when comparing the slope to 0. This indicates a significant relationship between increasing pH and increasing CO_2 removal. The effect of pH on CO_2 removal was not tested on the spray absorption column due to time constraints. Instead, we assumed that a similar trend will be observed in the spray column as in the bubble column.

Spray column

Spraying of alkaline solution into the scrubber removed a majority of the CO_2 present, leaving the gas with a composition of 2% to 14% CO_2 when alkaline saline

solution (pH = 12.8 ± 0.1) was used and 6% to 16% CO_2 when alkaline fresh water solution was used (Table 4.1).

Table 4.1 pH and percentage of CO_2 remaining and removed from synthetic biogas by spraying with different solutions.

Solution	pH	Percentage CO_2 remaining	Percentage CO_2 removed
Alkaline saline	12.8 ± 0.1	8 ± 6	80 ± 10
Alkaline fresh water (low sparger)	13.2 ± 0.1	0.3 ± 0.3	98.8 ± 0.7
Alkaline fresh water (raised sparger)	12.65 ± 0.08	11 ± 5	75 ± 9

*All are shown as an average of the three trials conducted at each condition. The percentage of CO_2 was taken when the composition was relatively stable. The percentage of CO_2 remaining in gas is the percent by volume of CO_2 in the total volume of gas out, while the percentage removed from the gas is percentage that has been removed based on the initial composition, which varied slightly depending on the initial composition of the gas.

During the initial freshwater trials, gas was observed coming out the water out port. The sparger was moved above the level of the port to prevent this phenomenon. When no gas was escaping through the water out port, the percentage of CO_2 remaining in the gas increased. Figure 4.4 compares the CO_2 levels of the collected gas over time of the spray column with a low sparger, and the spray column with the raised sparger. When gas escaped out the water out port, the pump on the CO_2 meter generated a negative pressure above the water column in the CO_2 scrubber. This accounts for some of the artifacts observed in the data set collected with the lowered sparger.

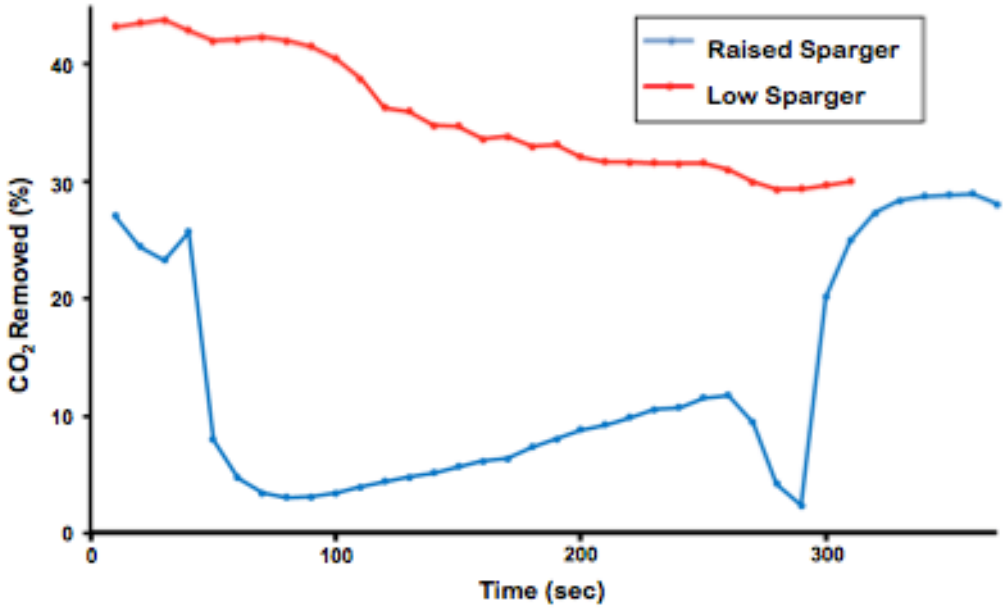

Figure 4.4 Percentage of CO_2 removed from synthetic biogas using the spray absorption column. Tap water is sprayed down while the sparger is below the water out port (low sparger) and raised above the water out port (raised sparger). The percentage of CO_2 removed was measured using a CO_2 meter (COZIR CM-0050).

Discussion

The final design of the CO_2 scrubber was a spray absorption column using alkaline media at pH 13. The scrubber was able to remove 75 ± 9% of the CO_2 from the 40% CO_2/N_2 gas mixture using freshwater solution and 80 ± 10% of the CO_2 using saline solution. On average, this left 8% CO_2 in the gas using a saline solution and 11% CO_2 using the freshwater solution. Using a saline solution this is within acceptable levels for natural gas (less than 10%) and using a freshwater solution, the CO_2 level remaining the gas is very close to acceptable levels. Some trials, however, had much higher levels of CO_2 remaining in the gas. Therefore, the pH of the solution was increased from pH 12, at which these tests were conducted, to pH 13. We assume that the trend of increasing CO_2 removal with increasing pH observed in the CO_2

bubble column applies to the spray column and continues to pH 13, thereby reducing the remaining levels of CO_2 to consistently less than 10%.

This pilot study, while promising, was done using a CO_2/N_2 artificial gas mixture and not actual biogas. Actual biogas contains CH_4 instead of N_2, and other trace gases that may affect absorption of the CO_2. The flow rates and pressures used in this study were also much higher than that produced by the anaerobic digester. Lower gas flow rates may result in higher removal of CO_2 as there is proportionally less gas flux than solution flux.

Chapter 5: Algae System

Introduction

Photosynthetic algae and few other autotrophic microorganisms metabolize CO_2 to produce sugars, which are used as a carbon and energy source for growth and a means to produce other compounds that can be used as biofuels (Weyer et al., 2010).

The equation for oxygenic photosynthesis is

$$2n\ CO_2 + 2n\ H_2O + photons \rightarrow 2\ (CH_2O)_n + 2n\ O_2 \qquad \text{Eqn. 7}$$

where light energy and water are required to convert CO_2 into sugars. Marine algae undergo a similar form of photosynthesis, where they take in HCO_3^- to obtain CO_2 for photosynthesis (Matsuda et al., 2001). Because CO_2 is readily available in biogas and photons are provided by sunlight, the algae require no additional starting compounds to perform photosynthesis. Therefore, photosynthesis provides a means to eliminate unwanted CO_2 and produce sugars without added cost.

Other microorganisms (i.e. purple and green sulfur bacteria) consume H_2S during metabolism and produce solid elemental sulfur (Biebl & Pfennig, 1977). The H_2S-consuming microorganisms can be used in a biological system to remove H_2S impurities from biogas; however, this was not tested in this study because it was beyond the scope of the experimental design.

The incorporation of algae in photobioreactors to purify biogas has several advantages over conventional chemical methods of CO_2 removal. Obtaining algae is relatively inexpensive because culturing algae requires minimal nutrients for their growth. Growth of the algae requires a light source as well, which does not

necessarily have to be expensive if illumination is provided by natural sunlight, which is not limited in supply. In addition, once the algae has performed its function and is considered “waste,” it can be harvested for more biofuels.

Photobioreactors are a new approach for the mass culture of algae with a variety of reactor designs. The helical design is advantageous because it typically has a higher surface area to volume ratio than other designs, reducing the maximum depth to which light must penetrate. A helical design also has the potential to be scaled up using multiple reactors in series (Xu et al., 2009). The light shines outwards from the inside of the helical tube coil to minimize the waste of light. High surface area-volume ratio and sufficient mixing must be maintained to maximize illumination in the photobioreactor (Ugwu, Aoyagi & Uchiyama, 2007; Jimenez, Cossio & Niell, 2003).

This section of the study is focused on designing and constructing a photobioreactor that would successfully facilitate the uptake of CO_2 through algal consumption using photosynthesis. What distinguished the helical photobioreactor design in this study from existing models were the methods of CO_2 addition and O_2 removal. The CO_2 was introduced into the photobioreactor as HCO_3^- rather than bubbling untreated biogas directly into the algal media. The photobioreactor contained a reservoir open to the atmosphere, where excess O_2 was removed. By separating out the CO_2 before removal from the photobioreactor, the potential hazard of a combustible mixture of CH_4 and O_2 was avoided.

This study tested the abilities of three different species of alga, *Phaeodactylum tricornutum, Botryococcus braunii,* and *Synechocystis* sp. PCC 6803

to fixate CO_2 via photosynthesis. These species were chosen for the study for various reasons. *P. tricornutum* is a well-known diatom with a short generation time, an ability to produce biofuel, and a capacity to uptake HCO_3^- as a form of dissolved CO_2 (Maheswari et al., 2005; Apt, Grossman, Kroth, 1996; Morais et al., 2009; Matsuda et al., 2001). *B. braunii* can produce large quantities of algal oil, a potential energy source (Metzger & Largeau, 2005). The *Synechocystis* sp. PCC 6803 was chosen because it was a readily available microorganism that addressed problems experienced during system testing. We hypothesized that both *B. braunii* and *P. tricornutum* would be able to thrive under high pH conditions and remove dissolved CO_2 from the media quickly and completely because they are both known to be robust and have relatively high growth rates.

Literature Review

Diatom *Phaeodactylum tricornutum*

Research in the area of carbon fixation revealed that diatoms, a major group of algae, were responsible for approximately 20% of global CO_2 fixation (Falkowski & Raven, 2007). The diatom *Phaeodactylum tricornutum* has a short generation time, a fully sequenced genome, and an ability to produce biofuel (Maheswari et al., 2005; Apt, Grossman, & Kroth, 1996; Morais et al., 2009). For these reasons, it has been selected as a microorganism of choice for our system.

Photosynthesis and Carbon Fixation

P. tricornutum performs photosynthesis, but the specific metabolic pathway remains relatively unknown. *P. tricornutum* contains the genes believed to be linked to both C_3 and C_4 photosynthesis (Valenzuela et al., 2012). Haimovich-Dayan et al. (2013) found that by using a process called RNA-interference to silence the gene

encoding pyruvate-orthophosphate dikinase (PPDK), an essential gene for the C_4 photosynthetic pathway, the rate of carbon fixation did not significantly decrease in *P. tricornutum*. As a result, despite lowered PPDK activity, the resultant similar photosynthetic rates provided evidence that an alternative photosynthetic pathway may be present in *P. tricornutum*. However, the researchers did note that silencing the PPDK gene could have activated alternative gene compensation mechanisms, thereby minimizing the effects of gene down-regulation on the photosynthetic rate (Haimovich-Dayan et al., 2013).

In a different study, *P. tricornutum* had been shown to activate multiple different carbon fixation pathways in situations, where nutrients like nitrates and phosphates were scarce. Valenzuela et al. (2012), demonstrated that when exogenous phosphates and nitrates were depleted, *P. tricornutum* genes associated with the C_3 photosynthetic pathway were not altered, but genes for the C_4 pathway were up-regulated. Along with up-expression of the C_4 pathway, different carbonic anhydrases were also up-regulated, and alternative pathways that use HCO_3^- became activated as well (Valenzuela et al., 2012).

Matsuda et al. (2001) evaluated such HCO_3^- alternative pathways for rates of HCO_3^- uptake by *P. tricornutum* in the form of dissolved CO_2 and evolution of O_2. Using artificial seawater with the addition of HCO_3^{--}, they cultivated *P. tricornutum* and evaluated the rates of photosynthesis. Through these experiments, Matsuda et al. (2001) found that the rate of O_2 evolution by *P. tricornutum* was higher than the rate of CO_2 formation. As a result, they concluded that HCO_3^- was readily taken up by *P. tricornutum* as a soluble substrate for photosynthesis. They also evaluated whether

changes in pH values and increasing concentrations of HCO_3^- would affect the growth of *P. tricornutum*, and they determined that no correlations existed between the effects of increasing pH and increasing the amount of HCO_3^- on growth rate (Matsuda, Matsuda, Hara, & Colman, 2001).

Growth Conditions

Preliminary literature review has revealed that copious amounts of research have already been conducted with regard to the optimal conditions required for growth of *P. tricornutum*.

Lighting

Mann and Meyers (1968) performed experiments in an effort to increase the rate of photosynthesis in *P. tricornutum*. In these experiments, strains of the diatom from the Indiana Culture Collection were grown in ASP-2 medium with slight adjustments under an optical system that consisted of two light beams with alternating intensities of light (Mann & Meyers, 1968). By varying the intensity of light and measuring the amount of O_2 produced, a positive linear relationship was observed between light intensity and the rate of carbon fixation. Other studies showed that the alternating light beam method produced the best results, with intensities varying between 4,000 and 5,500 lux (Yongmanitchai & Ward, 1992; Morais et al., 2009).

Temperature

Two prominent studies regarding *P. tricornutum* (Morais et al., 2009; Yongmanitchai & Ward, 1992) concluded optimal growth temperatures to be 21.5°C to 23.0°C and 18.0°C to 21.0°C, respectively. However, a study by Kviderova and Lukavsky (2003) revealed that the optimal temperature for growth of this diatom is between 15°C and 23°C. This iconic study used a simple but effective method called

crossed gradients to obtain these values. This method used agar with a thin layer of the diatom growing upon it; the agar was then provided with a temperature gradient in one direction and a light intensity gradient in the other direction. In this manner, all possible combinations of light intensity and temperature were evaluated for their direct effect on the growth rate of the diatom. The accuracy of these measurements has been supported through other studies on the link between light intensity and temperature. The light intensities that resulted in the most growth of the diatom, between 4,500 and 5,000 lux, were in accordance with the values used in studies by Yongimanitchai & Ward (1992) and Morais et al. (2009).

Glycerol

The landmark study performed by Morais et al. (2009) showed that the addition of glycerol, along with mixotrophic conditions, increased the growth rate of *P. tricornutum* by 30%. In these experiments, the cultures were obtained from Group Integrated Aquaculture UFPR in 2L Erlenmeyer flasks at temperatures between 18° and 21°C, at a light intensity of 5,500 lux. The dry mass was determined by extracting 150 mL of the sample and was separated into three samples. These samples were dried at 60°C and weighed. Guillard f/2 media was used; upon preparation, the media was cooled, and the glycerol was then added. Morais calculated a mathematical model for the velocity of growth for two groups; the control utilized an autotrophic medium and no glycerol while the experimental group contained glycerol and used a mixotrophic medium.

It is worth clarifying that autotrophic conditions involve the cells undergoing photosynthesis to perform vital functions, and heterotrophic conditions involve the cells already having the nutrients required in the absence of light. Under mixotrophic

conditions, both autotrophic and heterotrophic metabolisms were employed; both CO_2 and inorganic carbon were present in this method.

Production of fatty acids

A study by Yongmanitchai and Ward (1992) evaluated the production of Omega-3 fatty acids under different culture conditions. For their experiments, the researchers obtained cultures from the University of Texas (UTEX 640). Cultures were grown in 100 mL test tubes in Myers medium with a working volume of 75 mL (Mann & Meyers, 1968). The cultures were grown at 20°C and 4,000 lux with the aforementioned alternating light method. In order to determine the dry mass of the cultures, the diatoms were filtered through 0.8-µm filters, washed twice in saline solutions, and dried at 60°C. The lipids were extracted using the Bligh and Dyer (1959) and Holub and Skeaff (1987) methods. This study found that the growth of the fatty acids increased by 65% with the supplementation of vitamin B12.

Freshwater Algae *Botryococcus braunii*

Extensive research has been conducted on *B. braunii*, a freshwater green microalga, as a potential source of alternative energy. This is tied to its ability to produce hydrocarbons (Metzger & Largeau, 2005). Hydrocarbons can be implemented as a source of fuel. Because of its well-known growth conditions, its ability to fix CO_2, and its hydrocarbon-producing abilities, *B. braunii* was selected as a potential microorganism for the algal system.

*Photosynthesis and Carbon Fixation***.**

The specific photosynthetic pathway of *B. braunii* remains relatively unknown. However, it has been acknowledged that the majority of green algae perform C_3 photosynthesis (Xu et al., 2012). In the C_3 pathway, CO_2 is delivered

directly to RuBisCO, which uses the CO_2 to produce oxygen. Sydney et al. (2010) were able to quantify changes in the CO_2 fixation of *B. braunii* and other algal species in response to factors like nutrient consumption and metabolic changes. They cultivated *B. braunii* in 11 L *BioFlo* fermenters and after 15 days of cultivation discovered that the final biomass concentration reached 3.11 $g \cdot L^{-1}$ and a biomass doubling time of 2.9 days. They found the CO_2 fixation rate of *B. braunii* to be 496.98 $mg \cdot L^{-1}$ day^{-1}. It must be noted that in other literature sources, CO_2 fixation rates have reached upwards of 1100 $mg \cdot L^{-1}$ day^{-1}. Sydney et al. (2010) attribute this difference to different mediums and growth conditions used in cultivation of *B. braunii* along with the tendency of this particular algae to produce high amounts of hydrocarbons that can influence growth rate.

Growth conditions

Lighting

Literature review has shown that *B. braunii* cultures exposed to intense illumination, 10,000 lux, are able to attain biomass concentration of 7 $kg \cdot m^{-3}$ as compared to those exposed to lower irradiance levels, 3000 lux, which attained a concentration of 3 $kg \cdot m^{-3}$ (Banerjee et al., 2002; Kojima & Zhang, 1999). The algal biomass doubled under continuous 24-hour illumination rather than a 12-hour light and dark cycle. Continuous light also resulted in a four-time increase in the hydrocarbon concentration.

Temperature

A recent study conducted by Yoshimura, Okada, & Honda (2013) monitored the growth rate of *B. braunii* at different temperatures. They found that the algae could not grow at temperatures below 5°C and above 35°C. The doubling time was

the shortest, 1.4 days, at 30°C. Another study found that the optimal temperature for both hydrocarbon synthesis and growth was between 25 and 30°C (Banerjee et al., 2002).

CO_2 and pH

CO_2 plays a large role in *B. braunii* growth because the algae obtains a majority of its energy from carbon fixation. *B. braunii* can grow phototropically, mixotrophically, and heterotrophically (Tanoi, Kawachi, & Watanabe, 2011). Carbon sources can decrease the algae's doubling time from over a week to less than 2 days. Many studies have calculated the growth rate of *B.* braunii when it is exposed to different concentrations of CO_2. One study aerated the algae culture with 0.3% CO_2-enriched air (Banerjee et al., 2002). The algae exposed to CO_2 had a doubling time of 40 hours as opposed to the control, which had a doubling time of 6 days. Another notable study also tested the effects of different concentrations of CO_2 on the growth rate (Yoshimura, Okada, & Honda, 2013). This study found that a supply of CO_2 was necessary to maintain the growth rate. They found that a CO_2-enriched air concentration of between 0.2 and 5% was ideal. Growth decreased when the concentration was raised above 5% and stopped completely at a concentration of 50%. Chirac et al. (1985) found that air enriched with 1% CO_2 not only decreased the doubling time of the *B. braunii* culture to 2 days but also increased the hydrocarbon production five-fold. The addition of CO_2 to the culture decreased the pH. Addition of buffer was found to help stabilize the pH.

Hydrocarbon production

B. braunii is notable because of its ability to produce and store large amounts of hydrocarbons during its active growth phase (Metzger & Largeau, 2005). It uses

atmospheric CO_2 to produce long-chain hydrocarbons. Different strains of *B. braunii* have been shown to produce different types of hydrocarbons. Studies have found that hydrocarbons can comprise up to 75% of *B. braunii's* dry mass (Banerjee et al., 2002). Hydrocarbons can be extracted from the algal culture by pressing out or through solvent extraction. Once isolated from the algae, they can be used for energy by either being burnt directly or by being modified for use in engines.

***Cyanobacteria Synechocystis* sp. PCC 6803.**

The cyanobacteria, *Synechocystis* sp. PCC 6803 is a freshwater organism that is able to survive in a wide range of pH, temperature, UV light, and carbon dioxide concentrations. It can grow both phototrophically and heterotrophically, producing a high lipid concentration when it reaches its specific growth rate (Kim, Vannela, Zhou, & Rittmann, 2011). Lopo et al. (2012) conducted an experiment for which they cultured 2 mL of the cyanobacteria in 4.5 mL cuvettes covered with parafilm. They found that there was optimal growth at a temperature of 33°C and a light intensity of 40 $\mu E/m^2s$. Another study found that long-term exposure to temperatures of 22 or 44°C caused irreversible damage to *Synechocystis* sp. PCC 6803 (Sheng et al., 2011). Growth rate, biomass production, and nutrient utilization were reduced significantly. When used in a bench-scale photobioreactor, the specific growth rate reached a peak of 1.7 L/day (Kim, Vannela, Zhou, & Rittmann, 2011). In order to achieve maximum growth rates, *Synechocystis* sp. PCC 6803 was cultured in BG-11 media supplemented with phosphate (Zhang, Pakrasi, & Whitmarsh, 1994).

Both algae and cyanobacteria can produce high concentrations of lipids that can be turned into fuel. However, unlike algae, *Synechocystis* sp. PCC 6803 lipid growth is correlated with biomass production (Sheng, Vannela, & Rittmann, 2011).

Lipids are formed by growth of thylakoid membranes and occur without environmental stresses or added sugars. Additionally, cyanobacteria are easier to metabolically engineer for increasing lipid concentration because the entire genome sequence of *Synechocystis* sp. PCC 6803 is already known.

Photobioreactor

Photobioreactor designs

Algae have been commercially cultured for over 40 years (Xu et al., 2009). The first cultures were cultivated in open systems, such as ponds, which used sunlight for illumination. These ponds were often closed-loop channels that circulated algae cultures. Open-system cultures are inexpensive but are easily contaminated by competing organisms, which are detrimental to algal growth. Ponds also require a large area because of the one-sided illumination and have lower biomass productivity than closed systems.

Due to the various disadvantages of open systems, many different closed systems have been devised. Tubular photobioreactors circulate algae through transparent tubes via pumps or airlift systems. Airlifts can increase CO_2 and O_2 exchange in the algae and reduce cell damage compared to pumps but are harder to implement (Xu et al., 2009). Despite the mixing of algal cultures, algal growth may accumulate on inner walls of the tubes, restricting illumination (Ugwu, Aoyagi & Uchiyama, 2007).

Tubular photobioreactors

Tubular photobioreactors are particularly suitable for large-scale use. The reactor design is highly flexible and can maintain high surface-to-volume ratios for large reactor volumes. The diameter of the tubes is often limited to 0.1 m to maintain

a high surface-volume ratio and to maximize illumination (Jimenez, Cossio & Niell, 2003). The length of the tube also is restricted by the required circulation of the algae. Longer tubes allow O_2 to accumulate, inhibiting photosynthesis; O_2 concentrations over 35 mg/L are toxic to many algal species (Xu et al., 2009). In addition, CO_2 gradients may be established in long tubes, with high concentrations near gas entry and low concentrations near gas exit. This leads to pH gradients and insufficient CO_2 available for algal consumption at one end. Large-scale models may therefore require a series of several reactor units.

Helical photobioreactors

Helical photobioreactors are a subset of tubular bioreactors with the transparent tubing arranged in a vertical helical structure. The helix coils around an open circular space, forming either a cylindrical or cone shape (Singh & Sharma, 2012). Tube diameter and length are restricted by the same phenomenon in most tubular bioreactors. In addition, there is a high energy cost for pumps and airlifts when scaled up. However, in comparison with other types of photobioreactors, helical systems occupy a much smaller ground area and provide a more advantageous ratio between energy input and photosynthetic efficiency of algae (Singh & Sharma, 2012).

Flat plate photobioreactors

Flat plate photobioreactors are another common design and solve potential problems of O_2 buildup. Flat plate reactors are composed of many thin, transparent panels that are placed parallel to one another. Tubes that mix air with the cultures are placed at the bottom of the panels. The panels are exposed to light on either one or both sides and are often designed to change their positions in order to face the sun at optimal angles. Because the panels are thin, they have high surface area-to-volume

ratios and can be placed very close to one another, greatly reducing the area the system occupies. Unfortunately, like tubular bioreactors, algae may adhere to walls of the panels during growth, reducing illumination of the culture. The system is also particularly difficult to clean and maintain at a constant temperature.

Air-lift/bubble-column photobioreactors

Air-lift and bubble-column photobioreactors are vertical bioreactors that inject gas from the bottom of the bioreactor. In general, they are compact, inexpensive, and easy to use. Air-lift systems perform better than bubble columns on small scales because air-lift bioreactors have more consistent flow patterns that efficiently keep cells suspended and move cells between light and dark zones. However, size is limited by lighting since an increase in diameter of the column decreases the amount of light transmittance to the culture.

Lighting

Research by Bartual and Galvez (2002) studied the effect of light exposure patterns on the growth of the diatom *P. tricornutum*. Temperature was maintained at 17.5 ± 0.5 Cº. Fluorescent lamps were utilized to maintain the light intensity at saturating (150 μmol/m^2·s) and subsaturating (30 μmol/ m^2·s) levels. The optimal light intensity was also found to be 150 μmol/m^2·s. These conditions were determined to provide saturating levels of illumination. This was proven to not affect the metabolism of *P. tricornutum* due to the C_4 method of metabolism employed by this diatom, which allows it to dissipate excess light very effectively (Haimovich-Davan et al., 2012).

According to Qin (2005), the optimal light condition for *B. braunii* is an intensity of 60 W/m^2 with an exposure time of 12 h/day. Goldman and Carpenter

(1974) showed that the ideal light intensity for green algal growth was approximately 50 W/m^2. A study conducted by Ge, Liu and Tian (2011) cultured *B. braunii* in a photobioreactor using continuous cool white fluorescent light at 150 $\mu mol/m^2 \cdot s$.

Methodology

Preliminary tests were conducted to determine if algae would survive in environments similar to that of the designed photobioreactor. The algae must be able to endure high pH and HCO_3^- concentrations because CO_2 is fed into the photobioreactor through an alkaline aqueous solution. The general growth rates of *P. tricornutum* and *B. braunii* were found as well to serve as a baseline for the photobioreactor experiment. Because the *Synechocystis* sp. PCC 6803 was added into the experimental methods after the component pilot studies had concluded, there were no preliminary experiments done on the cyanobacterium.

Algal growth of *P. tricornutum*

The first algal species tested was *P. tricornutum*, a salt-water diatom. The stock culture was obtained from Dr. Ganesh Sriram's lab at the University of Maryland. *P. tricornutum* was cultured at 25°C, which is roughly room temperature. Because *P. tricornutum* is a marine species, the proper salinity was maintained to ensure optimal growth. *P. tricornutum* was cultured in a modified f/2 medium containing trace metal compounds, vitamin solution, and Instant Ocean (Appendix E).

P. tricornutum was initially cultured in 250 mL flasks on a small shaker with light exposure provided by low-wattage lamps. Once cultures reached a higher concentration with an optical density of 0.500 at a wavelength of 600 nm, they were transferred into a large tank. The tank was placed on a laboratory rocker that laterally

tipped periodically to mix the cultures. Twice a week, 1 L of culture was removed and was replaced by 1 L of fresh modified f/2 medium to regulate growth and volume of the culture. Two low-wattage lamps provided an adequate supply of light for our system. Twice a week, pH and concentration of the species were measured. pH was measured with triple pad pH strips. Optical density was measured using a spectrophotometer (Pharmacia Biotech Ultrospec 2000). To convert optical density into a concentration, a Beer's law plot was constructed. Volumes of 5, 10, 15, 20, and 25 mL of the algal cultures were transferred to 50 mL conical tubes. The tubes were then centrifuged for 5 minutes at 1000 rpm. After the supernatant was removed, the algae was incubated and dried. The dry weight was then measured, and the cultures were resuspended in 5 mL of media. Optical density was then measured for these resuspended cultures.

The optical density concentrations, measured at a wavelength of 600 nm, were plotted against concentration in g/mL. From this Beer's law plot, optical density measurements could be converted to a concentration by dividing absorbance values by the slope of the Beer's law plot. A Beer law's plot was only constructed for *P. tricornutum*. Due to faulty equipment and measurement issues a Beer's law plot was unable to be constructed for *B. braunii*. Despite establishing a growth standard for *P. tricornutum*, doubling time and growth rate for *P. tricornutum* proved to be difficult to determine based on unexpected growth fluctuations.

Alternative mixing techniques for *P. tricornutum*

It is worth noting that due to size limitations, the rocker would not serve as an adequate stirring mechanism on an industrial scale. Our experiments attempted to evaluate alternative stirring mechanisms while also testing the robustness of our algae

under various growth conditions. An alternative system used to test the algae was composed of a smaller tank with a built-in light-emitting diode (LED) light. A water pump was used as the method for stirring. 2 L of *P. tricornutum* was cultured in this smaller tank. Once a week, 1 L of culture was removed and replaced by 1 L of fresh modified f/2 medium. pH and concentration of the species were measured twice a week. A lower pressure cascade filter was also tested. This filter mixed the system by drawing water from the bottom of the tank and cascading it onto the culture from the top. The same methods as above were used to grow the algae. Qualitative observations were used to determine whether these mixing methods were feasible options in the construction of the algal system.

Bacterial growth prevention in *P. tricornutum* cultures

To avoid bacterial growth in our cultures, antibiotics were added to the system. Penicillin and ampicillin were the antibiotics of choice due to their generalized effects on various bacteria that could be harmful to our system. 1 µL of antibiotics was added per mL of culture.

Addition of bicarbonate to *P. tricornutum*

Before exposing our species to biogas, the effect of HCO_3^- on the species was tested to see how the algae would grow under different CO_2 concentrations. Three experimental groups and one control group, all of which contained 50 mL of algae submersed in 500 mL of f/2 medium, were set up. The control flask did not contain any sodium bicarbonate ($NaHCO_3$). The first group contained 1.175 g of $NaHCO_3$, which represented the maximum amount of CO_2 that the species would receive. This amount was based on the initial estimation that our anaerobic digester would produce roughly 5 L of biogas per day at a composition of 50% CO_2 (Appendix G). It was not

determined until after this experiment that the actual CO_2 percentage in our biogas was lower. The second group contained half the maximum amount (0.5875 g $NaHCO_3$) while the last group contained a quarter of the maximum amount (0.2938 g $NaHCO_3$). The four flasks were placed in an incubator at 25^oC and a shaker at 60 rpm. The algae samples received illumination from four 60-W lamps that were placed above the flasks inside the incubator. The pH and concentration were measured three times a week. Due to the variability of optical density for different samples of the same experimental group, three concentration measurements were taken for each of the four flasks at a wavelength of 600 nm. In addition, to avoid extraneous variables, the positions of the flasks within the incubator were rotated with respect to the light sources three times a week.

Algal growth of *B. braunii*

B. braunii was chosen for its high carbon fixation rate and its production of hydrocarbons. It is also a freshwater algae, so salinity would not play a role in its growth. *B. braunii* was cultured at room temperature in a Chu-13 medium (Appendix F), which required a nitrogen source in the form of potassium nitrate and trace amounts of other nutrients. The culture was grown in an incubator at approximately 60 rpm with light exposure provided by 4 60-watt lamps. The cultures were initially kept in large Erlenmeyer flasks; once cultures reached a high concentration, they were then transferred to a large tank. Approximately 3 times a week, 1 L of fresh media was added to the large tank. Optical density was measured using a spectrophotometer (Ultrospec 2000) and pH was taken with triple pad pH strips.

Bacterial growth prevention in *B. braunii* cultures

In contrast with *P. tricornutum* cultures, *B. braunii* cultures were not administered antibiotics because they did not have a history of contamination.

Addition of bicarbonate to *B. braunii*

$NaHCO_3$ was added in four different quantities to test the effects on pH and growth rate. The procedure mirrored that used for the $NaHCO_3$ experiments with *P. tricornutum*. However, while the *P. tricornutum* experiments only involved addition of $NaHCO_3$ all at once, a dripping method was also evaluated when testing *B. braunii*. $NaHCO_3$ was dripped in using a separatory funnel at a rate of approximately 1 mL every 8 seconds. The optimal flow rate was obtained by testing the effects of different flow rates and concentrations on the algal growth rate. It is important to note that no more than 6.72 g of $NaHCO_3$ was added per day. Measurements of pH and optical density were taken every day. Because the drip method introduced a dilution factor through the additions of $NaHCO_3$ solution, as opposed to the batch method that introduced solid $NaHCO_3$, only the total growth of the cultures under the drip method were adjusted.

Addition of NaOH to *B. braunii*

After the optimal $NaHCO_3$ concentration was identified, NaOH solutions were added to the algal solutions to study the growth rate at a pH level of 12. In this experiment, 1.25 mL of 1M NaOH was added to 125 mL of water and 1.25 mL of Chu-13 media to make a pH 12 NaOH solution. 125 mL of each NaOH solution was then added to a separatory funnel, and solution was dripped into the algal culture at an average rate of 1 drop every 10 seconds. Optical density and pH measurements were taken before and after addition of NaOH.

Photobioreactor

Set-up

Before construction, all necessary parts were surface sterilized with 70% ethanol and autoclaved water. Clear PVC tubing with a diameter of 1.9 cm was used for construction of the helical photobioreactor. The tubing was approximately 45.7 m in length and was coiled into a helical shape with a 27.9 cm diameter, rising to a height of 1.12 m. This shape was secured using zip-ties and a wooden support structure. Both ends of the photobioreactor were equipped with a ball valve to control flow. A diaphragm pump (Flojet 4YD41) connected a reservoir to the bottom of the photobioreactor, pumping the culture from the reservoir to the bioreactor at a rate of 0.00022 m^3/s . The top of the bioreactor was connected to the reservoir, allowing the algal culture to recycle back to the reservoir after flowing upwards through the coil. Four light fixtures (Spectralux 901618) were centered in the space inside the helical coil and provided light for the algal culture. CO_2 laden water from the CO_2 scrubber entered the photobioreactor through the reservoir. The top port of the reservoir connected to the recycling system.

Pilot study

Before the final design was implemented, a similar photobioreactor was tested using tubing with a diameter of 3.8 cm coiled around a diameter of 35.56 cm and a pump rate of 1 L/min.

Once the photobioreactor was set up, f/2 media for the *B. braunii* algal culture was pumped into the reservoir to fill the reactor. Composition of the media can be found in Appendix B. Sterilized water was used as the solvent, and air bubbles were minimized in the reactor. A culture of *B. braunii* was fed into the photobioreactor. *B.*

braunii was used because large volumes had been cultured. Qualitative observations were taken to see how the algae would grow and to make sure the light intensity was appropriate. The original plan was to also test how *P. tricornutum* would grow in the pilot photobioreactor design, but it was not completed due to time constraints.

Light intensity study

To determine the amount of light that would dissipate into photobioreactor, a photometer (LiCor LI-185B) was held about 10.16 cm away from the light fixtures (Spectralux 901618). It was important to determine the light intensity of the fluorescent lights because it contributes to algal growth. Six trials were conducted in which the light intensity was measured in lux. Multiple trials were completed to represent the different photometer readings taken at the various points along the circumference of the photobioreactor. This was done to mimic the variation in the distances of the tubing from the light fixture because the light fixtures were not exactly in the center of the structure. The light intensity of the photobioreactor lights was then compared to that of sunlight.

Results

Algae

Standard growth conditions

The growths of *P. tricornutum* and *B. braunii* under optimal growth conditions were investigated through measurements of optical density. *P. tricornutum* was grown in f/2 medium, and *B. braunii* was grown in Chu-13 medium under a 24-hour light cycle.

Fluctuations in the optical density of *P. tricornutum* were observed over a 48-day period of monitoring growth rate. During this period of time, 1 L of fresh media

was added to the cultures three times a week, along with the removal of 1 L of algae. To account for this dilution of the culture, total growth, total relative growth, and relative concentration were calculated. Optical density measurements over the 48-day period were adjusted by the dilution factor to determine total growth, which indicates the expected optical density values had the cultures not been diluted. The total growth was then normalized to the first optical density measurement to determine values for total relative growth. Optical density measurements were subsequently converted into concentrations through the use of a standard Beer's law plot of absorbance (OD600) against concentration (g/mL) (Figure 5.1).

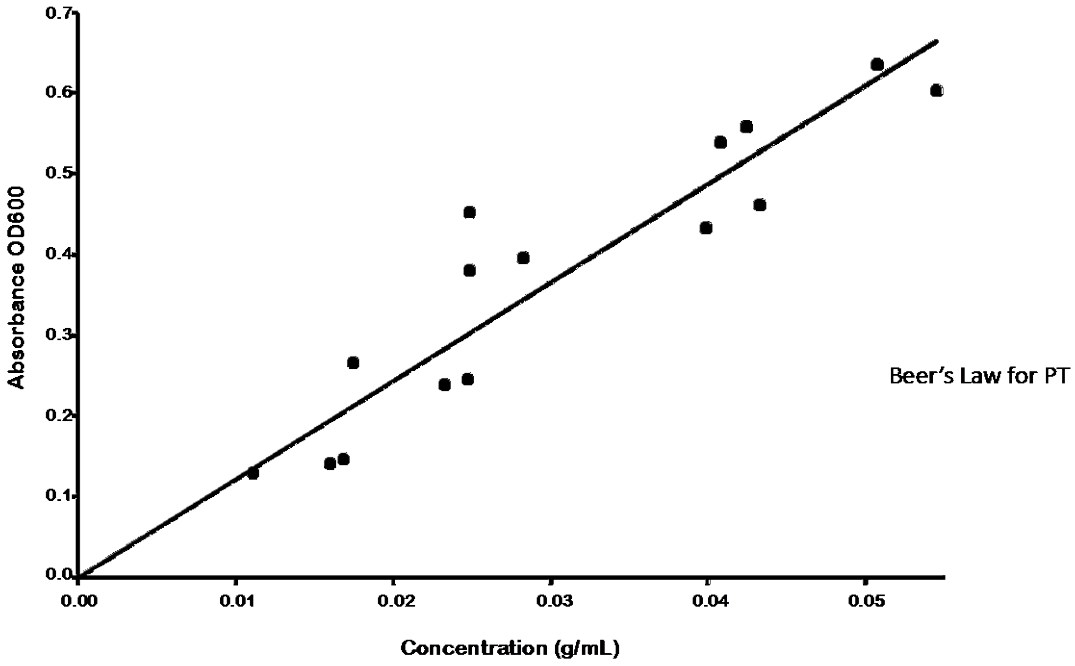

Figure 5.1. Beer's Law Standard Plot for the growth of *P. tricornutum*. Concentrations were determined through dry weight measurements prepared from various volumes of an algal culture of *P. tricornutum* and absorbance was measured for the re-suspended pellets in f/2 media. Each point represents the average of 3 optical density for one re-suspended pellet. A linear regression fit had a R^2 value of 0.8545 and a slope of 24.365. This is used to convert absorbance values to concentrations for *P. tricornutum*.

Relative concentration was determined by multiplying the concentration by its respective dilution factors. Initially, over the first week, *P. tricornutum* maintained a steady growth at a concentration of around 0.2 g/mL. However, after the first week, the concentration decreased significantly to approximately 0.05 g/mL and only reached a relative maximum of 0.175 g/mL over the next 20 days of study. However, from day 40 to 48, the growth increased substantially from a relatively stagnant concentration of 0.142 g/mL to 0.750 g/mL by the end of the study (Figure 5.2).

Optical density was also measured and recorded for *B. braunii* over a 15-day period of growth. During this period of time, 250 mL was removed from each of the four flasks and replaced with 250 mL of fresh media three times a week. Similar to *P. tricornutum*, the dilution factors were taken into account in the adjustment of the optical density measurements and subsequent normalization of the total growth to determine a total relative growth for *B. braunii*. *B. braunii* reached a maximum relative total growth of 6.178. pH remained mostly constant between 8.25 and 9.5.

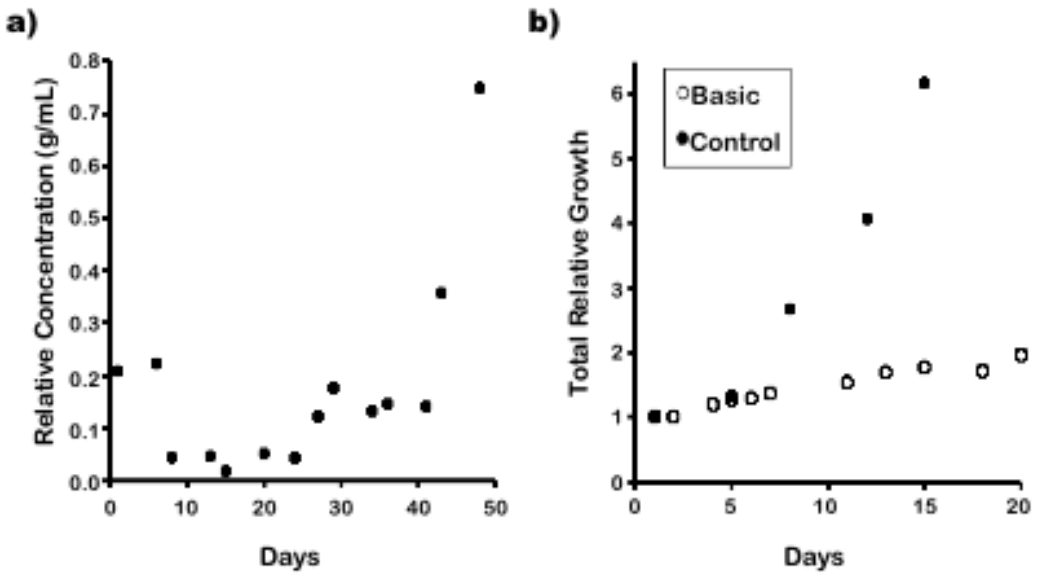

*Figure 5.2***.** Relative growth of *Phaeodactylum tricornutum* and *Botrycoccus braunii* under optimum pH conditions. (A) *P. tricornutum* was grown in f/2 media over a period of 48 days. Relative concentration was determined by standardizing absorbance at OD 600 to Beer's law plot (Figure 5.1). (B) *B. braunii* was grown in Chu-13 media over the period of twenty days. Total relative growth of *B. braunii* exposed to pH 12 NaOH solution (white) and total relative growth of *B. braunii* grown at its optimum pH of 7 (black) was measured. Each point represents the average of 3 optical density measurements.

Carbon feeding

The effects of $NaHCO_3$, the algae's primary source of carbon, on the growth of *P. tricornutum* and *B. braunii* were investigated by varying the concentrations of $NaHCO_3$ based on initial measurements of biogas production from the anaerobic digester. Corresponding concentrations were added to different cultures to represent the full amount, half of the amount, and a quarter of the amount of CO_2 that the algae would be exposed to in an ideal system. The results for *P. tricornutum* are presented in Figure 5.3

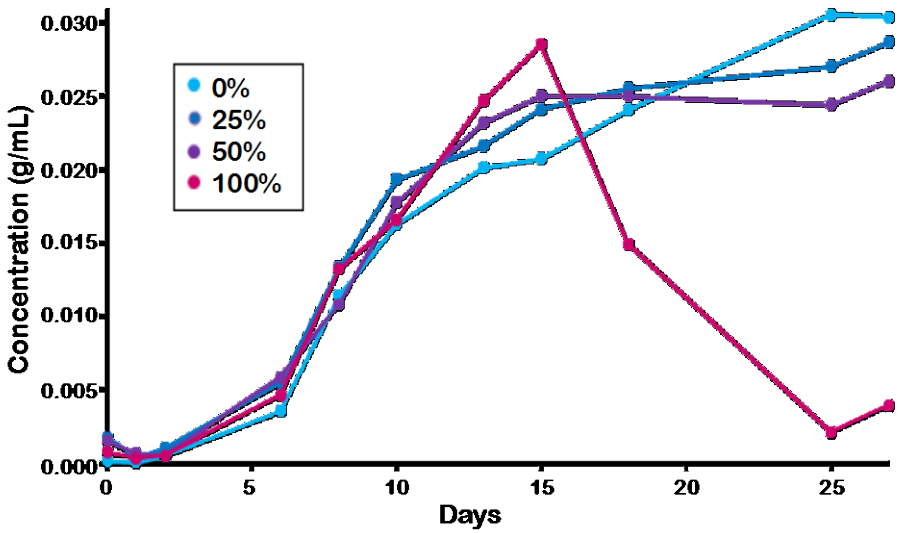

Figure 5.3. Effects of different $NaHCO_3$ concentrations on the growth of *Phaeodactylum tricornutum*. Growth concentrations of four cultures of *P. tricornutum*, grown in f/2 media, were measured. Cultures were given concentrations of $NaHCO_3$ that mimicked concentration of CO_2 produced from anaerobic digester (See Appendix). Absorbance at OD600 was measured for cultures and standardized to concentrations using the Beer's Law Plot (Figure 5.1).

$NaHCO_3$ had a minimal effect on the growth of *P. tricornutum*. At a full strength concentration of $NaHCO_3$, the maximal optical density differed from the control culture by a concentration of 0.1 g/mL. However, after 15 days, the optical density of the culture with a full strength concentration of $NaHCO_3$ dropped severely from a concentration around 0.03 g/mL to close to 0 g/mL. This drop in concentration was attributed to contamination, which caused the algae to die off completely. Contamination did not impact the other cultures.

Different methods of $NaHCO_3$ administration were evaluated within this study. For *B. braunii*, the effects of $NaHCO_3$ on growth rate were evaluated based on both a full batch and dripping method. In the full batch method, concentrations of $NaHCO_3$ were administered to the algae directly at the start, whereas the dripping method administered $NaHCO_3$ drop-wise at a rate of 36-45 ml/hr, each drop was predicted to be about 0.05 mL. The results of the batch method and dripping method

are presented in Figure 5.4.

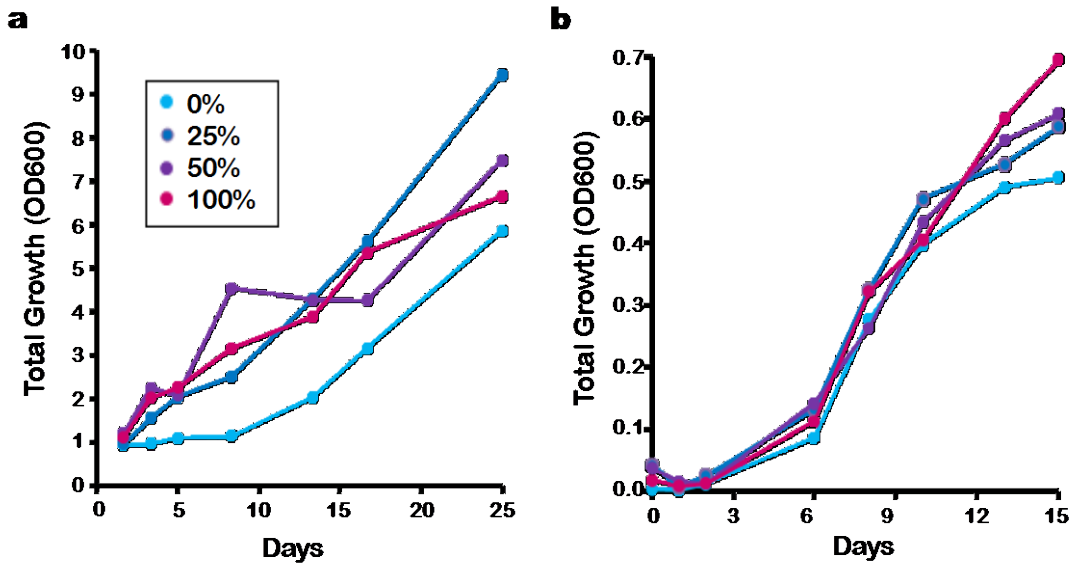

Figure 5.4. Effects of different $NaHCO_3$ concentrations on growth of *Botrycoccus braunii* when administered under (a) drip method and (b) batch method. *B. braunii* was grown in Chu-13 media and $NaHCO_3$ additions to cultures mimicked concentration of CO_2 produced by the anaerobic digester (See Appendix). Drip method consisted of dripping 125 mL of dissolved $NaHCO_3$ in water at a rate of 36-45 ml/hr into cultures. Batch method consisted of adding corresponding concentrations of solid $NaHCO_3$ at the start of the experiment. Each point represents the average of 3 optical density measurements.

A significant increase in growth rate was observed when $NaHCO_3$ was administered at higher concentrations to *B. braunii*. Maximum growth of *B. braunii* was observed under full strength conditions, where high concentrations of $NaHCO_3$ were administered to the algae. There was a significant increase in overall growth of *B. braunii* when $NaHCO_3$ was administered through the dripping method as opposed to the batch method. At a full strength concentration of $NaHCO_3$, the maximum concentration of *B. braunii* in the dripping method reached a total relative growth of about 10, while in the batch method the total relative growth reached 0.7. The significant difference in values between the dripping method and batch method can be attributed partially to the dilution factor, which only affected the dripping method

cultures. As a result, the batch culture growth was not exposed to an increased maximum carrying capacity for growth because $NaHCO_3$ was added only as a batch at the start of the experiment. The dripping method cultures were exposed to increasing amounts of $NaHCO_3$ over the course of the study.

pH Buffering Capacity

The effects of addition of highly alkaline aqueous solution on the growth of *B. braunii* were investigated by exposing the cultures to NaOH pH 12 solution. The total relative growth remained steady from about 1 to 1.963 and the pH remained fairly uniform between 8.25 to 9.5. However, a large deviation existed between the growth of *B. braunii* at its optimum pH in comparison with its growth when exposed to pH 12 solution. The maximum total relative growth was around 6 at the optimum pH and a maximum total relative growth of 2 for the cultures with the addition of the alkaline solution (Figure 5.2).

Photobioreactor

Pilot study

The study reveals many problems with the photobioreactor design. *B. braunii* formed large clumps and adhered to the walls of the tubing, causing the fluid running through the photobioreactor to become clear. The aggregations of algae on the walls reduced the illumination of the culture and prevented proper growth. Additionally, the diaphragm pump failed after 3 days.

Light intensity study

Table 5.1. Light flux of the photobioreactor lights was measured approximately 10.16 cm from the light.

Trials	Lux
1	1600
2	1250
3	1500
4	1600
5	1400
6	1300
Average	*1442 ± 149.7*

Light intensity 10.16 cm from the light fixtures was about 1442 lux. This intensity is the average intensity that the tubing of the photobioreactor is exposed to. Sunlight has a light intensity of 18500 lux. The lights in the photobioreactor have an intensity that is only 7.8% of that of sunlight.

Discussion

Based on initial studies of algal growth under various conditions, *B. braunii* showed a slightly steadier and more consistent growth than *P. tricornutum*. As a result, *B. braunii* was initially chosen for addition into the helical photobioreactor system. However, unforeseen problems arose when the algae was grown in the helical photobioreactor. Fouling, a process characterized by aggregating algae on material surfaces, occurred on the interior of the tubes of the photobioreactor. Adherence of *B. braunii* to the tubing may have been caused by the lack of turbulence and flow in the reactor as well as visible kinks in the tubing that created an impediment to flow. In general, *B. braunii* may also have been more naturally susceptible for adherence. Other problems associated with this were low light transmittance into the photobioreactor due to the thick density of the algae and an inability to measure the growth concentrations due to the algae aggregating on the bottom of the tubes rather than being suspended in solution. In order to ameliorate these issues, the diameter of

the PVC tubing was decreased in order to increase the velocity of the flow inside the reactor and improve mixing. The type of tubing, PVC, was kept the same in the final design due to limitations in budget. A new pump was used with a faster flow rate. *B. braunii* was replaced by *P. tricornutum* in the updated design to see if another species would not aggregate or stick to the tubing walls.

Hypothetically, the change from *B. braunii* to *P. tricornutum* and systematic changes would rectify the issues faced when *B. braunii* was introduced into the helical photobioreactor. *P. tricornutum* was not known to aggregate and stick to material surfaces, and changes in the pump velocity and tubing size would have increased the turbulence within the photobioreactor.

Although *B. braunii* was chosen for the initial tests of the helical photobioreactor, pilot studies indicated that growth was fairly similar between *P. tricornutum* and *B. braunii*.

The data from the pilot studies indicated that both species of algae had the capacity to survive and thrive in the presence of high concentrations of HCO_3^-. The HCO_3^- studies determined the threshold of algal survival in the presence of CO_2. These experiments also introduced a potential method to evaluate the metabolic capacities of the algae through the association of algal growth and the rate of CO_2 consumption. Generally, algal species are able to metabolize HCO_3^- to produce sugars that typically increase the growth of the algae. Based on the initial assumption that the projected system design would produce about 5 L/day of biogas, the corresponding amount of CO_2 was calculated and dispensed to both *P. tricornutum* and *B. braunii* in the form of HCO_3^- at a full concentration, half concentration, and

quarter concentration. Both species grew best when exposed to a full concentration of $NaHCO_3^-$. Over 15 days, the full strength culture of *P. tricornutum* reached a concentration of 0.3 g/mL. In comparison, the control group with no HCO_3^- only reached a concentration of 0.2 g/mL on day 15. *B. braunii* was tested with $NaHCO_3^-$ with both a dripping method and batch method of addition. At a full concentration, the total growth of *B. braunii* under the dripping method had roughly a 10 times greater increase in total growth than that of the batch method, though this difference is partially influenced by the dilution of the culture using the drip method, which continuously increased the carrying capacity of the culture. Despite the difference in methods, the *B. braunii* had a higher relative growth when exposed to the full concentration of $NaHCO_3^-$ as opposed to its control group. In addition, *B. braunii* demonstrated the aptitude to grow when exposed to highly alkaline solutions. The pH trials determined that *B. braunii* had the buffering capacity to handle additions of high alkaline solutions. *B. braunii* maintained a steady pH of between 8.25 and 9.5. In addition, its growth remained fairly steady with a total relative growth from 1 to 1.963 over the 20-day study period. Thus, from the results of the pilot studies, the problems in growing *B. braunii* in the photobioreactor were largely unexpected.

These growth issues led to several limitations in the assessment of the two algal species. Due to the inability to successfully measure growth of *B. braunii* in the photobioreactor, the algae's direct metabolism of HCO_3^- was not directly tested. From the results of the HCO_3^- studies, the growth of the algae suggested that both *B. braunii* and *P. tricornutum* were able to metabolize the HCO_3^-. In addition, the buffering capacity of *P. tricornutum* to maintain growth when exposed to highly

alkaline solutions was not evaluated. Due to time constraints, *P. tricornutum* was not tested in the photobioreactor under system testing conditions prior to the actual testing of the system.

Chapter 6: Water Recycling

Introduction

In order to increase the sustainability and cost-efficiency of the system, the water used in the CO_2 scrubber and photobioreactor was recycled. The residual algae needed to be filtered out of the recycled water before it could be reused in the CO_2 removal system. Two methods of filtration were considered for the water recycling column, membrane filtration and sand filtration. We hypothesized that our custom-built water recycling system would effectively filter out algae, yielding water that could be returned back to the CO_2 scrubber and reused for multiple cycles.

Literature Review

Membrane filtration

One method of removing algae from water is membrane filtration. This method involves a pressure-driven flow through a semipermeable membrane that traps impurities. A study by Lateef, Soh, and Kimura (2013) showed that direct membrane filtration could be used in wastewater treatment as it effectively removed 75% of organic matter in wastewater. The membrane can also be cleaned with sodium hypochlorite (NaOCl) or citric acid (Lateef, Soh & Kimura, 2013).

Sand filtration

Sand filtration can be divided into slow sand filtration (SSF) and rapid sand filtration (RSF). SSF uses a biofilm that forms on the surface of the sand bed to decompose organic materials. SSF systems can have flow rates between 0.1 and 0.2 m^3/hour and is typically used in the biofiltration industry. On the other hand, RSF functions either by trapping passing particles in spaces between sand particles or

through the adherence of passing particles to sand particles. The sand used in RSF can be cleaned by generating a backflow of water through the filter. RSF usually handles flow rates between 5 and 30 m^3/hour and will remove solids larger than 0.35 mm in diameter (Bar-Zeev et al., 2012). SSF was selected for this project due to its simplicity, microorganism size, and low energy consumption and operating costs.

Methodology

A sand filtration method was used to remove the algal species in the water coming from the algae tank. Initial preliminary studies were conducted using a 2-L plastic bottle that was cut at approximately 15 cm from the bottom. These studies were conducted as a proof of concept before moving on to a final filtration column design. The final filtration column was constructed, using PVC piping with a diameter of 10.2 cm and a height of 76.2 cm. The interior of the column consisted of a 15.2-cm layer of fine sand with a 2.5-cm layer of gravel above and below the sand for packing (See Figure 6.1).

Figure 6.1 Diagram of water recycling column. The recycling column was constructed with a PVC column filled with layers of fine sand and gravel. Black gardening filters were placed between each layer, separating the sand and gravel. *B. braunii* algal solution entered the column from an opening at the top, and algae was filtered out as the solution passed down the column. Algae-free water exited through an outlet at the bottom of the column and returned to the CO2 scrubbing column for reuse.

The sand and gravel layers were separated by filter fabric to prevent mixing between the layers. The water from the algae tank was fed through the top of the filtration column and was then allowed to flow through an opening at the bottom of the column. Microbial species in the water typically accumulate at the top of the sand layer, allowing for convenient cleaning of the column by replacing the upper portion of the sand layer.

To test the effectiveness of our system in filtering out the algae, the optical density of the outlet water from the filtration system was measured, and these measurements were compared with those of a 5-L feed of algae-laden inlet water. The flow rate through the filtration column was also determined as a function of the volume of liquid feed.

Results

Initial trials conducted for proof of concept showed that the algae appeared to accumulate on top of the sand layer. Optical density measurements taken after adding 5 L of algae-laden water are shown in Table 6.1 below. The effect of the volume of liquid feed on the flow rate through the column can be seen in Figure 6.2 below.

Table 6.1. Optical density measurements for sand filtration column.

Trial	Optical Density before filtration	Optical Density after filtration
1	0.435	0.000
2	0.443	0.001
3	0.445	0.000

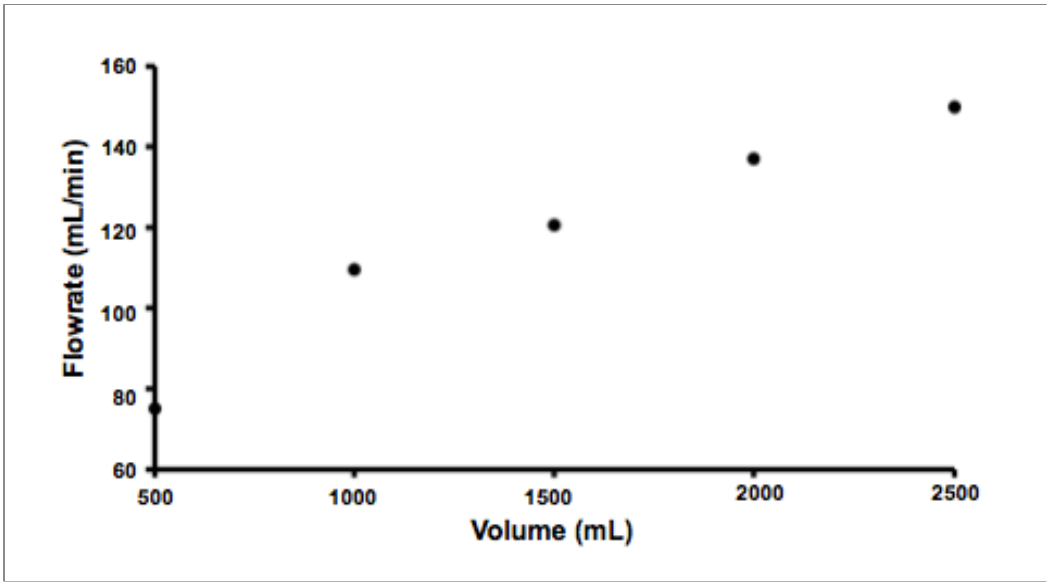

Figure 6.2. The rate of filtration of the sand filter. *B. braunii* algal solution was used to test the filtration rate.

Discussion

The sand filtration method using layers of gravel and fine sand succeeded in eliminating the algae from water. The outlet flow rate and input volume of. inlet feed

had a positive, near-linear relationship (See Figure 6.2). The measurements of flow rate and inlet feed were used to ensure that the filtration column would not flood with increases in the flow rate of our overall system. One problem encountered was that the filter fabric, separating the layers of gravel and sand, had a tendency to stretch, increasing the pore size. This allowed sand to leave the column outlet and possibly contaminate the filtered water returning to the CO_2 column. In addition, the sand used in the filtration column required extensive washing in order to remove smaller grains that could potentially pass through the pores of the filter fabric.

To address some of these issues, several aspects of the column can be adjusted to provide more effective filtration. One of these aspects involves decreasing the average grain size of the sand to trap a greater range of particles and contaminants within the sand layer. In accordance with this change, the pore size of the filter fabric that separates the gravel and sand layers can be reduced to prevent small sand particulates from escaping into the recycled water. Lastly, a transparent material can be used to construct the column to more clearly discern when replacement of the sand layer is required.

Chapter 7: Component Studies Conclusion

After testing each system component separately, several modifications were made to the original designs. The final working models for each component after these modifications are as follows. The biogas generator was an 18.9 L anaerobic digester maintained at 32°C by heating blankets. The culture was inoculated with manure and fed daily with 10 g soy flour in 100 mL of water. This is an OLR of 0.714 $kg_{TS}/(m^3*day)$. The digester was mixed by manual rocking after each addition of feed, but was otherwise unmixed. The digester was able to generate pressures up to 1.2 psig with an average flow rate of 4.12 ± 0.170 L/day. The average biogas composition produced by the digester was 69.9 ± 5.29% CH_4, 30.1 ± 5.29% CO_2, and 3520 ± 624 ppm H_2S as measured by GC/MS. The H_2S composition matches that of the biogas obtained from many landfills and a higher H_2S concentration better demonstrates the removal power of the system. The CO_2 composition of the produced biogas, however, is lower than average landfill biogas (37-41%). While this is not ideal, the CO_2 concentration is still sufficiently high to demonstrate the removal power of the system. Biogas is also highly variable in composition, so the composition of the biogas produced from our anaerobic digester is acceptable as a substitute for landfill biogas for testing our purification system.

The H_2S scrubber was an iron oxide adsorption column filled with acid-treated fine steel wool. The steel wool provides a source of iron oxide, which reacts with the H_2S, and provides a packing to increase reaction surface area. The data indicates that H_2S was removed to less than 1 ppm (resolution of the meter) from greater than 500 ppm (maximum of the meter). The H_2S concentration as measured

by GC/MS was ~3520 ppm. The $CuSO_4$ absorption column similarly removed H_2S to less than 1 ppm. However, the $CuSO_4$ absorption column was more expensive, generated large amounts of waste, and required a substantial pressure to overcome the water column. Since the anaerobic digester could generate a limited maximum pressure, the iron oxide adsorption column was chosen over the $CuSO_4$ column. As expected, both scrubbers completely removed H_2S from biogas. However, the $CuSO_4$ absorption column proved to be unviable for testing of our system.

The final CO_2 scrubber model was a spray column using an alkaline aqueous solution maintained at pH 13. The column was filled with ceramic raschig rings to increase the surface area of gas transfer to and dispersion of the solution. Scrubbing solution was pumped in the top through a spray nozzle at a flow rate of 566 mL/min, and an equivalent gravity-driven flow came out the bottom. Gas was introduced just above the water out port using an air stone sparger. A small water column was maintained to keep gas out of the water out port. The spray column removed 75 ± 9% of the CO_2 from the introduced 40% CO_2/N_2 gas mixture using freshwater and 80 ± 10% of the CO_2 using saltwater, leaving ~10% CO_2 in the purified gas. This was not the ideal goal of 5%, but it was very close to the minimum requirement of less than 10% CO_2. The solution flow rates were not ideal, but were defined by the available pumps. Increasing the water flow rate may therefore improve the CO_2 removal rate. The gas flow rate in these tests, 4.7 L/min or 6800 L/day, was also much higher than that produced by the digester, 4.1 L/day. The CO_2 absorption column is expected to work more effectively with the lower gas flow rate.

The final photobioreactor design was a tubular helix with fluorescent lights in

the center which provided a constant 1440 lux. The helix was 27.9 cm diameter by 1.12 m and constructed of 1.9 cm diameter PVC tubing. The tubing connected to a series of two open reservoirs. The circulation pump flow rate was 0.00022 m^3/s . *P. tricornutum* was selected as the alga to test in the system studies because *B. braunii* adhered the sides of the photobioreactor, blocking light and leading to cell death. A faster pump and smaller tubing were also used in the final design to increase flux within the photobioreactor, thereby reducing adherence. *B. braunii* was able to grow steadily with the addition of pH 12 solution, but growth was still reduced. *P. tricornutum* was not tested for this because of time constraints and contamination issues. Both algae grew well otherwise and improved growth when exposed to bicarbonate levels expected to be introduced during system testing. Growth of *P. tricornutum* in the photobioreactor was not measured due to time constraints and was instead used in system testing immediately.

The recycling column was a multi-layered gravity sand filtration column consisting of layers of fine sand and gravel in a PVC pipe. Testing showed that the filter successfully removed algae below detectable levels using spectrophotometry. The flow rate through the filter varied between 20 and 50 mL/min.

Chapter 8: System Studies

Introduction

Working models for each of the components were finalized after testing for functionality. The individual components were all combined into one connected system.

Component testing showed that each component of the purification system was functional. We hypothesized that after connecting each individual component, biogas produced by the anaerobic digester would exit the CO_2 scrubber, consisting primarily of CH_4 with approximately 10% CO_2 and very little, if any, traces of H_2S. The CO_2 would be fed into the photobioreactor, and the leftover CH_4 would be collected. The photobioreactor would appropriately mix the algal culture, and algal growth would be observed, suggesting usage of CO_2 by the algae. Water recycling would successfully filter out algae from the photobioreactor and return the water to the CO_2 scrubber.

Methodology

All final models of the anaerobic digester, H_2S scrubber, CO_2 column, photobioreactor, and water recycling column were connected together, and functionality of the system as a whole was analyzed. A diagram of the whole system is shown below in Figure 8.1.

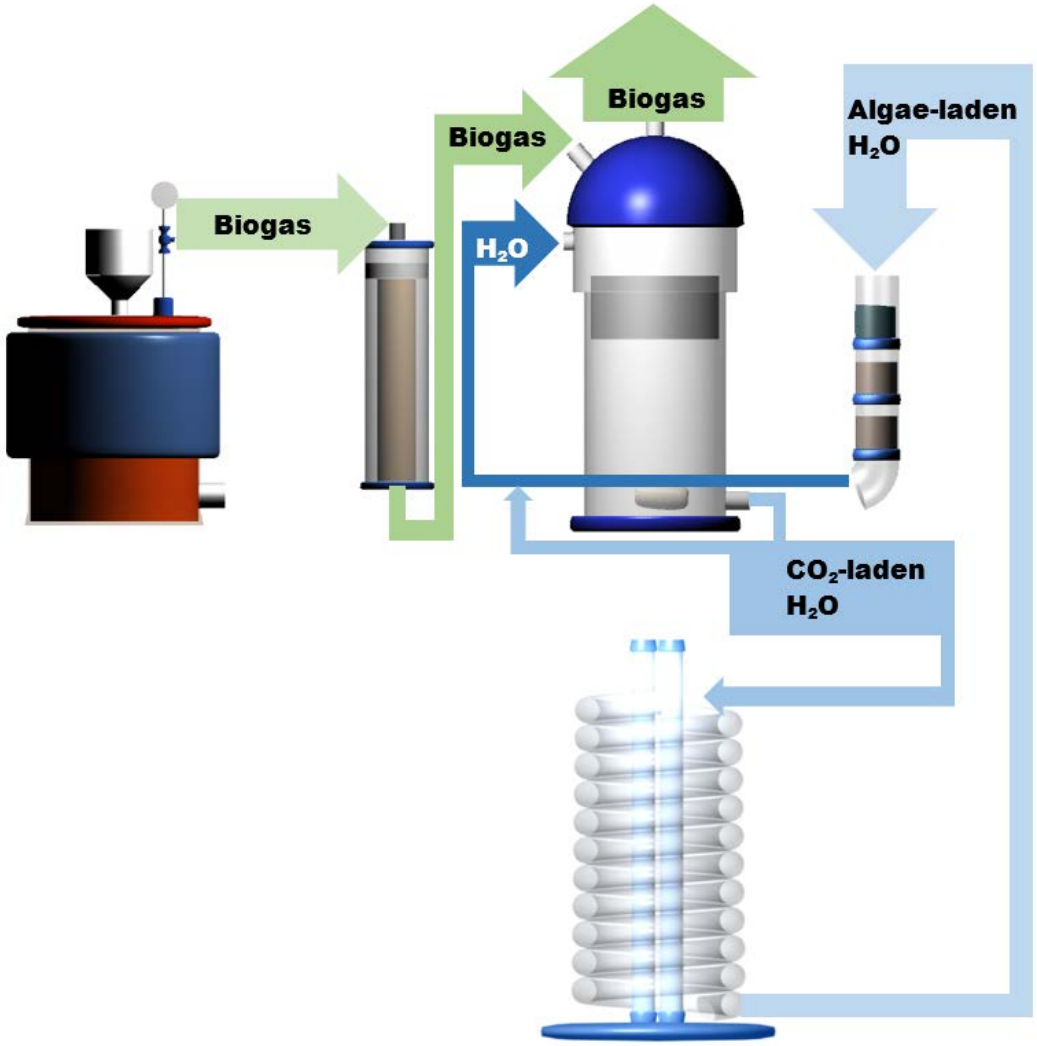

Figure 8.1. Diagram of whole system. Anaerobic digester produces biogas that flows into the H_2S scrubber, then the CO_2 absorption column. The purified biogas exits the CO_2 absorption column while CO_2-laden aqueous solution flows into the photobioreactor. The CO_2-stripped solution enters the sand filter that recycles the water for the CO_2 column.

In the final system, the anaerobic digester produced biogas at an average rate of 4.12 ± 0.170 L/day with an average composition that was similar to that of landfill biogas (69.9 ± 5.29% CH_4, 30.1 ± 5.29% CO_2, and 3520 ± 624 ppm H_2S). The digester generated a maximum pressure of 1.2 psig. The H_2S scrubber used the steel wool method and was able to remove H_2S from a concentration of approximately 3520 ppm to less than 1 ppm. The steel wool method was chosen over the $CuSO_4$

scrubbing method because steel wool was less expensive than $CuSO_4$, did not require a large pressure gradient, and did not generate waste that would be costly to dispose of. The CO_2 scrubbing column used a spray method with a pH 13 alkaline solution. It was able to remove 75 ± 9% of the CO_2 and left approximately 10% CO_2 in the purified gas. This gas was collected in sample bags and analyzed for composition using GC/MS. Although the composition of the purified gas does not reach natural gas standards (0% to 8% CO_2) (Speight, 2007), increasing water flow rate may improve the removal rate of CO_2. The photobioreactor employed a helical design with more turbulence than the original model. It was tested using *P. tricornutum* and *Synechocystis* sp. PCC 6803. *B. braunii* was not tested because it showed a tendency to adhere to interior walls of the PVC tubing, which decreased light penetration to the culture and therefore prevented growth of the culture. The water recycling system in the final system was able to successfully filter out algae using a sand filtration method.

After connecting all system components *P. tricornutum* was added into the reservoir and was cycled through the photobioreactor. The optical density of the culture was measured after an hour. Fluid level in the reservoir was kept underneath the port to the recycling system. Once the algal culture was fully mixed inside the bioreactor, CO_2-laden alkaline solution from the CO_2 column entered the reactor through the reservoir. Equal volumes of algal culture exited the photobioreactor and entered the recycling system over time.

However, due to the salinity of the media required for the growth of *P. tricornutum*, salts in the Chu-13 medium reacted with alkaline solution, resulting in

precipitation. In addition, the *P. tricornutum* culture was later found to have been contaminated with bacterial growth. As a result, the system was tested with *Synechocystis* sp. PCC 6803, a readily available freshwater cyanobacterium. However, this culture also appeared to adhere to the walls, possibly due to the addition of the alkaline CO_2-laden water. In order to reduce the pH of the *Synechocystis* sp. PCC 6803 culture, 15 mL of concentrated 37% w/w hydrochloric acid (HCl) was added on the second day, lowering the pH from 10.8 to 7.5. The pH was decreased again on the sixth day by adding 5 mL of the same HCl solution.

Results

Algal growth of *P. tricornutum* in photobioreactor.

Set-up of the whole system on the first day showed that the cyanobacteria was well-distributed throughout the photobioreactor. However, adhesion to the interior surface of the photobioreactor tubing was observed for the *Synechocystis* sp. PCC 6803 culture after one day. Initial cultures of the cyanobacteria in flasks did not show adhesion to the flask surface, which suggests that the adhesion seen in the photobioreactor may be due to the alkalinity of the CO_2-laden water. In addition, a high pH of 10.8 was maintained one day after introduction of the alkaline solution, indicating that the cyanobacteria may be unable to self-buffer the alkaline solution.

Algal growth of *Synechocystis* sp. PCC 6803 in photobioreactor.

Set-up of the whole system on the first day showed that the cyanobacteria was well distributed in the photobioreactor. However, adhesion to the interior surface of the photobioreactor tubing was observed for the *Synechocystis* sp. PCC 6803 culture after one day. Initial cultures of the cyanobacteria in flasks do not show adhesion to

the flask surface, which suggests that the adhesion seen in the photobioreactor may be due to the alkalinity of the CO_2-laden water. In addition, a high pH of 10.8 was maintained one day after introduction of the alkaline solution, suggesting that the cyanobacteria are unable to self-buffer the alkaline solution. Figure 8.2 below shows images of algal adherence to the PVC tubing of the photobioreactor on the second day.

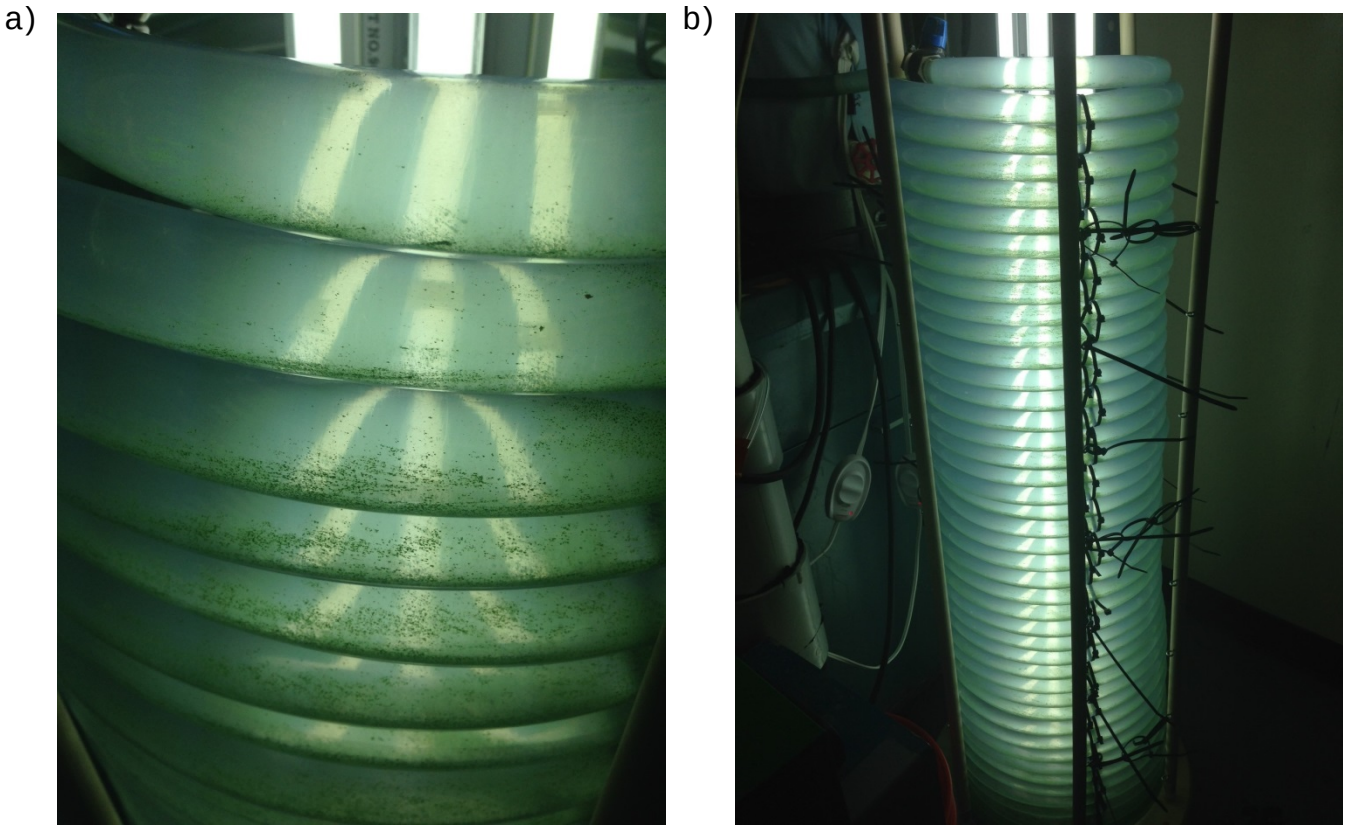

Figure 8.2. Adherence of *Synechocystis* sp. PCC 6803 to photobioreactor tubing on second day at pH 10.8. **(a)** A close up image of the photobioreactor shows regions of green growth on the sides of the tubing, indicating that *Synechocystis* sp. PCC 6803 was adhering to the interior walls of the PVC tubing. **(b)** This image of the whole photobioreactor shows that adherence is seen throughout the coil.

Three days after the initial introduction of cyanobacteria into the photobioreactor, the culture was visibly greener in color, indicating the possibility of

growth. However after the sixth day, the *Synechocystis* sp. PCC 6803 culture appeared to have settled down at the bottom of each coil of tubing in the photobioreactor. No adhesion was present, but the culture was also not completely mixed, which may suggest death. 5 mL of HCl was added on the seventh day to further lower the pH of the culture from 8.15. However, a majority of the algae in the photobioreactor was dead on the twelfth day. More images of the *Synechocystis* sp. PCC 6803 culture in the photobioreactor can be seen in Appendix H.

Biogas composition analysis.

GC/MS results showed that there was no H_2S or CH_4 gas in the sample bags, even though a substantial amount of gas was collected. This may have been due to an anomaly with the GC/MS machine.

Discussion

Whole system trials with *P. tricornutum* show that saltwater microorganisms may not be an optimal species for use with an alkaline solution. Chu-13 media used to culture *P. tricornutum* contained calcium salts that reacted with hydroxide ions in the alkaline CO_2-laden aqueous solution that was introduced into the photobioreactor, forming a calcium hydroxide precipitate. This precipitate caused the culture to turn cloudy, which seriously limited the amount of light transmittance through the photobioreactor. The cloudiness of the culture also prevented accurate measurement of optical density. In addition, the *P. tricornutum* stock culture was found to be contaminated, which compromised algal growth and the validity of the trials. Thus, *Synechocystis* sp. PCC 6803 was tested instead.

Trials with *Synechocystis* sp. PCC 6803 showed adherence to the PVC tubing, despite increasing turbulence inside the photobioreactor, using a pump with a higher

flow rate and tubing with a smaller diameter. While adherence was observed after introduction of the alkaline solution, it was not observed in original cultures of *Synechocystis* sp. PCC 6803 in flasks. This suggests that *Synechocystis* sp. PCC 6803 does not normally form filaments, and high pH may have been a factor that caused adherence of cells to tubing walls. Although less adherence was observed after decreasing the pH by adding HCl, the culture still appeared to be unviable due to the change in color from green to brown. Thus, lack of adherence may have been due to cell death and not necessarily due to a decrease in pH. In addition, persistence of a high pH (10.8) on the second day suggests that the cyanobacteria are unable to self-buffer. This may be due to a low initial density of algal culture, which prevents the algae from successfully buffering the solution after addition of alkaline solution.

GC/MS results indicated that there was a complete removal of H_2S and CH_4, which is problematic. A lack of CH_4 indicates that the gas was lost at some point in the system or during and after extraction. However, positive pressure coming out of the CO_2 column indicates the presence of gas in the sample bag. A mix-up in samples and/or issues with the GC/MS machine may have accounted for such anomalies. However, due to time limitations, no further GC/MS tests were conducted, and the issue was not further investigated.

Chapter 9: Scale-up Model and Cost Analysis

System model

In this industrial scale model, biogas is introduced into a CO_2 absorption column which removes the CO_2 from the biogas. An aqueous solution is pumped from a reservoir through the CO_2 absorption column and another pump transfers the solution from the column back to the reservoir at the same rate. Another set of pumps transfers some of the solution from the reservoir to the photobioreactor and back. A fifth pump circulates the solution through a tube arranged in a set of helices. The helices contain algae, which removes the CO_2 from solution and uses it and light, provided by lights in the center of each helix, to grow.

Growth rate of algae

The flow rate of the transfer between the CO_2 absorption system and the photobioreactor was based on the specific growth rate (μ_{max}) of the photosynthetic microorganisms. The growth is modeled using the Michaelis-Menton kinetics:

$$\mu = \frac{\mu_{max} * C_{CO2}}{K_m + C_{CO2}} \qquad \text{Eqn. 8}$$

where C_{CO2} is the CO_2 concentration in the photobioreactor and K_m is the CO_2 concentration at which the actual growth rate (μ) $= 0.5\mu_{max}$. Assuming that $K_m << C_{CO2}$, it can be approximated that $\mu = \mu_{max}$. The transient algal concentration in the photobioreactor is modeled as

$$\frac{dC_C}{dt} = C_C(\mu - \frac{1}{\tau}) \qquad \text{Eqn. 9}$$

where the terms in the parenthesis represent the algal growth and removal rate of algal cells from the photobioreactor, respectively. In order maintain growth in the

photobioreactor, where $\frac{dC_C}{dt}$ is greater than or equal to zero, the specific growth rate, μ, must be greater than the inverse of residence time, τ.

μ_{max} values found from various studies are shown below in Table 9.1. The minimum residence time (τ_{min}) is calculated by taking the inverse of μ_{max}.

Table 9.1. Specific growth rate and minimum residence time of various algal species.

Species	**μ_{max} (s^{-1})**	**τ_{min} (s)**
Botryococcus braunii (An *et al.*, 2003)	8.33×10^{-6}	120,000
Phaeodactylum tricornutum (Perez, Pina, & Rodriguez, 2008)	1.78×10^{-5}	56,200
Synechocystis sp. PCC6803 (Kim *et al*., 2011)	1.97×10^{-5}	50,800

Landfill Biogas: Input of CO_2 into the photobioreactor

The average landfill in Maryland (Environmental Protection Agency, 2013) produces biogas at a rate of roughly 1.13 m^3/s. Assuming 30% (by volume) of biogas is CO_2 and 70% is CH_4, according to the biogas composition results of this study, the flow rate of CO_2 entering the CO_2 absorption column is 0.34 m^3/s. The mass flow rate of CO_2 is 670 g/s.

Volume of the photobioreactors

The required volume of the photobioreactor to consume all of the CO_2 generated by the landfill is found using

$$\left(\frac{dC_C}{dt}\right)_{max} = \mu C_{C,max} = \frac{\dot{m}_{microbe}}{V} \qquad \text{Eqn. 10}$$

$$\therefore V = \frac{\dot{m}_{diatom}}{\mu C_{C,max}}$$

Assuming that the water will absorb the entire volume of CO_2 produced in the landfill biogas, the optimal algal densities ($C_{C,max}$) and the corresponding volume of

photobioreactor required to consume all of the CO_2 absorbed into the water are listed in Table 9.2.

Table 9.2 Optimal algal density and volume required to reach the optimal algal density for various algal species for a biogas flow rate of 1.13 m^3/s.

Species	**$C_{C,max}$ (g/m^3)**	**V (m^3)**
Botryococcus braunii (An et al. 2003)	7500	5,900
Phaeodactylum tricornutum (Silva Benavides et al. 2013)	1000	21,000
Synechocystis sp. PCC6803 (Kim and Vannela 2013)	1800	10,000

Sizing of the Photobioreactor

Two different scale-ups are shown in this section: scale-up A refers to scale-up of the photobioreactor containing the volumes listed in Table 9.2 for each algal species, while scale-up B refers to a scale-up model for a volume of 120 m^3. The volumes required to consume all CO_2 produced in landfill biogas that are used in scale-up A may be too large for industrial application, and thus modelling with a volume of 120 m^3 in scale-up B is also provided. Scale-up B is based on the growth of *P. tricornutum* because this algal species was tested most extensively out of the three species in this study.

The radius of the tubing is set to 0.05 m because this is the maximum thickness that allows for sufficient penetration of light for algal growth (Jimenez, Cossio & Niell, 2003). The corresponding cross-sectional area of the tubing is 0.00196 m^2. With this size of tubing, the photobioreactor would require certain lengths of tubing (l_{tubing}) in order to accommodate the volumes used for each scale-up model. These lengths are listed in Table 9.3.

The helix radii of the photobioreactor (r_{helix}) are set to 25 m and 2.5 m for scale-up A and scale-up B, respectively. Scale-up A photobioreactors are designed

with 25 m radius coils because the radius affects the light transmittance and height of the photobioreactor. A larger radius will decrease the height and decrease the light transmittance to the algal culture, and vice versa, thus the size of the coils does not affect the amount of light energy needed to provide a certain illuminance to the culture. Photobioreactors in scale-up A cannot afford to have a smaller radius because the excessive weight from the required height would be overbearing for tubing near the bottom of the coil.

Assuming each layer of the helix has a circular length equal to the circumference (c_{helix}) based on the r_{helix}, the total number of layers (N_{layers}) can be calculated by dividing the l_{tubing} by the c_{helix}. To clarify, each layer refers to one of the individual coils that makes up the helix of the photobioreactor. The N_{layers} for each scale-up model are listed in Table 9.3.

The total heights of each photobioreactor (h_{total}) are calculated by multiplying N_{layers} by the height of each layer. The height of each layer is assumed to be the sum of the diameter and thickness of the tubing. The thickness of the tubing is assumed to be twenty percent of the diameter. Hence, the height of each layer is 0.12 m. The h_{total} are tabulated in Table 9.3.

Each photobioreactor cannot be designed with the h_{total} listed in Table 9.3 because the tubing cannot handle the excessive weight due to tens of thousands of layers on top of one another. For this reason, the design is limited to heights of 100 m and 10 m for scale-up A and scale-up B photobioreactors, respectively. Even with this restriction, the photobioreactor would require a great deal of supporting structure to buttress weight on the layers of helix. Consequently, multiple photobioreactors are

required in series for the scale-up designs. The numbers of photobioreactors in series (N_{series}) are listed in Table 9.3.

Table 9.3. Dimensions of the photobioreactors.

Scale of Photobioreactor	**V (m^3)**	**l_{tubing} (m x 10^3)**	**r_{helix} (m)**	**C_{helix} (m)**	**N_{layers}**	**h_{total} (m)**	**N_{series}**
Scale-up A: *B. braunii*	5,900	3,000	25	160	19,000	2,300	23
Scale-up A: *P. tricornutum*	21,000	11,000	25	160	68,000	8,200	82
Scale-up A: *Synechocystis* sp. PCC6803	10,000	5,100	25	160	32,000	3,900	39
Scale-up B: *P. tricornutum*	120	61	2.5	16	3,900	470	47

As shown in Table 9.3 it would require numerous (up to 82) photobioreactors of enormous sizes for all scale-up models to completely treat the CO_2 produced in landfill biogas. This poses problems associated with available land, enormous weight pressing down on each layer of tubing, and high capital costs to build the photobioreactors.

Circulation flow rate of the photobioreactors

The volumetric flow rates of CO_2-laden aqueous solution ($\dot{V}_{solution}$) entering the photobioreactor are calculated as follows:

$$\dot{V}_{solution} = \frac{V}{1.5\tau_{min}} \qquad \text{Eqn. 11}$$

where the actual residence time (τ) is greater than τ_{min} by 50% to allow sufficient growth of algae in the photobioreactor. The flow rates required for each species is enumerated in Table 9.4.

Table 9.4. Volumetric flow rates of CO_2-laden aqueous solution for various algal species in photobioreactor.

Scale of photobioreactor	**V (m^3)**	$\dot{V}_{solution}$ **(m^3/s)**
Scale-up A: *B. braunii*	5,900	0.033
Scale-up A: *P. tricornutum*	21,000	0.25
Scale-up A: *Synechocystis* sp. PCC6803	10,000	0.13
Scale-up B: *P. tricornutum*	120	0.0014

Maximum CO_2 consumed by the algae in the photobioreactors

As noted before, landfills produce biogas at a rate of 1.13 m^3/s, with a composition of 30% CO_2 and 70% CH_4. Consequently, the mass flow rate of CO_2, $\dot{m}_{CO2}$, in the scale-up A photobioreactors is 670 g/s. Assuming 1.8 g CO_2 is consumed per gram of algae (Sudhakar et al. 2012), the maximum growth rate of algae, $\dot{m}_{algae}$, in the photobioreactor based on available CO_2 is 370 g/s.

Because the volume of the scale-up B photobioreactor (120 m^3) is roughly a hundred times smaller than scale-up A photobioreactors, much less CO_2 can be consumed by the algae in the 120 m^3 photobioreactor. Maximum CO_2 consumption in a 120 m^3 photobioreactor can be found using

$$\dot{m}_{algae} = \mu C_{C,max} \cdot V \qquad \text{Eqn. 12}$$

$$\dot{m}_{CO2} = 1.8 \cdot \dot{m}_{algae} = 1.8 \mu C_{C,max} \cdot V$$

and is tabulated in Table 9.5.

Table 9.5. Maximum algal growth, CO_2 consumption, and flow rate of biogas in the photobioreactors.

Scale of photobioreactor	$\dot{m}_{algae}$ **(g/s)**	$\dot{m}_{CO2}$ **(g/s)**	$\dot{V}_{CO2}$ **(m^3/s)**	$\dot{V}_{biogas}$ **(m^3/s)**
Scale-up A: *B. braunii*	370	670	0.34	1.13
Scale-up A: *P. tricornutum*	370	670	0.34	1.13
Scale-up A: *Synechocystis* sp. PCC6803	370	670	0.34	1.13
Scale-up B: *P. tricornutum*	2.1	3.8	0.0019	0.0064

As expected, the scale-up B model can purify roughly a hundred times less biogas than the scale-up A photobioreactors. Therefore, although the scale-up B photobioreactors may be more feasible in terms of size, it would produce considerably less revenue from the purified methane and potential algal oil, compared to the scale-up A photobioreactors. This is addressed in the following section.

Revenue

Purified Gas

If all of the biogas generated in an average landfill is purified, the system can produce CH_4 at an approximate rate of 0.79 m^3/s. We assume this stream of purified biogas to be of natural gas quality. The price of natural gas is approximately $4.66 per thousand cubic feet (Energy Information Administration, 2014) or $0.165 per m^2.

For the scale-up B photobioreactor, only a fraction of the available landfill biogas can be purified and utilized while taking advantage of all the captured CO_2 in the absorption column. The revenues generated from each photobioreactor, based on size and algal species, are tabulated in Table 9.6.

Table 9.6. Revenue from CH_4 purified by the 1200 L photobioreactor.

Scale of photobioreactor	$\dot{V}_{biogas}$ **(m^3/s)**	$\dot{V}_{CH4}$ **(m^3/s)**	**Revenue ($/yr)**
Scale-up A: *B. braunii*	1.13	0.79	4.11 mil
Scale-up A: *P. tricornutum*	1.13	0.79	4.11 mil
Scale-up A: *Synechocystis* sp. PCC6803	1.13	0.79	4.11 mil
Scale-up B: *P. tricornutum*	0.0064	0.0045	23,400

Algal Oil

Although this study did not attempt to extract algal oil from the growing algal biomass, this scale-up design takes into account this potential energy source to obtain a more comprehensive calculation of revenues that could be generated from the

photobioreactors. The potential productions of lipids and hydrocarbons from photobioreactors and revenues from the converted algal oils are tabulated in Table 9.7. The maximum oil contents of the algal biomass (Banerjee et al., 2002; Chisti, 2007; Sheng, Vannela, & Rittmann, 2011) are listed and multiplied by the $\dot{m}_{algae}$ to obtain rough estimates of the productions of algal oil ($\dot{m}_{oil}$). The volumetric production of algal oil is found using 864000 g/m^3 as the density.

The price of algal oil is set based on its energy content (80%) compared to crude oil (Chisti, 2007). According to the U.S. Energy Information Administration (2014), petroleum cost is roughly $3.50 per gallon in March 2014. We assume that algal oil is $2.80 per gallon or $740 per m^3 and has no processing cost to produce from the collected algal culture.

Table 9.7. The oil contents, potential production of algal oil, and the revenues from the algal oils.

Scale of photobioreactor	**Oil Content (% dry wt)**	$\dot{m}_{oil}$ **(g/s)**	$\dot{V}_{\mathbf{oil}}$ **(m^3/s x 10^{-4})**	**Revenue ($/yr)**
Scale-up A: *B. braunii*	~75%	280	3.2	7.5 mil
Scale-up A: *P. tricornutum*	~30%	110	1.3	3.0 mil
Scale-up A: *Synechocystis* sp. PCC6803	~8%	30	0.35	820,000
Scale-up B: *P. tricornutum*	~30%	0.64	7.4 x 10^{-3}	17,000

As Table 9.7 illustrates, *B. braunii* produces about 2.5 times more algal oil than *P. tricornutum*. Generating $7.5 or $3 million per year in scale-up A, photobioreactors augment the revenue significantly. For this reason, algal oil extraction is a key revenue-producing component of photobioreactors.

Cost Analysis

The system has several operating costs related to NaOH, pumps, and lights. The capital costs were not included due to insufficient literature data on the prices of

photobioreactors. The intent of this cost analysis is to determine if the revenues outweigh the operating costs of the system. Regardless of the capital cost, the revenue must be greater than the operating cost to justify implementing this system. If the economics predict a negative profit, or a loss, solely from operating costs and revenue, then it would be impossible to payback the capital costs.

Sodium Hydroxide

The amount of NaOH required is based on the upper bound of one mole of NaOH required per mole of CO_2 processed. This scale-up is based on the assumption that microorganisms are growing at their optimal state; hence, we assume the microorganisms buffer perfectly. Although our experiment did not provide comprehensive evidence to fully support this buffering assumption, this must be the case or the microorganisms would not survive as the pH would continue to escalate as more NaOH is added to compensate for the dissolved CO_2. Although dissolved CO_2 lowers the pH of the solution, the CO_2 is later removed by the algae thereby returning the effective pH of the solution back to the original based on the equilibrium of the following equations.

$$CO_2 + 2OH^- \rightarrow CO_3^{2-} + H_2O \qquad \text{Eqn. 13}$$

$$CO_2 + CO_3^{2-} + H_2O \rightarrow 2HCO_3^-$$

Therefore, the buffering effect of the algae is the only factor determining the amount of NaOH that needs to be added. The amount of NaOH is directly proportional to the flow of buffered solution from the photobioreactor to the CO_2 reservoir. This flow is proportional to the growth rate of the algae and the volume of the photobioreactor. The volume is directly proportional to the mass flux of CO_2 into

the system. The net proportionality constant between the needed NaOH and the flow of CO_2 is less than 1, but we use the upper bound of 1 for simplicity.

With those assumptions, the required addition rate of NaOH into the absorption column is tabulated in Table 9.8. Industrial price for NaOH is estimated to be approximately $0.40 per kg based on 2014 market prices.

Table 9.8. Cost of NaOH based on a mole to mole ratio of CO_2 and NaOH.

Scale of photobioreactor	$\dot{m}_{CO2}$ **(mol/s)**	$\dot{m}_{NaOH}$ **(g/s)**	**Cost ($/yr)**
Scale-up A: *B. braunii*	15	600	7.6 mil
Scale-up A: *P. tricornutum*	15	600	7.6 mil
Scale-up A: *Synechocystis* sp. PCC6803	15	600	7.6 mil
Scale-up B: *P. tricornutum*	0.087	3.5	44,000

Photobioreactor Circulation Pump

Because the scale-up photobioreactors need to have turbulent flow in the photobioreactor to prevent settling of the algae, the flow rates of the photobioreactor circulation pump were increased to maintain a constant linear velocity of the algal media as the experimental design of this study. The experimental design used a diaphragm pump (Flojet 4YD41) at a flow rate of 3.5 gal/min or 0.00022 m^3/s. The inner tubing radius was 0.0095 m. The linear velocity was then calculated to be 0.78 m/s. The flow rate of the scale-up photobioreactors was found by maintaining the same linear velocity in the wider tubing with inner radius of 0.05 m. Hence, the circulation rate is 0.0061 m^3/s.

The power of the pump is calculated by

$$P = \frac{Q \; x \; \rho \; x \; g \; x \; h_{total}}{\eta_{pump}} \qquad \text{Eqn. 14}$$

where Q is the flow rate [m^3/s], ρ is the density of the fluid, g is the gravity (9.81 m/s^2), h_{total} is the total height of the photobioreactors [m], and η_{pump} is the efficiency (0.6). By using this equation, only the pressure difference due to height is applied in the pump power. Viscosity and other forces are ignored for simplicity. For the circulation pump, Q is set as 0.0061 m^3/s, and ρ is assumed to be close to that of water and set as 1000 kg/m^3. The power and cost are listed in Table 9.9. The costs to power the pumps are found by multiplying the powers by the cost of electricity, estimated to be $0.0662 per kWhr.

Table 9.9. Power and cost of the circulation pumps

Scale of photobioreactor	**P (kW)**	**Cost ($/yr)**
Scale-up A: *B. braunii*	230	130,000
Scale-up A: *P. tricornutum*	810	470,000
Scale-up A: *Synechocystis* sp. PCC6803	390	230,000
Scale-up B: *P. tricornutum*	47	27,000

CO_2-laden Aqueous Solution Transfer Pump

The transfer rate of the CO_2-laden aqueous solution from the reservoir of the CO_2 absorption column to the photobioreactors is given in Table 9.4. The power required to operate this pump is calculated using Equation 14 and is tabulated in Table 9.10. Assuming the pressure is again solely due to h_{total}, and the density is close to that of water. The flow rate, Q, is given by $\dot{V}_{solution}$. The costs to power the pumps are found by multiplying the powers by the cost of electricity, estimated to be $0.0662 per kWhr.

Table 9.10. Flow rates and cost of CO_2-laden aqueous solution transferred from the CO_2 absorption column to the photobioreactors.

Scale of photobioreactor	$\dot{V}_{solution}$ **(m^3/s)**	**P (kW)**	**Cost ($/yr)**
Scale-up A: *B. braunii*	0.033	1,200	710,000
Scale-up A: *P. tricornutum*	0.25	33,000	19 mil
Scale-up A: *Synechocystis* sp. PCC6803	0.13	8,400	4.9 mil
Scale-up B: *P. tricornutum*	0.0014	11	6,300

Two transfer pumps are required for each scale-up photobioreactor. One pump transfers CO_2-laden aqueous solution from the reservoir of the CO_2 absorption column to the photobioreactor; the other transfers the solution back to the reservoir of the CO_2 absorption column from the photobioreactor. Therefore, the costs in Table 9.10 are doubled.

CO_2 Absorption Column Spray Pump

The scale-up photobioreactors use an additional pump that was not used in the experimental design. Another spray pump is implemented in the scale-up design because the experiment found it difficult to share one pump to spray the CO_2 absorption column *and* transfer the CO_2-laden aqueous solution to the photobioreactor. To simplify the process, the scale-up photobioreactors designate each of the two flows to its own pump.

The rate at which the alkaline solution is sprayed down the CO_2 absorption column is scaled up by assuming the following concerning the CO_2 absorption column:

1. The volume of the column increases proportionally to the increase in the CO_2 flow rate.
2. The height-radius proportion of the column remains constant.

3. The flux of the alkaline solution through the column increases proportionally to the increase in the CO_2 flux through the column using the scaled-up cross-sectional area.

The assumptions apply the CO_2 flow rates instead of the biogas flow rates because the CO_2 composition of the gas in the pilot study of the CO_2 spray absorption column (40%) is different from that of the scale-up photobioreactors (30%). Because the study focuses on the removal of CO_2, the CO_2 flux is used to scale up the systems proportionally.

The experimental design treated 3.15×10^{-6} m^3/s of CO_2; the scale-up photobioreactors treat 0.34 and 0.0019 m^3/s for the scale-up A and scale-up B, respectively. Applying the first and second assumptions, the volumes, radius, and height of the CO_2 absorption columns are found.

The CO_2 flux is calculated by dividing the CO_2 flow rate by the cross-sectional area of the CO_2 absorption column. The CO_2 flux in the experimental design was 4.0×10^{-4} m/s; it is 0.019 and 0.0034 m/s for the scale-up A and scale-up B, respectively. The flow rate and flux of the alkaline solution in the experimental design was 8.33×10^{-6} m^3/s and 0.0011 m/s, respectively. By applying the third assumption, the fluxes of the alkaline solution in the scale-up CO_2 absorption column are 0.050 m/s and 0.0090 m/s for the scale-up A and scale-up B, respectively. The flow rates of the alkaline solution are then found and listed in Table 9.11.

The powers required to operate this pump are calculated according to Equation 14 and tabulated in Table 9.11. Assume the pressure is solely due to the h_{scale}, and the density is close to that of water. The flow rate Q is given by $\dot{V}_{spray}$. The

costs to power the pumps are found by multiplying the powers by the cost of electricity, estimated to be $0.0662 per kWhr.

Table 9.11. Scale-up of the CO_2 absorption columns.

Scale of photobioreactor	**r_{scale} (m)**	**h_{scale} (m)**	**A_{scale} (m^2)**	**$\dot{V}_{spray}$ (m^3/s)**	**P (kW)**	**Cost ($/yr)**
Scale-up A	2.4	24	18	0.90	350	200,000
Scale-up B	0.42	4.2	0.56	0.0050	2.0	1,100

All scale-up A systems have the same cost associated with this particular pump because the CO_2 flow rate entering the CO_2 absorption columns are equal. Hence, the difference in algal species does not make any difference for this case. This alkaline solution transfer system requires two pumps. One sprays the solution from the alkaline solution reservoir down the CO_2 absorption column; the other transfers the solution from the column back to the reservoir. Therefore, the costs in Table 9.11 are doubled.

Lights

Lights are scaled up based on the intensity of light absorbed by the algae in the photobioreactors. The illuminance in the experimental design was 1,440 lux. The power required to power the lights can be calculated using

$$P = \frac{E_v \, x \, A}{\eta} \qquad \text{Eqn. 15}$$

where P is power [W], E_v is illuminance [lux], A is surface area [m^2], and η is luminous efficacy [lm/W]. The typical η value for fluorescent light is estimated to be 60 lm/W. By multiplying the total height (h_{total}) and circumference of the helix (c_{helix})

of the photobioreactors, the surface area (A) can be found. The calculated powers for each scale-up photobioreactors are listed in Table 9.12.

Table 9.12. Energy required to power and costs of the lights of the photobioreactors.

Scale of photobioreactor	**A (m^2 x 10^3)**	**P (kW)**	**Cost ($/yr)**
Scale-up A: *B. braunii*	360	8,600	5.0 mil
Scale-up A: *P. tricornutum*	1,300	31,000	18 mil
Scale-up A: *Synechocystis* sp. PCC6803	610	15,000	8.7 mil
Scale-up B: *P. tricornutum*	7.3	180	100,000

Total Operating Cost

The total operating costs associated with each scale-up design are given in Table 9.13. The costs due to the circulation pump are minimal compared to those of the other three operating costs. The lights are generally the highest operating costs followed by the NaOH costs.

Table 9.13. Total operating costs of the photobioreactors.

Scale of photobioreactor	**NaOH ($/yr)**	**Circ. Pump ($/yr)**	**Trans. Pump ($/yr)**	**Spray Pump ($/yr)**	**Lights ($/yr)**	**Total Cost ($/yr)**
Scale-up A: *B. braunii*	7.6 mil	130,000	1.4 mil	400,000	5.0 mil	14.5 mil
Scale-up A: *P. tricornutum*	7.6 mil	470,000	38 mil	400,000	18 mil	64.5 mil
Scale-up A: *Synechocystis* sp. PCC6803	7.6 mil	230,000	9.8 mil	400,000	8.7 mil	26.7 mil
Scale-up B: *P. tricornutum*	44,000	27,000	13,000	2,200	100,000	186,000

Net Profit or Loss

The net profit of the system is shown in Table 9.14 by subtracting the total revenue from the total operating cost.

Table 9.14. The net profit of the scale-up photobioreactors.

Scale of photobioreactor	**Revenue ($/yr)**	**Cost ($/yr)**	**Profit ($/yr)**
Scale-up A: *B. braunii*	11.6 mil	14.5 mil	-2.90 mil
Scale-up A: *P. tricornutum*	7.11 mil	38.3 mil	-57.4 mil
Scale-up A: *Synechocystis* sp. PCC6803	4.93 mil	22.2 mil	-21.8 mil
Scale-up B: *P. tricornutum*	40,400	176,000	-146,000

The negative profit values indicate losses; the operating costs are greater than the revenues for all scale-up designs. The system should be redesigned to consume less NaOH, utilize more efficient lighting system, and produce more algal oil to make it profitable. It is also important to note that this scale-up calculation only includes the utility costs; other costs, such as capital cost, are omitted. Those costs would augment the net loss, so several design alternatives must be made before pursuing this scale up.

Chapter 10: Conclusion

This study aimed to design a system to convert landfill biogas, a large untapped energy resource, into a natural gas substitute by removing H_2S and reducing CO_2 from the biogas. Algae was used as a biological method to remove CO_2 through photosynthesis. Algae has several advantages over conventional chemical CO_2 removal methods because algae is inexpensive to obtain, requires only light and minimal nutrients in addition to the CO_2 for growth, and the waste can be harvested for biofuels.

A custom-built anaerobic digester was used to generate biogas that mimicked the composition of landfill biogas, and an H_2S adsorption column removed H_2S from the produced biogas in order to test the system. The anaerobic digester was fed 0.714 $kg_{TS}/(m^3*day)$ of soy flour every day and maintained at 32°C. It produced 4.12 L/day of biogas with a composition of 70% CH_4, 30% CO_2, and 3520 ppm H_2S. This source of biogas was an acceptable substitute for landfill biogas. The H_2S adsorption column was packed with rusted steel wool, which was the source of iron oxide. The scrubber removed H_2S from the biogas to less than 1 ppm, though there were some anomalies in the data.

The CO_2 was separated from the biogas, using a spray absorption column packed with ceramic raschig rings. The alkaline solution was maintained at a pH near 13 and sprayed down the column at a flow rate of 566 mL/min. The CO_2 scrubber lowered the CO_2 concentration of a 40% CO_2/N_2 test mixture down to 8-10%. The CO_2-laden aqueous solution was then pumped into the photobioreactor to grow algae through photosynthesis.

Two different algal species were tested in the helical tubular photobioreactor: *P. tricornutum* and *Synechocystis* sp. PCC6803. The diameter of the tubing was 1.9 cm, the diameter of the coils was 28 cm, and the height of the photobioreactor was 1.1 m. The central lighting provided 1440 lux of illuminance. A diaphragm pump was used to provide constant mixing in the photobioreactor. Once the bicarbonate was consumed fully, the aqueous solution then flowed down the water recycling column. The water recycling system consisted of a PVC column that used a gravity sand filtration method to remove algae. It was able to filter out algae to below-detectable levels using absorbance.

Testing of the system as a whole was unsuccessful because of various problems leading to death of the algae. These include pump failure, adherence of algae to the walls of the photobioreactor, escalating pH, and the formation of a precipitate. Therefore, the data presented is from the individual component studies which were designed to model the parameters of the entire system.

The parameters obtained from the testing of the system components were used in a cost analysis of a scaled-up version of the final system design on an industrial scale. The industrial model is a direct scale-up of the appropriate parameters of our system, so that application of our data is possible. The industrial model also uses pumps to drive and control every flow, as this is more practical in an industrial setting. The potential revenue is derived from the natural gas produced from the purification system and from the algal oil that can be collected from the photobioreactor. The initial construction costs of the system are ignored in this comparison, and instead, only the upkeep costs are used. The costs include the NaOH

addition, the light energy required to grow the algae, and the electrical energy required to run all five pumps, which pump the aqueous solution to and from the CO_2 scrubber, to and from the photobioreactor, and within the photobioreactor. The results of this cost analysis show an annual deficit for each of the algae tested in this study. *B. braunii* is expected to be the most productive with a yearly revenue of $11.6 million and cost of $14.5 million (loss of $2.9 million per year or 125%). *P. tricornutum* is expected to produce $7.11 per year, but with an extensive annual cost of $64.5 million (loss of $57.4 million per year or 910%). The *Synechocystis* sp. PCC6803 model predicts an even lower revenue of $4.93 million per year and a high cost of $26.7 million per year (loss of $21.8 million per year or 540%).

Each parameter of the system acts in a complex manner on the costs of the system, so pinpointing the reasons for these deficits is difficult. Ultimately, the algae grows too slowly, given the amount of energy put into the system, to be cost effective. NaOH accounts for $7.6 million of the yearly costs and indirectly reduces the growth rate of the algae. Adjusting these parameters would both increase revenue and decrease costs. The enormous physical size of the scaled-up system may also be unfeasible, so initial construction costs may be extremely high. However, despite this cost inefficiency, the system is not fundamentally flawed and just needs to be optimized.

Several procedural factors must be kept in mind when examining the conclusions of this study, stemming from the accumulated problems encountered throughout experimentation. Foremost among these, the system was never successfully tested in its entirety. Therefore, most conclusions are based on the

studies done on each component separately. However, these studies were designed to mimic the conditions found in the entire system as closely as possible and should be applicable to a scale-up model and future studies.

Most of the data collected was from the CO_2 and H_2S meters used in the experiment. These meters were observed to fluctuate in response to minor changes in flow and pressure. Additionally, the meters had a long response time to changes in gas composition. Extensive steps and calibration tests were performed to try to minimize the error resulting from this problem. However, error in the values for CO_2 and H_2S levels may have been higher than reported.

Finally, the system components were tested with synthetic biogas or biogas produced from the constructed anaerobic digester. The aim of the study was to apply the data to landfill biogas; however, landfill biogas was never actually used in the testing of the system. The synthetic biogas used N_2 as a substitute for the insoluble methane, and the biogas produced from the anaerobic digester had a lower CO_2 percentage than that found in average biogas. Nevertheless, the compositions of these gases were sufficient for the purposes of the study.

Keeping these factors in mind, the system as originally designed, would not be cost-effective on an industrial scale. Regardless, our system was successful in converting mimicked landfill biogas into a natural gas substitute.

Chapter 11: Future Directions

In our study, we successfully built and tested working models for each of the components and connected them in series to complete the whole purification system. However, the system we designed and tested was not cost-effective. With some modifications, the system could function with lower operating costs, which, in turn, could increase the overall profit from the system.

Design Modifications

Large concentrations of NaOH, used to create an alkaline solution that scrubbed CO_2 from the biogas, posed many problems in our experiments and constituted a significant cost factor in our system. A method of removing CO_2 from the system that does not require NaOH should be implemented to eliminate a major cost, avoid the numerous problems associated with a basic solution, and maintain algal growth at its optimum pH. Furthermore, if the algal growth rate was increased, less volume would be needed in the photobioreactor, thus a smaller photobioreactor that requires less energy to circulate the contents and less lighting could be used. However, in our study, high NaOH concentrations were linked to increased CO_2 removal. Therefore, changes to the CO_2 column would be needed to compensate for this loss in efficiency. The size of and flow rate through the CO_2 scrubber would need to be increased, resulting in higher costs. However, the economic benefits of eliminating NaOH and scaling down the photobioreactor should outweigh the added costs from the proposed changes to the CO_2 scrubber. Additionally, if NaOH was not used in the CO_2 scrubber, then a salt water algae could be used without the risk of precipitate formation.

Further research should also be done on alternative algae species that may work better in the purification system. The three species that were tested, *P. tricornutum, B. braunii,* and *Synechocystis* sp. PCC6803, adhered to the walls of the photobioreactor tubing, impairing growth of the culture by reducing light penetration and circulation. In order to address such issues and ensure the integrity of the system, we would need to use an algae that neither sticks to surfaces nor forms debris in the tubing. The alternative species should also have a high growth rate and an ability to metabolize a high amount of CO_2 at a fast rate. As would be the case in a system that does not utilize NaOH, higher growth rates and optimal concentrations of algae can be paired with a smaller photobioreactor to reduce costs. An algal species that produces more algal oil would also lead to greater cost efficiency of our system.

Pumps should also be incorporated between each component of the system to replace any gravity transfers, 5 pumps in total. This would lead to greater control of the flow of gas and liquid throughout the system. To account for mechanical failures, backup pumps should be connected in parallel for each pump in the system. This way, in the event of pump failure, as we encountered in our system studies, a backup pump would immediately take over, allowing the system to function continuously. This is especially important for a biological system in which any downtime could lead to decimation of the algal culture.

Experimental Modifications

Several improvements could be made to the current design that would improve the reliability of our results and the ease of testing new designs. Instead of producing biogas using an anaerobic digester, biogas should be directly obtained from

either pressurized landfill biogas or pressurized synthetic biogas in order to achieve a more static composition. These alternatives would provide enough pressure to overcome the water resistance in our system and a wide range of controllable flow rates. The increased pressure would allow us to conduct further testing on the CO_2 bubble absorption column, as the pressure would effectively push the gas through the column. This column would be beneficial to use given its higher CO_2 removal rate and reliability in past experiments.

A more valid method of measuring the levels of CO_2 and H_2S in the biogas would allow for a more accurate determination of the efficiency of the scrubbing components. The meters used in our experiments resulted in unreliable data. The H_2S meter required a steady flow of gas, which we were unable to provide in our system. Furthermore, the meter could not measure above 500 ppm, which meant that we could not accurately determine the H_2S concentration in the range of the biogas produced from the anaerobic digester. Additionally, the CO_2 meter gave variable readings, and its response time was delayed, leading to large errors. Different meters should give more stable, accurate readings.

Designing a method to internally monitor the parameters within the H_2S, CO_2, and water recycling columns would allow for qualitative observations and measurements. Such observations would allow for a higher degree of troubleshooting and understanding of the overall system. This could be accomplished by using transparent columns, so the contents of the column could be visually monitored.

The photobioreactor should be started with a high concentration of algae. A denser starting culture would be able to more effectively maintain homeostasis and allow the system to be tested more readily.

Future Experiments

Future studies could expand upon the research we conducted. In our experiment, we chose to purify H_2S using iron oxide; however, biological alternatives do exist. Several species of algae can metabolize H_2S (Biebl & Pfennig, 1977). Using a biological system to remove H_2S has similar benefits to using one to remove CO_2: lower upkeep costs, more environmentally sustainable, and non-hazardous waste.

Metabolic engineering of algae is another possible avenue of research to increase cost efficiency. Algae can be modified in several ways to have a higher photosynthetic rate. One such method is the engineering of algae to produce more photosynthetic enzymes or growth factors. This higher photosynthetic rate would increase the overall growth rate of the algae and reduce the costs of the overall system. Additionally, the issue of algal culture contamination could be eliminated by combining genetic modification and antibiotics. The algae would be genetically modified to be resistant to an antibiotic of choice, which would be added to the starting culture; the genetic modification would ensure that the antibiotic would not harm the algae while destroying other contaminating agents. Maintaining a pure culture would increase the efficiency of the algae in processing CO_2.

Using biological metabolism to purify biogas is a promising means of biofuel production. In particular, the system presented in this study, with the modifications addressed above, may be an effective means of purifying landfill biogas. We

recommend further laboratory-scale tests before large-scale tests and implementation in industry.

Appendices

Appendix A – CAD Diagrams

A.1 Anaerobic Digester

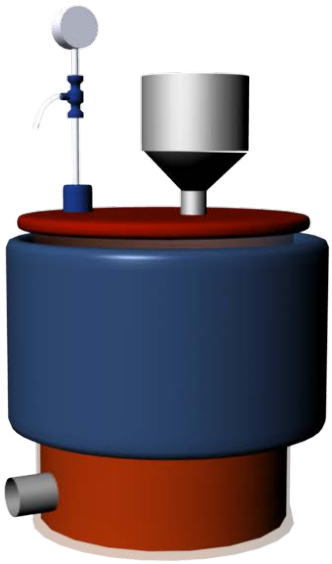

A.2 H_2S Scrubber

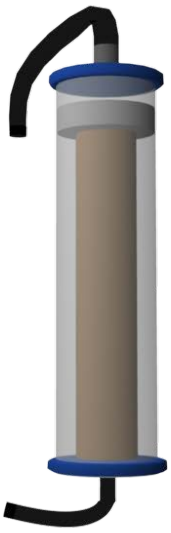

A.3 CO_2 Scrubber

A.4 Photobioreactor

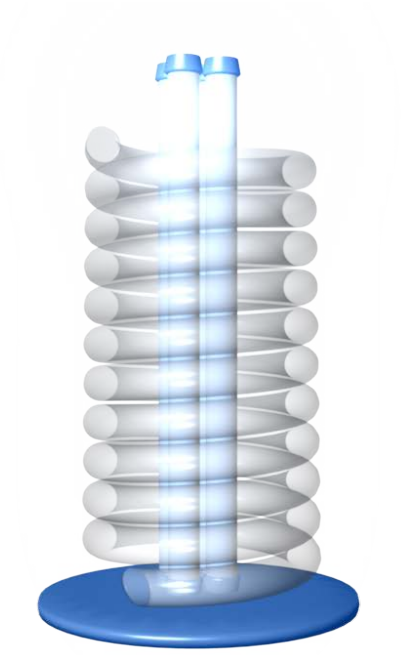

A.5 Water Recycling Column

Appendix B - Whole System Diagram

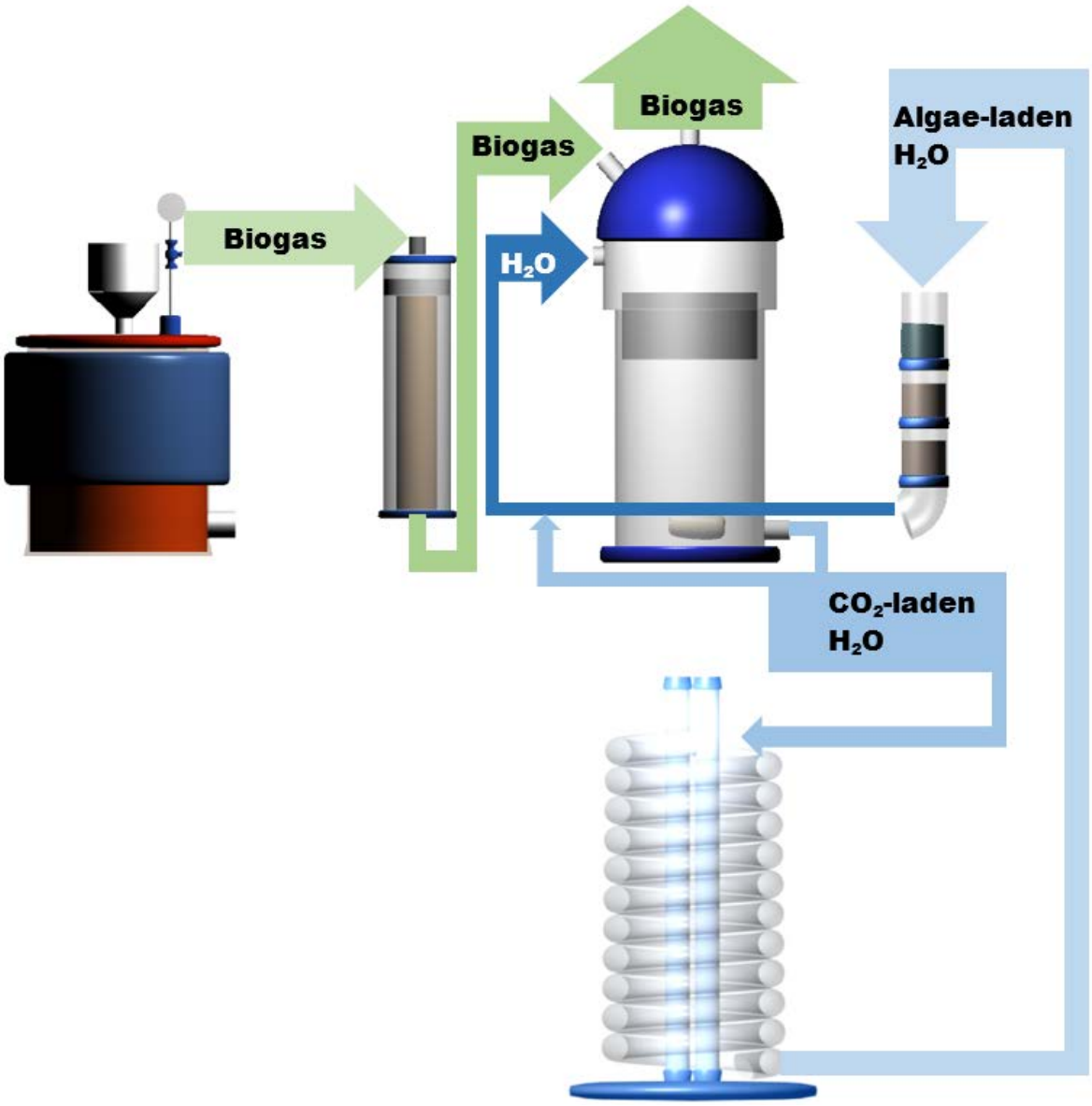

Appendix C - Calculating Biogas Generation Rate in Digester

1. Plot a pressure [Pa] vs. time [s] curve.
    a. Note: this should be a linear curve for constant biogas generation.
2. Record the slope of the pressure vs. time curve.
    a. The slope of this curve will be referred to as $\frac{dP}{dt}$ $[\frac{Pa}{s}]$.
3. Record the temperature [K] and volume of gas space in the digester [m^3].
    a. The temperature refers to the inoculum and substrate temperature, not the wall temperature.
    b. The volume of gas space is equal to the total volume of the digester minus the volume of inoculum and substrate in the digester.
4. Convert $\frac{dP}{dt}$ to $\frac{dn}{dt}$, molar change over time by applying the ideal gas law.
    a. Assume that biogas is an ideal gas.
    b. $\frac{dn}{dt} = \frac{dP}{dt}\frac{V}{RT}$, where R is the ideal gas constant $[\frac{m^3 Pa}{K \cdot mol}]$.
5. Convert $\frac{dn}{dt}$ to biogas generation rate by applying the molecular weight $[\frac{g}{mol}]$ and density $[\frac{g}{m^3}]$.
    a. The molecular weight and density of biogas are calculated based on the composition of the biogas.
    b. $Biogas\ generation\ rate = \frac{dn}{dt}\frac{MW}{density}\ [\frac{m^3}{s}]$
6. Convert the units as needed.

Appendix D - CO_2 Concentration Calculations

1. CO_2 concentration in CO_2 laden water at pH 12:
   F_{co2}=0.4 scfh=11.328 L/min V_{H2O}=18L
   t=10 min r_{co2}=0.74

   Where F_{co2} is the flow rate of the CO_2 into the column, t is the amount of time the trial was run, r_{co2} is the fraction of CO_2 removed with partially saturated water, and V_{H2O} is the volume of water run through the column.

   (11.328 L/min)*(10 min)/(24.45 mol/L)=4.63 mol CO_2

   (4.63 mol)*(0.74)=3.42 mol CO_2 removed

   (3.42 mol CO_2)/(18 L H_2O)=0.19 M

2. Volume of water necessary for CO_2 scrubber in overall system

   F_b=2.44 L/day X_{CO2}=0.543
   [CO_2]=0.19 M

   Where F_b is the flow rate of the biogas into the system, X_{CO2} is the mol fraction of CO_2 in the biogas, and [CO_2] is the concentration of CO_2 in the outflowing water.

   (2.44 L/day)*(0.543)/(24.45 mol/L)=0.054 mol/day CO_2

   (0.054 mol/day)/(0.19 M)=0.28 L H_2O/day

   This is the minimum amount of water that should be used in the column. Solubility will be better if the volume of water is higher.

Appendix E – f/2 Media for *Phaeodactylum tricornutum*

Compound	**mL**
$NaNO_3$ (75.0 g/L dH_2O)	1.0
$NaH_2PO_4 \cdot H_2O$ (5.0 g/L dH_2O)	1.0
$Na_2SiO_3 \cdot 9H_2O$ (30.0 g/L dH_2O)	1.0
L1 Trace Metal Solution (see below)	1.0
Vitamin Solution	0.5
Filtered Seawater (0.036 g/mL)	to 1000

L1 Trace Metal Solution

Compound	**Amount**
$FeCl_3 \cdot 6H_2O$	3.15 g
$Na_2EDTA \cdot 2H_2O$	4.36 g
$CuSO_4 \cdot 5H_2O$ (9.8 g/L dH_2O)	0.25 mL
$Na_2MoO_4 \cdot 2H_2O$ (6.3 g/L dH_2O)	3.0 mL
$ZnCl_2$ (22.0 g/L dH_2O)	1.0 mL
$CoCl_2 \cdot 6H_2O$ (10.0 g/L dH_2O)	1.0 mL
$MnCl_2 \cdot 4H_2O$ (180.0 g/L dH_2O)	1.0 mL
$NiCl_2$ (2.7 g/L dH_2O)	1.0 mL
Na_3VO_4 (1.84 g/L dH_2O)	1.0 mL
K_2CrO_4 (1.94 g/L dH_2O)	1.0 mL

Vitamin Solution

Compound	**Amount**
Biotin (0.1 g/L dH_2O)	10.0 mL
Thiamine HCl	200.0 mg
Distilled H_2O	to 1.0 L

Appendix F – Modified Chu-13 Medium for *Botrycoccus braunii*

Compound	**mg/L**
KNO_3	400
K_2HPO_4	80
$CaCl_2 \cdot 2H_2O$	107
$MnSO_4 \cdot 7H_2O$	200
$C_6H_5FeO_7$	20
$C_6H_8O_7$	100
$CoCl_2$	0.02
H_3BO_3	5.72
$MnCl_2 \cdot 4H_2O$	3.62
$ZnSO_4 \cdot 7H_2O$	0.44
$CuSO_4 \cdot 5H_2O$	0.16
Na_2MoO_4	0.084
0.072 N H_2SO_4	1 drop
Deionized water	1 L

Appendix G - Calculating amount of sodium bicarbonate to test CO2 effect on algae

This is based on a predicted production of 5 L of biogas per day from our anaerobic digester with a composition 50% CO2.

$$\frac{2.5\ L\ CO_2}{} \times \frac{1\ mol\ CO_2}{22.4\ L\ CO_2} \times \frac{84\ g\ NaHCO_3}{1\ mol\ NaHCO_3} = 9.4\ g\ NaHCO_3$$

Our original plan was to have a 4 L culture of algae. The sodium bicarbonate tests were conducted on 500 mL samples of algae, so the approximated NaHCO3 amounts were adjusted appropriately.

$$\frac{9.4\ g\ NaHCO_3}{4\ L\ algae} = \frac{x\ g\ NaHCO_3}{0.5\ L\ algae}$$

$$x = 1.175\ g\ NaHCO_3\ \ for\ 500\ mL\ algae\ sample$$

This calculated out to the following weights of NaHCO3 to be added to the corresponding samples:

$$full\ strength = 1.175\ g\ NaHCO_3$$
$$half\ strength = 0.5875\ g\ NaHCO_3$$
$$quarter\ strength = 0.2938\ g\ NaHCO_3$$

Appendix H - Images of *Synechocystis* culture in the photobioreactor

The following images were taken on March 13, 2014. This was a few hours after the cyanobacteria was added to the photobioreactor. There was no alkaline water in the reactor yet. There was ample circulation and no sticking of the *Synechocystis* to the tubing. The pH was 10.8.

The following images were taken on March 14, 2014. One day after the cyanobacteria was added and alkaline water was dripped into the photobioreactor, the cyanobacteria began sticking to the tubing walls. The solution in the photobioreactor was almost clear. There was almost no sign of cyanobacteria being circulated. The pH was 10.8. This high value suggests that the cyanobacteria cannot self-buffer the high pH alkaline solution. 15 mL of concentrated HCl (37% w/w) was added to lower the pH to about 7.5.

The following images were taken on March 16, 2014. This was 3 days after the initial addition of cyanobacteria. The solution is slightly greener in color than on March 14. There is still excessive sticking on the walls of the tubing. This could suggest that there was algal growth. The pH was 8.15. This value was still a little high but the cyanobacteria seems to be adapting to the new environment.

The following images were taken on March 19, 2014. This was 6 days after the initial addition of cyanobacteria. There seem to be cyanobacteria deposits settled on the bottom of each coil of tubing. The cyanobacteria is no long sticking to the walls, but it is also not fully mixed in the solution. This may indicate either death of the culture of continued growth. This must be confirmed by further experimentation. The pH was 8.15.

Glossary

Adsorption
the accumulation of gases, liquids, or solutes on the surface of a solid or liquid

Alkaline
describing a solution that has an excess of hydroxide ions (i.e. a pH greater than 7)

Amine
any of a group of organic compounds of nitrogen, such as ethylamine, $C_2H_5NH_2$, that may be considered ammonia derivatives in which one or more hydrogen atoms have been replaced by a hydrocarbon radical

Atomizer
a device for converting a substance, especially a perfume or medicine, to a fine spray

Carbon fixation
during photosynthesis, the process by which plants convert carbon dioxide from the air into organic molecules

Caustic
A material or substance capable of burning, corroding, dissolving, or eating away by chemical action

Exothermic
a chemical reaction that releases heat into its surroundings

Filament
a chainlike series of algae cells

Fouling
the settlement of algae or other microorganisms

Heterotrophically
obtaining energy by taking in organic substances

Hydrocarbon
any of numerous organic compounds, such as benzene and methane, that contain only carbon and hydrogen

Ideal gas law

the equation of state of an ideal gas which is a good approximation to real gases at sufficiently high temperatures and low pressures; that is, PV = RT, where P is the pressure, V is the volume per mole of gas, T is the temperature, and R is the gas constant

IDLH

the value at which a substance is immediately dangerous to life and health as defined by the Centers for Disease Control and Prevention

Inoculum

a quantity or suspension of cells, microorganisms, or viruses used to start a new culture or to infect another culture; something used to inoculate

Mixotrophically

obtaining energy from both autotropic (inorganic substances resulting from chemosynthesis and photosynthesis) and heterotrophic (organic substances) mechanisms

Optical density

the degree of opacity of a translucent medium expressed by log I_0/I, where I_0 is the intensity of the incident ray, and I is the intensity of the transmitted ray

Parts per million (ppm)

ratio to determine the molecular presence of a particular substance per million parts in relation to others. Often used in chemical analysis, ppm is a critical measure for determining the significant presence or absence of a particular substance in a medium

Phototrophically

obtaining energy from sunlight for the synthesis of organic compounds

Precipitate

a solid or solid phase separated from a solution

Rotameter

a variable-area, constant-head, rate-of-flow volume meter in which the fluid flows upward through a tapered tube, lifting a shaped weight to a position where upward fluid force just balances its weight

Substrate

the substance that is affected by the action of a catalyst; for example, the substance upon which an enzyme acts in a biochemical reaction

Supernatants

the clear fluid above a sediment or precipitate

Volatile fatty acid

fatty acids with a carbon chain of six carbons or fewer. They are now usually referred to as short-chain fatty acids (SCFA)

Bibliography

Abatzoglou, N. & Boivin, S. (2008). A review of biogas purification processes. *Biofuels, Bioproducts & Biorefining, 3*(1), 42-71.

An, J.-Y., Sim, S.-J., Lee, J. S., & Kim, B. W. (2003). Hydrocarbon production from secondarily treated piggery wastewater by the green alga *Botryococcus braunii*. *Journal of Applied Phycology, 15*(2-3), 185-191.

Andriani, D., Wresta, A., Atmaja, T. D. & Saepudin, A. (2013). A review on optimization production and upgrading biogas through CO_2 removal using various techniques. *Appl Biochem Biotechnol, 172*(4), 1909-1928.

Appels, L., Baeyens, J., Degreve, J., & Dewil, R. (2008). Principles and potentials of the anaerobic digestion of waste-activated sludge. *Progress in Energy and Combustion Science, 34,* 755-781. doi:10.1016/j.pecs.2008.06.002

Apt, K. E., Grossman, A. R. & Kroth-Pancic, P. G. (1996). Stable nuclear transformation of the diatom *Phaeodactylum tricornutum*. *Molecular and General Genetics MGG, 252*(5), 572-579.

Bandosz, T. (2002). On the adsorption/oxidation of hydrogen sulfide on activated carbons at
ambient temperatures. *Journal of Colloid and Interface Science, 246*(1), 1-20.

Banerjee, A., Sharma, R., Chisti, Y., & Banerjee, U. C. (2002). *Botryococcus braunii* : A renewable source of hydrocarbons and other chemicals. *Critical Reviews in Biotechnology, 22*(3), 245-279.

Bar-Zeev, E., Belkin, N., Liberman, B., Berman, T. & Berman-Frank, I. (2012). Rapid sand filtration pretreatment for SWRO: Microbial maturation dynamics and filtration efficiency of organic matter. *Desalination, 286(1),* 120-130.

Bartual, A. & Galvez, J. A. (2002). Growth and biochemical composition of the diatom *Phaeodactylum tricornutum* at different pH and inorganic carbon levels under saturating and subsaturating light regimes. *Botanica Marina, 45*(6), 491-501.

Benavides, A. M. S., Torzillo, G., Kopecky, J., & Masojidek, J. (2013). Productivity and biochemical composition of *Phaeodactylum tricornutum* (Bacillariophyceae) cultures grown outdoors in tubular photobioreactors and open ponds. *Biomass and Bioenergy, 54*(2), 115-122.

Biebl, H., & Pfennig, N. (1977). Growth of sulfate-reducing bacteria with sulfur as electron acceptor. *Archives of Microbiology, 112*(1), 115-117.

Bligh, E. G. & Dyer, W. J. (1959). A rapid method of total lipid extraction and purification. *Canadian Journal of Biochemistry and Physiology, 37*(8), 911-917.

Bolzonella, D., Cavinato, C., Fatone, F., Pavan, P., & Cecchi F. (2012). High rate mesophilic, thermophilic, and temperature phased anaerobic digestion of waste activated sludge: A pilot scale study. *Waste Management, 32*, 1196-1201. doi:10.1016/j.wasman.2012.01.006

Bouzaza, A., Laplanche, A. & Marsteau, S. (2004). Adsorption-oxidation of hydrogen sulfide on activated carbon fibers: effect of the composition and the relative humidity of the gas phase. *Chemosphere, 54*(4), 481-488.

Centers for Disease Control and Prevention. (1994). *Documentation for immediately dangerous to life or health concentrations (IDLHs).* Retrieved from http://www.cdc.gov/niosh/idlh /7783064.html.

Chen, P., Shi, W., Du, R., & Chen, V. (2008). Scrubbing of CO_2 greenhouse gases, accompanied by precipitation in a continuous bubble-column scrubber. *Industrial and Engineering Chemical Research, 47*(16), 6336-6343.

Chirac, C., Casadevall, E., Largeau, C., & Metzger, P. (1985). Bacterial influence upon growth and hydrocarbon production of the green alga *Botryococcus braunii. Journal of Phycology, 21*(3), 380-387.

Chisti, Y. (2007). Biodiesel from microalgae. *Biotechnology Advances, 25*(3), 294-306.

Demirbas, A. (2010). Use of algae as biofuel sources. *Energy Conversion and Management, 51*(12), 2738-2749.

Dienst, D., Georg, J., Abts, T., Jakorew, L., Kuchmina, E., *et al*. (2014). Transcriptomic response to prolonged ethanol production in the cyanobacterium *Synechocystis* sp. PCC6803. *Biotechnology for Biofuels, 7*(1), 21.

El-Bishtawi, R. & Haimour, N. (2004). Claus recycle with double combustion process. *Fuel Processing Technology, 86*(3), 245-260.

Energy Information Administration (2014). Gasoline and Diesel Fuel Update. Retrieved March 20, 2014, from http://www.eia.gov/petroleum/gasdiesel/

Environmental Protection Agency. LFG Energy Project Profiles. Retrieved March 20, 2014, from http://www.epa.gov/lmop/projects-candidates/profiles.html

Environmental Protection Agency (2013a). An Overview of Landfill Gas Energy in the United States. from http://www.epa.gov/lmop/documents/pdfs/overview.pdf

Environmental Protection Agency. (2013b). Energy Projects and Candidate Landfills. Retrieved March 25, 2014, from http://www.epa.gov/outreach/lmop/projects-candidates/index.html#map-area

Environmental Protection Agency. (2013c). *Natural gas*. Retrieved from http://www.epa.gov/ cleanenergy/energy-and-you/affect/natural-gas.html.

Fajardo, A. R., Cerdan, L. E., Medina, A. R., Fernandez, F. G. A., Moreno, P. G., & Grima, E. M. (2007). Lipid extraction from the microalga *Phaeodactylum tricornutum*. *European Journal of Lipid Science and Technology, 109*(2), 120-126.

Falkowski, P. G. & Raven, J. A. (2007). *Aquatic photosynthesis.* Princeton, NJ: Princeton University Press.

Ge, Y., Liu, J. & Tian, G. (2011). Growth characteristics of *Botryococcus braunii* 765 under high CO_2 concentration in photobioreactor. *Bioresource Technology, 102*(1), 130-134.

Goldman, J. C. & Carpenter, E. J. (1974). A kinetic approach to the effect of temperature on algal growth. *Limnology and Oceanography, 19*(5), 756-766.

Haimovich-Dayan, M., Garfinkel, N., Ewe, D., Marcus, Y., Gruber. A., *et al.* (2013). The role of C_4 metabolism in the marine diatom *Phaeodactylum triconutum*. *New Phytologist, 197*(1), 177-185.

Hoegh-Guldberg, O. & Bruno, J. F. (2010). The impact of climate change on the world's marine ecosystems. *Science, 328*(5985), 1523-1528.

Holub, B. J. & Skeaff, C. M. (1987). Nutritional regulation of cellular phosphatidylinositol. *Methods Enzymol, 141*, 234-244.

International Panel on Climate Change (2001). Climate Change 2001: Synthesis Report. from http://www.ipcc.ch/pdf/climate-changes-2001/synthesis-syr/english/summary-policymakers.pdf

Jaffrin, A., Bentounes, N., Joan, A. M. & Makhlouf, S. (2003). Landfill biogas for heating greenhouses and providing carbon dioxide supplement for plant growth. *Biosystems Engineering, 86*(1), 113-123.

Jimenez, C., Cossio, B. R. & Niell, F. X. (2003). Relationship between physicochemical variables and productivity in open ponds for the production of *Spirulina*: A predictive model of algal yield. *Aquaculture, 221*(1), 331-345.

Kabil, O. & Banerjee, R. (2010). Redox biochemistry of hydrogen sulfide. *Journal of Biological Chemistry, 285*(29), 21903-21907.

Kapdi, S. S., Vijay, V. K., Rajesh, S. K. & Prasad, R. (2005). Biogas scrubbing, compression and storage: perspective and prospectus in Indian context. *Renewable Energy, 30*(8), 1195-1202.

Kim, H. W., Vannela, R., & Rittmann, B. (2013). Responses of *Synechocystis* sp. PCC 6803 to total dissolved solids in long-term continuous operation of a photobioreactor. *Bioresource Technology, 128*, 378-384.

Kim, H. W., Vannela, R., Zhou, C., & Rittmann, B. (2011). Nutrient acquisition and limitation for the photoautotrophic growth of Synechocystis sp. PCC6803 as a renewable biomass source. . *Biotechnology and Bioengineering, 108*(2), 277-285.

Kojima, E., & Zhang, K. (1999). Growth and hydrocarbon production of microalga Botryococcus braunii in bubble column photobioreactors. *Journal of Bioscience and Bioengineering, 87,* 6, 811-815.

Kviderova, J. & Lukavsky, J. (2003). The cultivation of *Phaeodactylum tricornutum* in crossed gradients of temperature and light. *Algological Studies, 110*(1), 67-80.

Lateef, S. K., Soh, B. Z. & Kimura, K. (2013). Direct membrane filtration of municipal wastewater with chemically enhanced backwash for recovery of organic matter. *Bioresource Technology, 150*, 149-155.

Lastella, G., Testa, C., Cornacchia, G., Notornicola, M., Voltasio, F., & Sharma, V. K. (2002). Anaerobic digestion of semi-solid organic waste: biogas production and its purification. *Energy Conversion & Management, 43*, 63-75.

Lashof, D. A. & Ahuja, D. R. (1990). Relative contributions of greenhouse gas emissions to global warming. *Nature, 344*, 529-531.

Leu, J., Sheahan, C., & Fu, P. (2011). Metabolic engineering of algae for fourth generation biofuels production. *Energy & Environmental Science, 4*(7), 2451-2466.

Liu, X., Wang, W., Shi, Y., Zheng, L., Gao, X., Qiao, W., & Zhou, Y. (2012). Pilot-scale anaerobic co-digestion of municipal biomass waste and waste activated

sludge in China: Effect of organic loading rate. Waste Management, 32, 2056-2060. doi: 10.1016/j.wasman.2012.03.003

Lopo, M., Montagud, A., Navarro, E., Cunha, I., Zille, A., *et al*. (2012). Experimental and Modeling Analysis of *Synechocystis* sp. PCC 6803 Growth. *Journal of Molecular Microbiology and Biotechnology, 22*(2), 71-82.

Lu, J., Zheng, Y. & He, D. (2006). Selective absorption of H_2S from gas mixtures into aqueous solutions of blended amines of methyldiethanolamine and 2-tertiarybutylamino-2-ethoxyethanol in a packed column. *Separation and Purification Technology, 52*(2), 209-217.

Ma, H., Cheng, X., Li, G., Chen, S., Quan, Z., *et al*. (2000). The influence of hydrogen sulfide on corrosion of iron under different conditions. *Corrosion Science, 42*(10), 1669-1683.

Maat, H., Hogendoorn, J. A. & Versteeg, G. F. (2005). The removal of hydrogen sulfide from gas streams using an aqueous metal sulfate absorbent: Part I. The absorption of hydrogen sulfide in metal sulfate solutions. *Separation and Purification Technology, 43*(3), 183-197.

Maheswari, U., Montsant, A., Goll, J., Krishnasamy, S., Rajyashri, K. R., *et al*. (2005). The diatom EST database. *Nucleic Acids Research, 33*(1), 344-347.

Mann, J. E. & Myers, J. (1968). On pigments, growth, and photosynthesis of *Phaeodactylum tricornutum*. *Journal of Phycology, 4*(4), 349-355.

Mann, G., Schlegel, M., Schumann, R., & Sakalauskas, A. (2009). Biogas-conditioning with microalgae. *Agronomy Research, 7*(1), 33-38.

Markham, A. E. & Kobe, K. A. (1941). The solubility of gases in liquids. *Chemical Reviews, 28*(3), 519-588.

Matsuda, Y., Matsuda, Y., Hara, T., & Colman, B. (2001). Regulation of the induction of bicarbonate uptake by dissolved CO_2 in the marine diatom, *Phaeodactylum tricornutum. Plant, Cell & Environment, 24*(6), 611-620.

Metzger, P. & Largeau, C. (2005). *Botryococcus braunii:* a rich source for hydrocarbons and related ether lipids. *Applied Microbiology and Biotechnology, 66*(5), 486-496.

Morais, K. C., Ribeiro, R. L., Santos, K. R., Taher, D. M., Mariano, A. B. & Vargas, J. V. (2009). *Phaeodactylum tricornutum* microalgae growth rate in heterotrophic and mixotrophic conditions. *Thermal Engineering, 8*(1), 84-89.

Nagao, N., Tajima, N., Kawai, M., Niwa, C., Kurosawa, N., *et al*. (2012). Maximum organic loading rate for the single-stage wet anaerobic digestion of food waste. *Bioresource Technology, 118*, 210-218. doi: 10.1016/j.biortech.2012.05.045

Nagl, G. (1997). Controlling H_2S emissions. *Chemical Engineering, 104*(3), 125-131.

Oilgae. Algae Oil Information. Retrieved March 20, 2014, from http://www.oilgae.com/algae/oil/oil.html

Osorio, F., & Torres, J. C., (2009). Biogas purification from anaerobic digestion in a wastewater treatment plant for biofuel production. *Renewable Energy, 34*(10), 2164-2171.

Papadias, D. D., Shabbir, A., & Romesh, K. (2012). Fuel quality issues with biogas energy – An economic analysis for a stationary fuel cell system. *Energy*, *44*(1), 257-277.

Perez, E. B., Pina, I. C., & Rodiguez, L. P. (2008). Kinetic model for growth of *Phaeodactylum tricornutum* in intensive culture photobioreactor. *Biochemical Engineering Journal*, *40*(3), 520-525.

Petersson, A. & Wellinger, A. (2009). Biogas upgrading technologies-developments and innovations. *IEA Bioenergy*, 12-15.

Qin, J. (2005). Bio-Hydrocarbons from Algae: Impact of temperature, light and salinity on algae growth: Rural Industries Research and Development Corporation, Australia.

Rasi, S., Veijanen, A., & Rintala, J. (2007). Trace compounds of biogas from different biogas production plants. *Energy, 32*, 1375-1380. doi:10.1016/j.energy.2006.10.018

Shafiee, S. & Topal, E. (2009). When will fossil fuel reserves be diminished? *Energy Policy, 37*(1), 181-189.

Sheng, J., Kim, H. W., Badalamenti, J., Zhou, C., Sridharakrishnan, S., *et al*. (2011). Effects of temperature shifts on growth rate and lipid characteristics of *Synechocystis* sp. PCC6803 in a bench-top photobioreactor. *Bioresource Technology, 102*(24), 11218-11225.

Sheng, J., Vannela, R., & Rittmann, B. (2011). Evaluation of methods to extract and quantify lipids from*Synechocystis* PCC 6803. *Bioresource Technology*, *102*(2), 1697-1703.

Siefers, M. K. (2000). History of Silage, Sorgum Silage Production, and Nutritive Value of Pelleted Poultry and Restaurant Waste. Manhattan, KS: Kansas State University.

Singh, R. N. & Sharma, S. (2012). Development of suitable photobioreactor for algae production – A review. *Renewable and Sustainable Energy Reviews, 16*(4), 2347-2353.

Sorokin, C. & Krauss, R. W. (1958). The effects of light intensity on the growth rates of green algae. *Plant Physiol, 33*(2), 109-113.

Speight, J. (2007). *Natural Gas: A Basic Handbook*. Houston, Texas: Gulf Publishing Co.

Sudhakar, K., Premalatha, M., & Sudharshan, K. (2012). Energy balance and exergy analysis of large scale algal biomass production. *The 2nd Korea-Indonesia Workshop & International Symposium on Bioenergy from Biomass.*

Sydney, E. B., Sturm, W., de Carvalho, J. C., Thomaz-Soccol, V., Larroche, C., *et al.* (2010). Potential carbon dioxide fixation by industrially important microalgae. *Bioresource Technology, 101*(15), 5892-5896.

Tanoi, T., Kawachi, M., & Watanabe, M. (2011). Effects of carbon source on growth and morphology of *Botryococcus braunii. Journal of Applied Phycology, 23*, 25-33.

Themelis, N. J., & Ulloa P. A. (2007). Methane generation in landfills. *Renewable Energy, 32*, 1243-1257. doi:10.1016/j.renene.2006.04.020

Tippayawong, N. & Thanompongchart, P. (2010). Biogas quality upgrade by simultaneous removal of CO_2 and H_2S in a packed column reactor. *Energy, 35*(12), 4531-4535.

Ugwu, C. U., Aoyagi, H. & Uchiyama, H. (2008). Photobioreactors for mass cultivation of algae. *Bioresource Technology, 99*(10), 4021-4028.

Valenzuela, J., Mazurie, A., Carlson, R., Gerlach, R., Cooksey, K., et al. (2012). Potential role of multiple carbon fixation pathways during lipid accumulation in *Phaeodactylum tricornutum*. *Biotechnology for Biofuels*, 5(1), 1-17.

Weyer, K. M., Bush, D. R., Darzins, A., & Wilson, B. D. (2010). Theoretical maximum algal oil production. *Bioenergy Research*, 3(2), 204-213.

Wurts, W. A. & Durborow, R. M. (1992). Interactions of pH, carbon dioxide, alkalinity and hardness in fish ponds. *Southern Region Aquaculture Center*, Publication No. 464.

Xu, J., Fan, X., Zhang, X., Xu, D., Mou., et al. (2012). Evidence of Coexistence of C_3 and C_4 Photosynthetic Pathways in a Green-Tide-Forming Alga, *Ulva prolifera*. PLoS ONE 7(5): e37438. doi: 10.1371/journal.pone.0037438.

Xu, L., Weathers, P. J., Xiong, X. & Liu, C. (2009). Microalgal bioreactors: Challenges and opportunities. *Engineering in Life Sciences, 9*(3), 178-189.

Yongmanitchai, W. & Ward, O. P. (1992). Separation of lipid classes from *Phaeodactylum tricornutum* using silica cartridges. *Phytochemistry, 31*(10), 3405-3408.

Yoshimura, T., Okada, S., & Honda, M. (2013). Culture of the hydrocarbon producing microalga *Botryococcus braunii* strain Showa: Optimal CO_2, salinity, temperature, and irradiance conditions. *Bioresource Technology, 133*(0), 232-239. doi: http://dx.doi.org/10.1016/j.biortech.2013.01.095

Yuan, W. & Bandosz, T. J. (2007). Removal of hydrogen sulfide from biogas on sludge-derived adsorbents. *Fuel, 86*(17), 2736-2746.

Zhang, L., Pakrasi, H., & Whitmarsh, J. (1994). Photoautotrophic Growth of the Cyanobacterium Synechocystis sp. PCC 6803 in the Absence of Cytochrome c553 and Plastocyanin. *The Journal of Biological Chemistry, 269*(7), 5036-5042.

Zhou, Y., Zhang, Z., Nakamoto, T., Li, Y., Yang, Y., *et al*. (2011). Influence of substrate-to-inoculum ratio on the batch anaerobic digestion of bean curd refuse-okara under mesophilic conditions. *Biomass and Bioenergy, 35*, 3251-3256. doi:10.1016/j.biombioe.2011.04.002

Zicari, M. (2003). Removal of hydrogen sulfide from biogas using cow-manure compost. Master of Science thesis, Graduate School of Cornell University.